Structure-Function relationships of Flavoproteins and their Cofactors studied by Mass Spectrometry

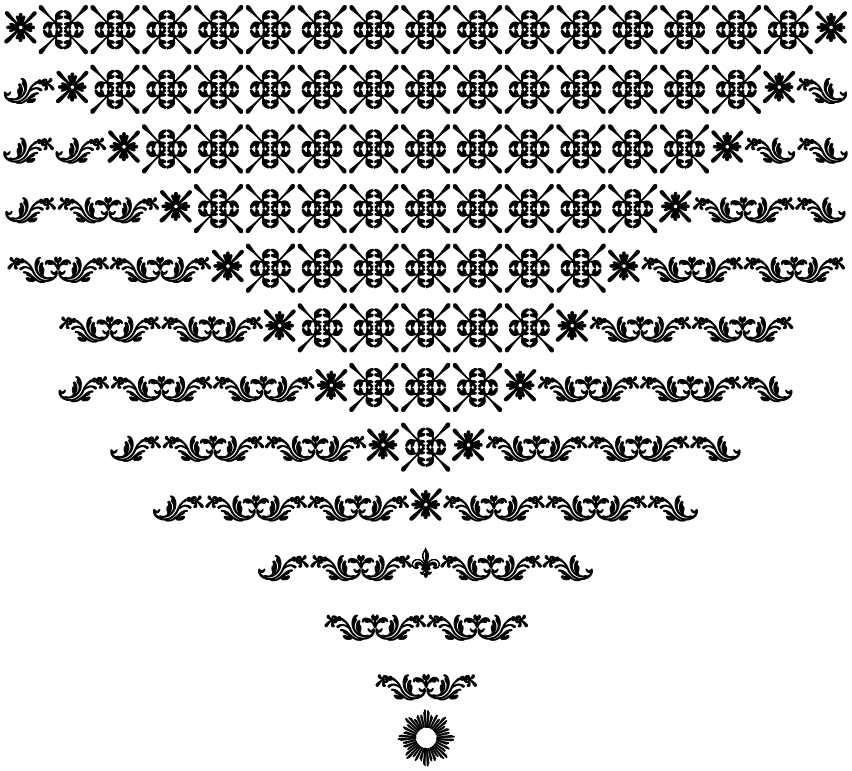

Structure-Function relationships of Flavoproteins and their Cofactors studied by Mass Spectrometry

Structuur-Functie relaties van Flavine-bevattende Eiwitten bestudeerd met behulp van Massaspectrometrie
(met een samenvatting in het Nederlands)

Relations Structure-Fonction des Flavoprotéines avec leurs Cofacteurs étudiées par Spectrométrie de Masse
(résumé en Français)

Proefschrift

ter verkrijging van de graad van doctor aan de Universiteit Utrecht op gezag van de Rector Magnificus, Prof. Dr. W. H. Gispen, ingevolge het besluit van het College voor Promoties in het openbaar te verdedigen op maandag 07 November 2005 des middags te 12:45 uur

door

Nora Tahallah

Geboren op 07 April 1972 te Algiers (Algerije)

Promotor: Prof. Dr. Albert J. R. Heck
Verbonden aan het Departement Scheikunde van de
Faculteit β-Wetenschappen der Universiteit Utrecht

Co-promotor: Dr. Robert H. H. van den Heuvel
Verbonden aan het Departement Scheikunde van de
Faculteit β-Wetenschappen der Universiteit Utrecht

Front cover: *Inspired from a 1947 lithograph in brown by Maurits Cornelis* ***Escher***
"Up and Down", also named "High and Low"

Isn't structure description all a matter of technique, sample state (solid, liquid, gaseous) in other words… a matter of point of view?

Back cover: *Adapted from an oil on canvas by Salvador* ***Dalí***
"Swans Reflecting Elephants" (1937). Critical-paranoiac method to make elephants appear from the reflection of the swans in water.

I don't know if John B. Fenn was inspired by Dalí or if Dalí has anticipated mass spectrometry…
Isn't Electrospray the most elegant way to make the elephants swimming in solution fly, as gracefully as swans, through a mass spectrometer?

Printing: Ponsen & Looijen B.V.

ISBN: 90-393-4086-2

Het in dit proefschrift beschreven onderzoek werd gefinancierd door het gebied Chemische Wetenschappen (CW) van de Nederlandse Organisatie voor Wetenschappelijk Onderzoek (NWO).

The work described in this thesis was financially supported by the Council for Chemical Sciences (CW) of the Netherlands organization for Scientific Research (NWO).

Je dédie cet ouvrage à :

Мамо,
Ти ме научи що е сила
Бабо,
Ти ме научи що е милост
Sonia,
A toi, si longtemps mon second moi
Nina,
A toi, notre seconde maman
Mila,
A toi qui tiens encore le monde dans tes mains
Claude,
A toi, un père comme aucun autre
Деди,
Ти ме научи що е благородност
Stéphane,
A toi qui m'as donné la plus belle nièce au monde
Вуйчо,
Ти ми показа що е дипломация
Papa,
A toi que j'espère avoir retrouvé pour de bon
Gwendal,
A toi qui m'as donné des ailes et qui voyages à mes côtés

« Не е важно никога да не падаш…
Важното е да знаеш всеки път,
на крак пак да се изправяш. »

Баба и Мама

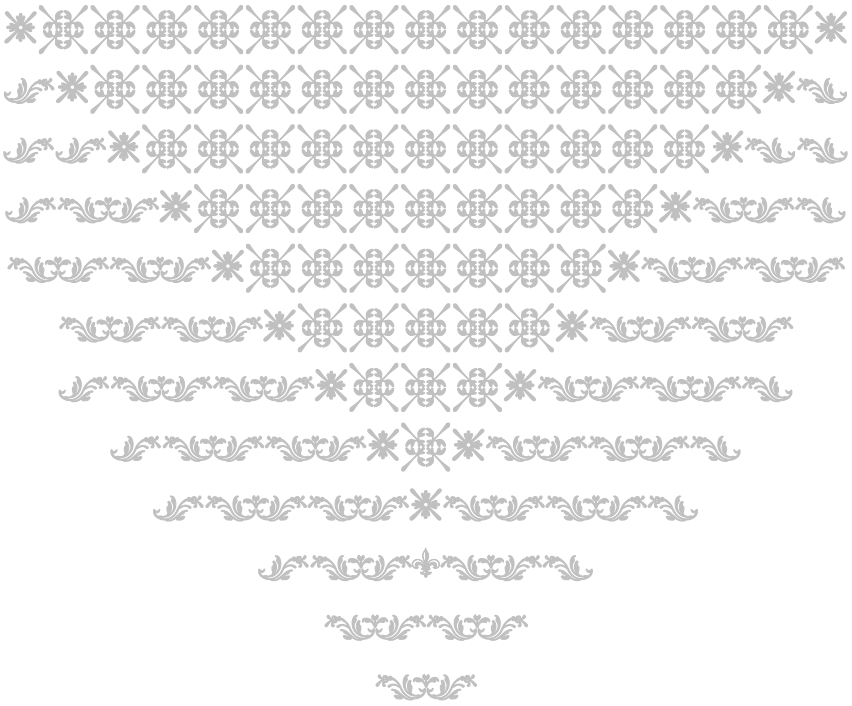

Table of contents

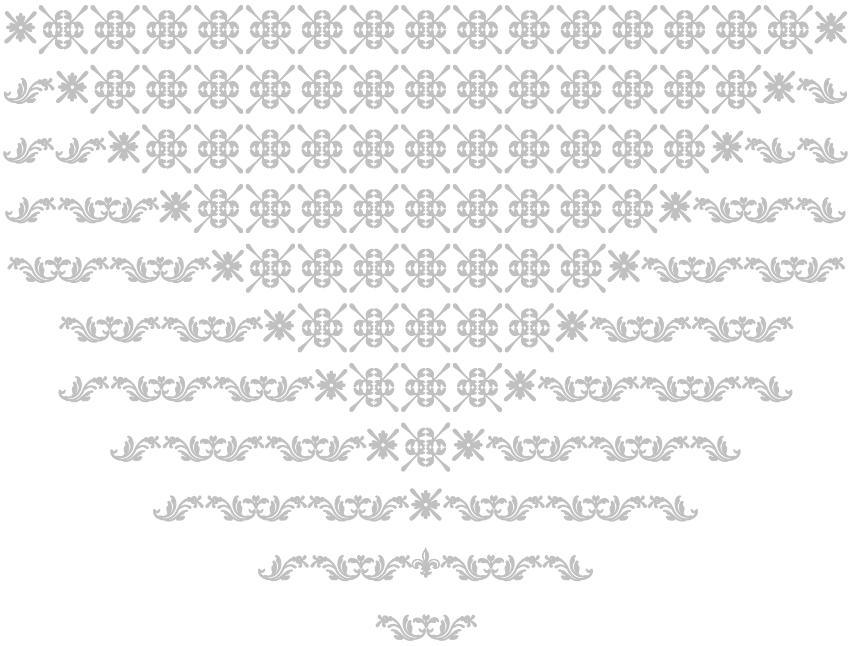

Chapter 1

General Introduction

«It is, by no means, easy to state what flavoenzymes are in chemical or biochemical terms.»
RETSU MIURA

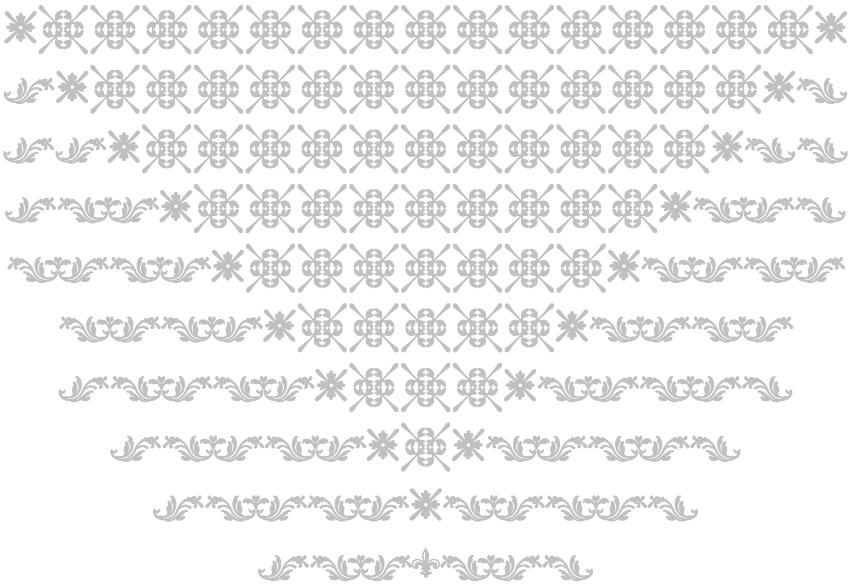

It is nowadays well established that interactions of proteins with other proteins, DNA/RNA and/or other biomolecules are fundamental in cell communication and life-sustaining processes. By strong physical, albeit noncovalent, interactions proteins can form the functional heterogeneous macromolecular complexes that are ribosomes, proteasomes or spliceosomes, as well as homooligomeric macromolecular assemblies, *i.e.* with identical protein subunit. The study of protein interactions is thus of vital importance for the understanding of biomolecular processes. Up to now, structural analyses of noncovalent protein complexes are mostly performed by techniques like nuclear magnetic resonance (NMR), X-ray crystallography, light scattering, sedimentation equilibrium by ultracentrifugation, size-exclusion chromatography, electrophoresis, etc. The focus of this thesis is the mass spectrometry-based analysis of noncovalent protein assemblies, a relatively new approach in the field of structural biology.

In this opening chapter are first shortly described some of the more established structural methods dedicated to the investigation of noncovalent protein interactions, as well as a short history of the constantly expanding role of mass spectrometry in structural biology. Then are enumerated the main mass spectrometry-based methodologies used for the work exposed in this thesis. Finally, the large family of flavoproteins, proteins investigated in this research, is introduced.

A) Noncovalent interactions

1– Noncovalent interactions and protein assemblies

It seems that almost no molecule in cellular biology works alone. The functioning of proteins in cells is highly dependent and regulated by specific noncovalent interactions with other molecules such as proteins, DNA, RNA, metal ions, heme and/or cofactors[1]. Protein interactions affect all processes in a cell; they organize and manage cell proliferation, differentiation, function, ageing and death and govern macromolecular assembling and disassembling, thereby defining the organisms' normal physiology[2]. Structural proteins need to interact and form extensive networks in order to shape organelles and whole cells. Vital functional macromolecular machineries, such as ribosomes or RNA polymerases, are held together by protein-protein interactions and the same goes for multi-subunit channels and receptors in membranes. The forces that mediate these noncovalent protein interactions include Van der Waals, electrostatic and hydrophobic effects and hydrogen bond interactions. Through extensive analysis of protein-protein interactions a hypothesis has been put together, which states that all proteins in a cell are connected through a

huge network in which protein-protein interactions can form and dissociate constantly[3]. Many biochemical studies have shown that the disruption of such protein-protein interactions, or improper association thereof, may lead to malfunctioning of the body possibly resulting in infectious, tumoral and neurodegenerative diseases or even death. Next to the more heterogeneous protein or protein-DNA assemblies, there exists in nature a plethora of proteins, including many enzymes, that interact with each other to form homooligomers (assemblies of identical subunits). It is not exactly clear what the role of such an extensive oligomerization is, although it has been proposed that oligomerization aids in protein stability (against proteases or heat-shocks) and that, additionally in protein oligomers, the multitude of active sites may lead to positive cooperativity.

2– Biophysical techniques to investigate noncovalent interactions

As mentioned above homo- and heteroprotein oligomers are a recurrent theme *in vivo*; they are essential in signaling pathways and biological functions. The investigation of these interactions and how they are controlled is crucial for the understanding of proteins stability, enzymes regulations, cellular mechanisms and other essential processes. A multitude of experimental methods exist nowadays for the detection and analysis of *in vitro* and *in vivo* noncovalent protein-protein and protein-ligand interactions. The work described here has been performed on a particular class of proteins called flavoproteins (see section **E** of this chapter). Therefore, examples of generic biophysical techniques in structural biology are highlighted below, which have proven to be particularly valuable for the analysis of interactions that involve flavoproteins.

One of the earliest and most common methods to study protein structure, including protein quaternary structure, is UV-visible difference spectroscopy[4]. Especially for flavoproteins, this is a helpful technique: the isoalloxazine ring of the flavin cofactor in its oxidized form gives flavoproteins a yellow color as it absorbs the light around 360 and 450 nm. Monitoring the spectral changes during enzymatic reactions or oligomerization processes can provide information on mechanisms, dissociation constants and conformational changes in the flavin environment[5-7]. Although they may be used to point at changes in the oligomerization, it is evidently not directly possible to measure the oligomerization status of a flavoprotein by analysis of the flavin spectral properties.

Next to UV-visible difference spectroscopy, circular dichroism spectroscopy (CD) may offer a very useful contribution to monitor changes in protein conformation possibly induced by ligand binding or protein oligomerization. CD signals, and changes therein, may reflect conformational changes and give a quantitative information on secondary and tertiary structures[8,9]. Changes in CD signals can be directly proportional to the amount of protein-ligand complexes in the sample, therefore used to determine binding constants[10]. However, the CD signal is a sum of

all CD active moieties in the protein or protein complex. Hence, difficulties in analyses of multi-protein complexes, or multi-flavin and/or heme containing proteins, may arise[11]. Besides, it is also possible that certain protein-ligand interactions or changes in protein conformation are CD blind, *i.e.* the association does not lead to overall differences in the CD spectrum, which hampers the measurements of conformational changes. Thermodynamics of folding/unfolding of monomers and oligomers can also be determined by CD spectroscopy using unfolding experiments through thermal or chemical denaturation[12,13].

Another powerful technique often used in structural biology, is fluorescence spectroscopy, which may provide information on protein concentration, structure, ligand binding and reaction kinetics. Fluorescence excitation/emission and quenching properties are sensitive to the direct environment of the fluorescent chromophore, thus also sensitive to the interactions of the fluorophore with its surrounding. Typically, when an intrinsic fluorescent amino acid is protected from the environment, for instance when it is closely buried within the protein structure, the quenching of the fluorescence is higher[14]. Thus fluorescence and fluorescence quenching measurements can provide information on conformation, orientation and environment changes and can be used to study unfolding/refolding or association processes of proteins[15]. Again, the flavin present in flavoproteins may be used for fluorescence measurements as has been done in mechanistic enzyme studies[16,17].

Isothermal Titration Calorimetry (ITC) is a biophysical approach that is very helpful for studies of equilibrium protein-ligand and protein-protein interactions. In such an approach, the heat release is measured as a function of the titrated-in ligand concentration. The technique is rather unique in that it can provide simultaneously all thermodynamic parameters (ΔG, ΔH, ΔS and ΔC_P) of an association process[18-21]. However, although it is in practice possible to measure the stoichiometry of the binding event, ITC is difficult when a variety of species are present in solution.

Sedimentation equilibrium, or analytical ultracentrifugation, allows the determination of approximate molecular weight of proteins and protein complexes as well as equilibrium constants and stoichiometries and is very suitable for the study of homooligomers[22-24]. Owing to its chemical/physical properties, the method is not influenced by the shape of the molecules and enables a large scope of molecular mass detection, from 500 Da to over 50 MDa[25].

Although valuable and relatively simple and inexpensive to perform, UV-visible, CD, fluorescence spectroscopy, ITC and sedimentation equilibrium approaches provide rather limited detailed information about local (un)folding or interaction properties of proteins. Protein X-ray crystallography, electron microscopy, NMR and small-angle X-ray scattering are excellent

resources for detailed protein structural information. In the last decades these techniques have yielded an enormous amount of information varying from three-dimensional structures and dynamics of smaller proteins up to quaternary structures of whole viruses, like the 7 Å resolution data for hepatitis B virus particles, by electron microscopy[26]. In the measurements of protein-protein interactions, NMR chemical-shift perturbations, usually performed with isotopically labeled samples, can be very useful[27]. Although these methods provide high quality data, they also have their own intrinsic limitations, such as high sample consumption and low throughput. In addition, NMR and X-ray crystallography are mainly restricted to single proteins or protein domains and require homogeneous samples. For instance, NMR requires still relatively large amounts of very pure proteins and is therefore typically only used for the analysis of cloned and/or overexpressed proteins[28,29]. At present, a practical limit for the full analysis of the structure of a protein by NMR is approximately 50 kDa and therefore unfortunately beyond reach for most oligomeric flavoproteins[29].

3– Native Mass Spectrometry: An emerging biophysical technique to study noncovalent interactions

The last decade has seen the rapid development of a new field of research termed proteomics, which encompasses identifying structure, function and interactions of proteins and their role in biological processes. Proteomics thus entails the analysis of proteins on a large scale with the aim to measure their expression profiles, modifications, interactions and networks, localization and function. From the start mass spectrometry has played a pivotal role in proteomics. First primarily in the identification of proteins[30] but more recently also in the identification of proteins present within complex networks[31], in accurate measurement of protein expression levels and in the in-depth study of protein co- and post-translational modifications. These proteomics studies have further confirmed that the proteome world possesses an immense complexity. One of the intriguing views that have emerged out of these larger scale proteomics studies is that not many proteins "act on their own". It has been proposed that a cell can be described as a network of interlocking assembly lines[31,32], each of which is composed of large protein machineries. The constituents of these machineries may vary over time as a function of the environment induced by, for instance, signaling molecules or post-translational modifications. Although mass spectrometry-based proteomics technologies have been used to elucidate on a large-scale cellular protein networks, these technologies are not suited to study structure and dynamics of such intact protein machineries.

With the advent of the "soft" ionization techniques such as matrix assisted laser desorption ionization (MALDI) and electrospray ionization (ESI), the mass range of species amendable to mass spectrometric analysis has been increased immensely enabling the transfer into the gas-phase

of ionized noncovalent species with masses well over the million Dalton, *i.e.* the range of intact protein oligomers and functional machineries. This has led to the birth of a new field in biomolecular mass spectrometry that focuses on the analysis of intact proteins and protein complexes under pseudo-physiological conditions: native mass spectrometry. In-depth reviews on this relatively young field are available[33-36].

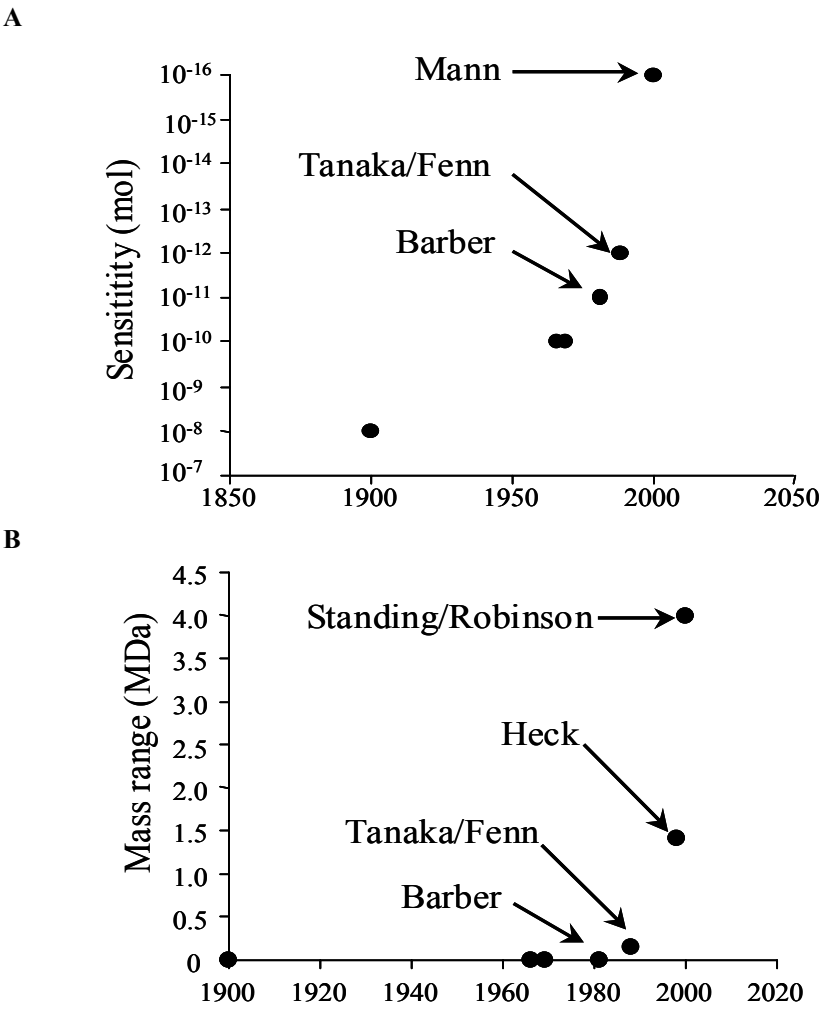

Figure 1. Evolution of electrospray ionization mass spectrometry over the last century. **A**, Increase of mass spectrometers' sensitivity and **B**, Improvement of the mass range capacity, during the last years as realized by several research groups (for refs. see text).

The optimization of experimental conditions, whereby noncovalent interactions can survive the transition from solution- to gas-phase and be detected intact, has paved the way to make native mass spectrometry a relevant alternative approach for the analyses of intact protein complexes and functional machineries, complementary to the more well-established structural biology techniques. **Figure 1** shows the evolution of mass spectrometry capabilities, in terms of sensitivity potentials (**Fig. 1A**) and mass detection range (**Fig. 1B**) of the mass spectrometers, over the last century. Especially the group of Standing has been a pioneer in this field as their study on 4-oxalocrotonate tautomerase[37] was one of the first mass spectrometry studies on protein oligomerization.

B) Mass spectrometry techniques

1– Introduction to Mass Spectrometry

Mass spectrometry is a more than a hundred years old biophysical analytical technique but is continually improved and has thereby only recently gained significant importance in its application to structural biology. Only since the late 1980s it is possible to analyze proteins, DNA and even viruses and to determine their quaternary structures. Native mass spectrometry offers the possibility to study very large intact protein assemblies in solution giving informations on molecular mass, stoichiometry, assembly, dynamics, cooperativity and ligand binding. The method allows the identification of complex building blocks composition, topology, quaternary structure and stability.

To perform mass spectrometric analyses the samples in solution need to be ionized and transferred into the gas-phase. Mass spectrometers are usually composed of three main regions. In the first stage samples are introduced into the ion source where the ionization takes place. Subsequently, the generated ions are directed by magnetic and/or electric fields towards an analyzer, which sorts them according to their mass-to-charge ratio *m/z*, with m being the ion mass and z its charge. An ion detector connected to a computer system registers the number of ions at each *m/z* value and produces mass spectra by translating the acquired ion electrical signals into ion abundances at each measured *m/z* value. One of the most extensively used analyzers in biomolecular mass spectrometry is the time-of-flight (ToF) analyzer, which is highly sensitive, allows rapid analyses and has a virtually unlimited *m/z* range. The combination of the continuous electrospray ion beam and the requirement for pulsed detection in ToF has been achieved by the orthogonal coupling of the ToF to other analyzers such as quadrupole mass analyzers in the so-called hybrid instruments (*e.g.* q-ToF instruments). Another advantage of such hybrid instruments is that they provide the opportunity to perform tandem mass spectrometry and obtain additional structural information. In typical q-ToF instruments, ions with an *m/z* range of up to 4 000 (*i.e.* complexes up to 60 kDa) can be first selected and then dissociated through collisional activation

within a collision cell. For the larger assemblies, giving signals above *m/z* 4 000, Robinson and co-workers have reported on a custom-built quadrupole with an *m/z* range extended to 32 000[38].

A fundamental parameter in every mass spectrometer is the high vacuum, critical for preventing ion-neutral collision. A properly adjusted and maintained high vacuum is typically essential for sensitivity, resolution and high quality spectra. However, it is now well established that a higher pressure than the standard operating values is vital for transmission of large molecular ions (see **Chapter 2**). The pressure can be raised by reducing the pumping speed in the first region or by introducing an additional gas flow[39,40]. Alternatively, a flow-restricting sleeve can be set around the first quadrupole[41]. It is believed that ions need to be translationally cooled down and focused by collisional damping as they acquire high kinetic energies when electrosprayed and accelerated by the electric fields in the ion source. The pressure parameters need to be carefully optimized since it has been reported that optimal conditions are *m/z* dependent and are reflected by significant changes in ion abundance in the resulting mass spectra. Therefore, specifically when different species in equilibrium are present in solution, one needs to be cautious when relating the relative abundances in the spectra to those in solution[42,43].

2– Ionization methods for noncovalent complexes

Introduction in the late 1980s of two new ionization techniques, namely matrix assisted laser desorption (MALDI)[44,45] and electrospray ionization (ESI)[46], gave a real impetus to biomolecular mass spectrometry and biomedical research in general as evidenced by the fact that Fenn and Tanaka have been awarded the Nobel Prize in chemistry in 2002 for their large contribution to the development of these ionization techniques.

Matrix Assisted Laser Desorption Ionization

Laser desorption ionization mass spectrometry of large proteins was first reported in 1988 by the groups of Karas & Hillenkamp. MALDI process is initiated by firing a pulsed laser beam, which desorbs and subsequently ionizes analyte molecules embedded in a laser-light absorbing matrix co-crystallized on a metal surface and placed inside the vacuum of the mass spectrometer. The use of the matrix minimizes analyte degradation by the intense laser beam as most of the energy is absorbed by the matrix. The analyte gets ionized by a plethora of gas-phase ion-molecule reactions whereby, in a final step, protons are transferred from the matrix molecules to the analyte resulting mainly in monocharged ions $[M+H]^+$. As singly charged ions are most prevalent in MALDI spectra, their interpretation is relatively straightforward[47]. MALDI offers high sensitivity (below the femtomole)[48] and has a high tolerance towards salts and other low-molecular weight contaminants making possible the analysis of complex biological mixtures without much further purification[49,50]. The method is extensively used in proteomics related peptide analysis.

Additionally and more relevant to the work described in this thesis, some more recent studies have shown that MALDI may allow the analysis of intact noncovalent complexes[51,52]. However the dried organic, often acidic (e.g. sinapinic acid or 2,5-dihydroxybenzoic acid), matrix is a far away environment from native or pseudo-physiological solution conditions and may result in the dissociation of noncovalent interactions during the ionization process.

To circumvent a few drawbacks from the conventional MALDI technique, Brutschy and co-workers have developed an alternative termed laser-induced liquid beam ionization/desorption mass spectrometry technique (LILBID-MS) whereby the desorption of ions takes place directly from solution[53]. In this approach a microscopic liquid beam introduced by an HPLC system passes a free flight where it is intersected by a laser beam directly desorbing the solvated ions. Samples can be dissolved in water making the sample preparation simple. Using this approach, tetrameric human hemoglobin could be successfully analyzed both in positive and negative ion mode. Lowering the laser energy produced a "softer" desorption process, reducing fragmentation in favor of the specific tetrameric conformation. Therefore LILBID-MS analyses provide a promising perspective for analyses of noncovalent assemblies.

Electrospray Ionization

In contrast to conventional MALDI, electrospray ionization enables the direct transfer of intact noncovalent macromolecular complexes from solution into the gas-phase. In the 1960s, Dole and co-workers established the foundations of what is now known as electrospray[54]. However, it was not until the second half of the 1980s that Fenn and co-workers developed the more modern form of the technique and used it successfully to analyze polymers and proteins[46,55]. They revealed the potential of the method for analyzing polymers and large biological molecules.

In electrospray, typically an electric potential (3-4 kV) is applied on a capillary containing the sample thereby enriching the liquid for positive/negative ions (in positive/negative detection mode). Forming the Taylor cone, charged droplets with an elongated meniscus at the tip of the capillary are expelled. Evaporation of solvent from the released droplets shrinks the droplet size and since the charge is conserved, at a critical radius, Coulombic repulsion overcomes the surface tension and leads to the fission of the droplets into much smaller droplets. The succession of shrinking and explosion leads to very small charged droplets and eventually results in highly charged gas-phase ions. This process occurs at atmospheric pressure and is very gentle with no significant fragmentation. The exact mechanism of how electrospray ionization leads to the formation of multiply charged ions is still not known in detail but is supposed to be different for large and small molecules (**Fig. 2**).

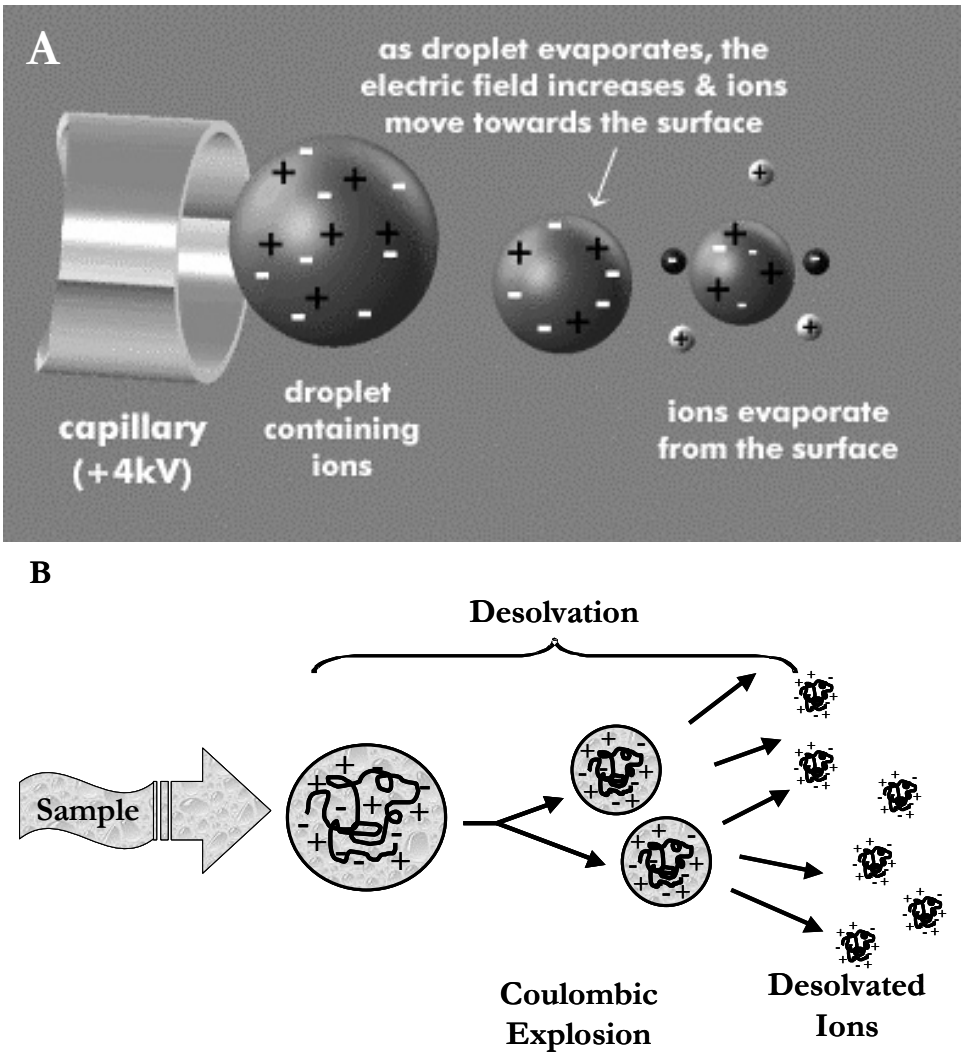

Figure 2. Proposed mechanisms for electrospray ionization. **A**, Ion evaporation model, from www.waters.com website. **B**, Charge residue model.

Iribarne and Thomson[56] suggested that small molecular ions can evaporate directly from the formed droplets (**Fig. 2A**). For larger globular proteins Dole *et al.*[54] have proposed a charged residue mechanism in which the water molecules totally evaporate from the droplets containing the native macromolecules (**Fig. 2B**). The current state of affairs concerning the electrospray ionization process has been reviewed in detail by Kebarle[57]. In the charge residue model, which is

evidently the most relevant for the studies described in this thesis, the residual charges accumulate throughout the ionization process on the proteins whereby they are transferred to the basic sites of the macromolecule. Therefore it is expected that the resulting charge a protein attains depends on the number of available basic sites[58]. Heck and Van den Heuvel[34] have compared a set of reported charge states and molecular masses in both positive and negative ion mode and concluded that in positive ion mode the experimental charge of a protein is ~90% of the charge predicted by Dole's model while it is only ~70% in negative ion mode. It has been suggested that the charge depends on the organic/inorganic buffer molecules present in the solvent[59]. When aqueous ammonium acetate is used as spray solution the protein attains more charges when compared to aqueous triethylammonium bicarbonate (TEAB), most probably linked to the higher gas phase proton affinity of TEAB[60].

The development of downscaled nanoflow electrospray ionization mass spectrometry (nano-ESI-MS)[61,62] has been vital for native mass spectrometry. Nano-ESI operating at a nanoliters per minute flow rate consumes only minute amounts (femto- to picomoles) of sample. In nano-ESI the sample is introduced in a small gold-coated glass capillary. The analyte is expelled by the potential (0.9-2 kV) applied to the capillary. The generated droplets are 100- to 1 000-fold smaller than those formed by conventional ESI. This results in much higher ionization and desolvation efficiencies.

C) Analysis of noncovalent interactions and intact protein assemblies by native mass spectrometry

1– Applications of native mass spectrometry

Recent reviews have described in detail the applications of native mass spectrometry for the analysis of noncovalent interactions and protein assemblies. Here are highlighted only a few recent examples, which reveal best the potential of the method. Formation and stability of protein complexes largely depend on environment conditions such as pH, salt, concentration and temperature. pH- or heat-induced conformational changes of distinct proteins are commonly measured by techniques such as calorimetry, circular dichroism and/or fluorescence spectroscopy, but monitoring changes in quaternary structure is more challenging.

Mass spectrometry analyses of the bifunctional kinase/phosphatase pointed to two different oligomeric states: a dimer at basic pH and a hexamer at neutral pH, most likely related to the kinase and phosphatase activity, respectively[63,64]. Benesch *et al.*[65] designed a mini-Peltier based thermo-controlled nano-ESI probe (10-100°C) to investigate the denaturation, aggregation, polydispersity and melting temperature of the 200 kDa dodecamer of the small heat shock protein

TaHSP16.9 directly reflected in the monitored ESI mass spectra. Related, Sobott *et al*.[38] followed by nano-ESI-MS subunit exchange between two small heat shock proteins PsHSP18.1 from pea and TaHSP16.9 from wheat and observed in line with previous TaHSP16.9 crystallographic data[66] that both proteins formed 200 kDa homodecamers. However, the mixture of both proteins at different molar ratios led to significant subunit exchange forming heterododecamers with a stoichiometry directly related to the initial concentration of each protein. Interestingly, the different oligomers exchanged specifically dimers suggesting first that the structures are globally very dynamic but with a very stable dimeric substructure and second that, *in vivo*, heat shock proteins of the same class and in the same location may exchange subunits.

Pinkse *et al.* reported a study of the multimeric urease, which confers to the gram-negative *Helicobacter pylori* its pathogenicity. The enzyme converts urea into ammonia to neutralize the gastric acids around the proliferating microorganism. The oligomerization dynamics of the heterocomplex enzyme were monitored by ESI-MS[67]. Consisting of 26.5 kDa α-subunits and 61.7 kDa β-subunits, Pinkse *et al.* showed that *H. pylori* urease forms primarily a heterododecamer $(\alpha\beta)_{12}$ of 1.06 MDa and is very sensitive to thermal dissociation into the heterohexamer $(\alpha\beta)_3$, corroborating the $((\alpha\beta)_3)_4$ structure proposed by the previous X-ray analyses[68].

Additionally, initial results on a pseudo-native membrane-bound detergent-solubilized oligomeric membrane protein complex by direct ESI-MS have been reported showing that the ESI technique can also be used for this difficult class of proteins. It was found that the rat membrane-bound microsomal glutathione transferase-1 protein forms a 53 kDa homotrimer binding one glutathione per monomer[69]. The group of Robinson[70] demonstrated by native ESI-MS that the *E. coli* ribonuclease E, responsible for RNA processing and degradation, assembles in a 248 kDa homotetrameric complex binding up to 4 RNA molecules.

Also ESI-MS analyses of the intact heterocomplexes of *E. coli* RNA polymerase core enzyme, a multi-subunit complex of around 389 kDa, with the sigma70 factor and the Rsd protein were carried out successfully[71,72]. As confirmed by gel electrophoresis, these ESI-MS studies showed that the binding of the Rsd regulator displaced the sigma70 factor from the polymerase and formed complexes with the enzyme and the factor suggesting that Rsd sequesters sigma70 and is an effector of RNA polymerase.

Finally, one of the most beautiful examples of the puissant contribution of native mass spectrometry to the characterization of intact heterogeneous assemblies is the analysis of the intact *E. coli* 70S ribosome by ESI-MS. This cellular machinery contains 54 proteins within two noncovalent subunits 30S and 50S attached to RNA molecules[73].

2– Tandem mass spectrometry of intact protein assemblies

Several mass analyzers provide an opportunity to obtain additional structural information by investigating dissociation patterns of ions produced by ESI or MALDI. In fact this is one of the most powerful approaches in proteomics where gas-phase ion dissociations are used for peptide sequencing. Fragmentation is induced by collisions of the generated ions, within a collision cell placed in the vacuum of the mass spectrometer, with other gaseous neutral molecules (typically inert rare gas molecules). The process is often referred to as collision induced (or activated) dissociation (CID or CAD). Such CID experiments are also known as tandem MS, MS/MS or MS^n experiments where n corresponds to the number of fragmentation steps the precursor ion and subsequent fragment ions are subjected to. In principle, native ESI mass spectrometry is aimed to bring protein assemblies intact into the mass spectrometer. It would manifestly be advantageous to dissociate the protein complexes inside the vacuum of the mass spectrometer to obtain further information about the stoichiometry, the molecular architecture and/or the binding energies of the interacting partners.

Nevertheless an important consideration that needs to be addressed in such studies is that the higher order structures of the desolvated gas-phase ionic protein complexes may deviate extensively from the structure of the complexes in solution. Therefore gas-phase MS/MS data on protein complexes need to be cautiously interpreted when related to the solution-phase properties. In several reported studies, gas-phase dissociation pathways observed by mass spectrometry were not in line with condensed-phase expectations. For example, MS dissociation of the tetrameric concanavalin A and adult human hemoglobin resulted principally in the formation of monomer and trimer product ions while in solution concanavalin A is composed of a homotetramer of two dimers and hemoglobin forms two heterodimers[74,75]. An often observed pattern in the gas-phase dissociation of protein complexes is that the fragmentation proceeds by the elimination of the smallest subunit, no matter how tight this is bound to the complex in solution. This pattern has been observed for a number of noncovalent complexes such as the $\alpha_2\beta_4$ heterohexamer of the archaeal GimC/prefolding homologue, which releases the small β-subunit when collisionally activated[76]. The ten-components transthyretin complex consists of a tetrameric transthyretin assembling with two thyroxins, two retinol-binding proteins and two retinols (Vitamin A). Again, under collisionally induced dissociation the whole complex releases first a single monomer of transthyretin[38].

However, more recently several gas-phase dissociation studies have provided useful information related to solution-phase properties of protein assemblies. For instance, gas-phase tandem MS dissociation of the intact ribosome under different pH conditions[77,78] showed that a lower pH in the sprayed solution promoted dissociation into monomeric ribosomal proteins and 5S

RNA and cofactors. Also, replacement of Mg^{2+} by Li^{+} in the ribosomes promoted facile dissociation of the ribosome in the gas-phase.

Similarly, McCammon *et al.*[79] investigated by MS/MS the stoichiometry and binding sites of tryptophane (Trp) molecules in the TRAP complex, revealing a single ring structure for the TRAP 12-mer binding up to 11 Trp molecules and a double ring structure of 24 subunits binding up to 22 Trp, depending on the Trp molecule concentration in the initial solution. The similarity in the dissociation pattern for both 12- and 24-mer (loss of 5 then 6 Trp per ring) allowed the authors to propose a global oligomerization mode of the protein complex depending on the environment. One of the nicest applications of tandem mass spectrometry is the analysis of αB-crystallin. αB-crystallin forms polydisperse oligomeric protein complexes, which cannot be separated/purified and are therefore extremely difficult to investigate by traditional structural biology approaches. ESI-MS of αB-crystallin produces an unresolved mass spectrum as all the charge states of the different present oligomers do overlap. MS/MS analysis was used on a selected isolated *m/z* peak, to deconvolute the oligomer distribution from the polydisperse oligomers of αB-crystallin[80].

From above it is clear that the technique of tandem mass spectrometry may be very helpful for the structural analysis of protein complexes by native mass spectrometry. Although the data obtained so far have revealed that gas-phase dissociation pathways may sometimes be in agreement with solution phase properties, they are also often in contradiction. Therefore, good care should be taken when the solution properties are addressed.

D) The structural role of cofactors in proteins

1– Flavin and pyridine nucleotide cofactors

Many proteins require cofactors in order to catalyze a chemical reaction. These organic or inorganic compounds such as metal ions, hemes, flavins (**Fig. 3A**) and pyridine nucleotides (**Fig. 3B**) interact often tightly with proteins to enhance reactivity, selectivity and efficiency of the enzymatic reactions. However, sometimes cofactors interact only weakly with proteins, *e.g.* the binding of NADPH to *p*-hydroxybenzoate hydroxylase is known to be very weak[81]. In recent years it is becoming clear that many of the cofactors may also contribute to the structural stability of proteins such as oligomerization and thermo-stability[82,83].

In this section, the structural function of two groups of cofactors, namely flavins and pyridine nucleotides, present in the proteins investigated in this work, is described. In addition, the cooperativity effect in proteins and in relation with cofactor binding will be introduced.

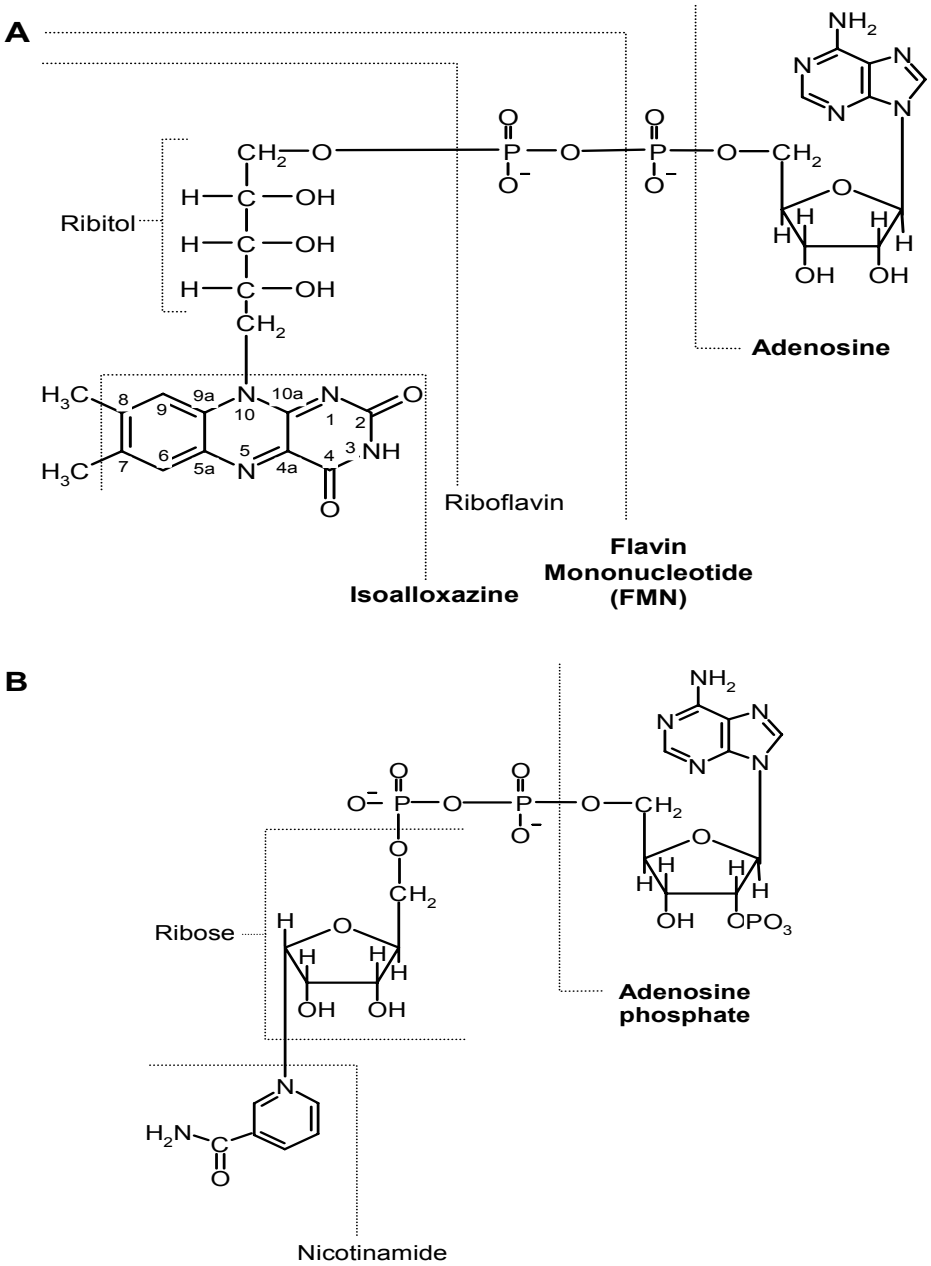

Figure 3. Flavoprotein cofactors and coenzymes. **A**, Structure components of the flavin cofactors Riboflavin, Flavin mononucleotide (FMN) and Flavin adenine dinucleotide (FAD). **B**, Nicotinamide adenine dinucleotide phosphate reduced form (NADPH).

Riboflavin (vitamin B2), which consists of an isoalloxazine ring system with a ribityl side chain, is the precursor of flavin molecules (**Fig. 3A**). Whereas plants and bacteria are able to produce riboflavin, mammals are dependent on their food for this compound take up. By the subsequent action of flavokinase and FAD synthase, riboflavin is converted into the cofactors flavin mononucleotide (FMN) and flavin adenine dinucleotide (FAD), respectively[6]. These cofactors are incorporated covalently or noncovalently into flavoproteins and are indispensable for enzymatic reactivity. The mechanistically relevant part of the flavin cofactor is the isoalloxazine ring system, which serves as a reversible reduction-oxidation catalyst in many biological redox processes[84]. This part of the molecule is also responsible for light absorption, giving the yellow color to flavins and flavoproteins (Latin: flavus = yellow).

Most flavoproteins interact noncovalently with flavin molecules, however, about 10% of the human cellular FAD is covalently attached through an amino acid of the protein. Prominent examples of this class of flavoenzymes are succinate dehydrogenase and monoamine oxidase[85,86]. To date, although the first covalent flavin-protein link was identified in succinate dehydrogenase already 50 years ago[87], there is no definite rational for the covalent flavinylation process. It has been shown that the covalent link allows the flavin to reach a proper redox potential, thereby efficiently assisting enzyme catalysis[88]. It is also suggested that the covalent flavin binding is important for increased resistance against proteolysis and altered reactivity of the cofactor, improved protein stability, but also gives the advantage of retaining activity in a flavin deficient environment[89-91].

Flavins may also be substrates instead of cofactors. An interesting example is the flavin reductase PheA2 from *Bacillus thermoglucosidasius*. The conversion of phenols into cathecols in this organism involves a two-component system: PheA2, which reduces the flavin, and PheA1, which uses the reduced flavin for the hydroxylation of phenol[92,93]. Native ESI-MS data have shown that PheA2 is a dimeric protein, which has per monomer one high affinity site for FAD and a second low affinity site for FAD **(Fig. 4)**. From these data, X-ray crystallography and biochemical data, it was concluded that PheA2 contains a high affinity FAD cofactor, which remains bound during the catalytic cycle and a weak affinity FAD substrate, which is transferred in its reduced state to PheA1[93].

Pyridine nucleotides such as NADH and NADPH (**Fig. 3B**) are essential cofactors for both energy metabolism and signal transduction and share this dual functionality with two other important nucleotides ATP and GTP. Pyridine nucleotides are synthesized via metabolic pathways starting from the enzyme-catalyzed oxidation of L-aspartate[94,95]. These compounds are then noncovalently incorporated into proteins. While flavin cofactors bind usually tightly throughout the catalytic cycle of an enzyme, pyridine nucleotides often interact tightly only in the reduced or

oxidized form. However, recent ESI-MS studies on the dimeric 4-hydroxyacetophenone monooxygenase (HAPMO) showed for the first time the continuous binding of NADP(H) to a Baeyer-Villiger monooxygenase thereby increasing the stability of the protein[43]. This may also be important for related BVMOs.

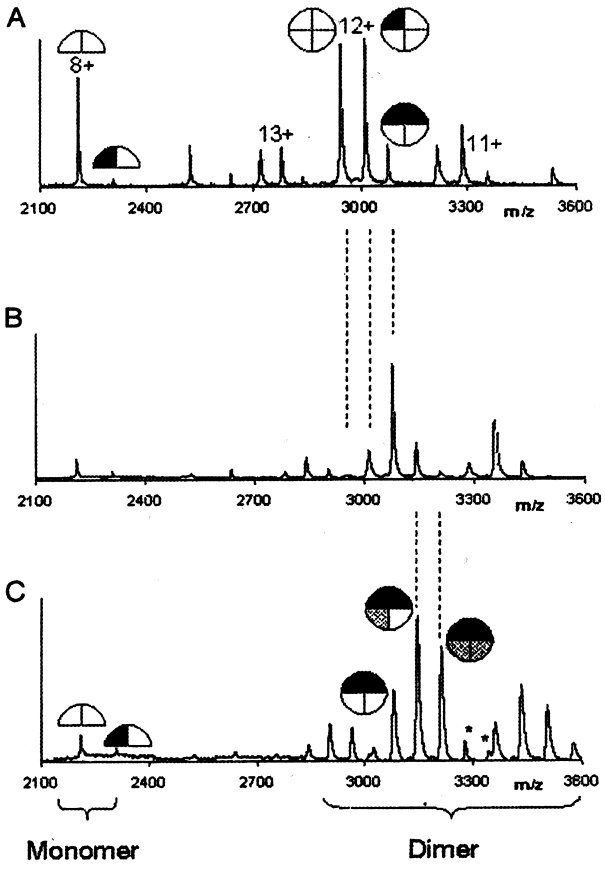

Figure 4. Nano-electrospray mass spectra of 4 μM holo-PheA2 in 40 μM ammonium bicarbonate, pH 8.0 mixed with **A**, 0 μM FAD, **B**, 40 μM FAD, and **C**, 100 μM FAD. FAD binding as cofactor is indicated in *black* and FAD as substrate in *gray* [Adapted with permission from *Ref.*[96]].

2– Protein stability

Protein-cofactor interactions have proven to be of prime importance for enzyme thermo-stability. Loss of enzyme thermal stability increases the risk of among others cardiovascular diseases and neural tube defects in humans. As an example, the covalent bond between FAD and monoamine oxidase seems not to be required for the catalytic activity but may function as a structural core for the active conformation in the membrane. The C406A mutant of monoamine oxidase A, which contains a noncovalently bound FAD, is active but loses rapidly and irreversibly

activity during incubation[97]. Similarly, cofactor-binding efficiency is crucial for the stability of bacterial methylenetetrahydrofolate reductase. The common polymorphism 677C->T in methylenetetrahydrofolate reductase causing the single point mutation Ala222Val reduces the affinity of the enzyme for the FAD cofactor and results in a lower thermal stability[98,99].

Another study towards the contribution of cofactors for the stability of the host protein is the FAD binding induced octamerization of the vanillyl alcohol oxidase (VAO) mutant H61T. Wild type VAO contains a covalently bound FAD cofactor whereas holo-H61T VAO contains a noncovalently bound FAD. While both wild type and holomutant form octamers, apo-H61T is present as a dimer[91,100]. Interestingly, X-ray crystallography of both apo- and holoforms of the mutant H61T revealed a highly homologous structure without any major conformational perturbations[101]. However, ESI-MS studies showed that when an excess of cofactor is added to the apoprotein, FAD binding induces octamerization, suggesting cooperativity between cofactor binding and stabilization of the enzyme quaternary structure[91].

3– Cooperativity effects

Oligomerization of proteins, in particular proteins involved in signal transduction, may be advantageous to provide means of allosteric interactions between the subunits. In some multimeric proteins these interactions may give rise to cooperative binding of ligands, which is believed to play a role in the regulation of their activity[102].

One of the first native mass spectrometry studies revealing cooperativity effects[103] is the titration of different glyceraldehyde-3-phosphate dehydrogenases and alcohol dehydrogenase with NAD^+. The researchers followed a mass spectrometry-based approach to directly determine only from a single ESI-MS spectrum all species with and without coenzyme present in equilibrium in solution, their relative abundance and the cooperativity. Their results were in agreement with the cooperative effect as measured by fluorescence studies, calorimetry and UV spectroscopy.

McCammon *et al.*[104] have probed, in another elegant study, the cooperativity in the human tetrameric transthyretin, a transporter of thyroxin hormone and retinol. Transthyretin, when misfolded or singly mutated, is believed to be involved in the amyloid fibrils formation process of several illnesses such as Alzheimer's disease, type II diabetes and the transmissible spongiform encephalopathies and the tetrameric transthyretin complex dissociation is expected to lead to amyloidosis[105].

It was shown by native mass spectrometry that thyroxine and the probed synthetic ligands were subject to different cooperative effects among which a negative cooperativity for thyroxine

binding. Similarly, Apiyo & Wittunng-Stafshede[9,106] studied unfolding of both holo- and apoforms of flavodoxin from *Desolvovibrio desulfuricans*. From this work it was concluded that cofactor binding to the unfolded state alters the kinetic pathway and speeds up the folding reaction, while it does not influence the GuHCl-induced unfolding process. However, Bollen et al.[107] showed later that not only the FMN influences the unfolding rate, as apo and holoflavodoxin unfold at significantly different denaturant concentration, but also that FMN does not bind to unfolded apoflavodoxin and does not increase the rate of the folding process. Furthermore, the two homologous proteins, serum amyloid A protein (SAP) and C-reactive protein (CRP) are pentameric proteins in solution[108]. Addition of a physiological quantity of Ca^{2+} to SAP induces protein decamers and higher order oligomers up to 30-mers. When mixed *in vitro*, SAP and CRP form heterodecamers consisting of two pentamers of each enzyme but addition of Ca^{2+} prevents heterooligomerization suggesting transient or minimal *in vivo* complexation of the two pentamers.

E) Flavoproteins studied in this project

In this section are presented the four intact flavoproteins investigated by native nano-ESI-MS. All proteins described in this work are oxidoreductase flavoenzymes. To date, only few studies (12, from which 8 in from group) report on the characterization of flavoproteins by native ESI-MS tools. **Table I** gives an overview of the available ESI-MS data on intact flavoproteins.

1–*para*-Hydroxybenzoate hydroxylase

para-Hydroxybenzoate hydroxylase (PHBH) is one of the numerous flavoproteins classified as oxygenases; that is, it incorporates one atom of molecular oxygen into its substrate. All oxygenases contain a cofactor, however, the identity of the cofactor varies. PHBH from *Pseudomonas fluorescens* is a flavin-containing monooxygenase, which uses NADPH as an external reducing agent to provide electrons[109,110]. It is the archetype of flavin-containing aromatic monooxygenases and the first from which a crystal structure was determined[111] (**Fig. 5A**). The enzyme aerobically degrades aromatic compounds derived either from natural lignin biodegradation[112,113] or environment pollution[114-116]. It catalyzes the convertion of 4-hydroxybenzoate into 3,4-dihydroxybenzoate, an intermediate step in the degradation of aromatic compounds by soil bacteria[117,118]. The protein is a homodimer[119] of about 90 kDa with each 45 kDa subunit containing a tightly bound noncovalent FAD cofactor[111]. Each monomer contains an active site cavity made entirely from residues of that monomer. The NADPH coenzyme interacts only weakly with the protein and there is no identifiable pyridine nucleotide-binding domain[120]. Only very recently an X-ray structure of a PHBH mutant (R222Q) was solved with the pyridine nucleotide bound to the protein[121].

Table I. Flavoproteins studied by native mass spectrometry.

Enzyme	Source Organism	Noncovalent Flavin Cofactor[a]	Oligomeric State	Oligomer MW[c] (Da)	Reference
Vanillyl alcohol oxidase **VAO**	*Penicillium Simplicissimum*	8α-(N^3-His) FAD[b]	**Octamer**	508 543	[91], [100]
apo-His61Thr VAO	*Penicillium Simplicissimum*	FAD	**Dimer**	127 121	[91]
holo-His61Thr VAO	*Penicillium Simplicissimum*	FAD	**Octamer**	506 809	[91]
Electron transferring flavoprotein **hETF**	*Human*	FAD	***α*,*β*-Dimer**	62 037	[122], [123]
Electron transferring flavoprotein **pETF**	*Pig liver*	FAD	***α*,*β*-Dimer**	61 821	[122]
p-hydroxybenzoate hydroxylase **PHBH**	*Pseudomonas fluorescens*	FAD	**Dimer**	90 200	[40]
Glutathione amide reductase **GAR**	*Chromatium gracile*	FAD	**Dimer**	98000	[124]
Flavoprotein reductase **FprA**	*Mycobacterium tuberculosis*	FAD	**Monomer**	51 040	[125]
Glutamate synthase **GltS**	*Synechocystis sp.*	FMN	**Dimer**	322 638	[34]
Isovaleryl-CoA dehydrogenase **IVD**	*Human*	FAD	**Tetramer**	not reported	[126]
Short chain acyl-CoA dehydrogenase **SCAD**	*Human*	FAD	**Tetramer**	174 006	[126]
hETF + Dimethylglycine dehydrogenase	*Human + Pig liver*	FAD	**Dimer**	155 084	[126]
pETF + Sarcosine dehydrogenase	*Pig liver*	FAD	**Dimer**	158 858	[126]
Flavin reductase **PheA2**	*Bacillus thermoglucosidasius*	FAD	**Dimer**	35 325	[92]
4-hydroxyacetophenone monooxygenase **HAPMO**	*Pseudomonas fluorescens ACB*	FAD	**Dimer**	145 232	[43]
Arg339Ala HAPMO	*Pseudomonas fluorescens ACB*	FAD	**Dimer**	145 103	[43]
Arg440Ala HAPMO	*Pseudomonas fluorescens ACB*	FAD	**Dimer**	145 092	[43]
Flavodoxin **FldA**	*Azotobacter vinelandii*	FMN	**Monomer**	19 995	[127]

[a] except for VAO binding a covalent 8α-(N^3-His) FAD, all other cofactors are noncovalently bound to the proteins. [b] covalent link. [c] MW: Molecular weight.

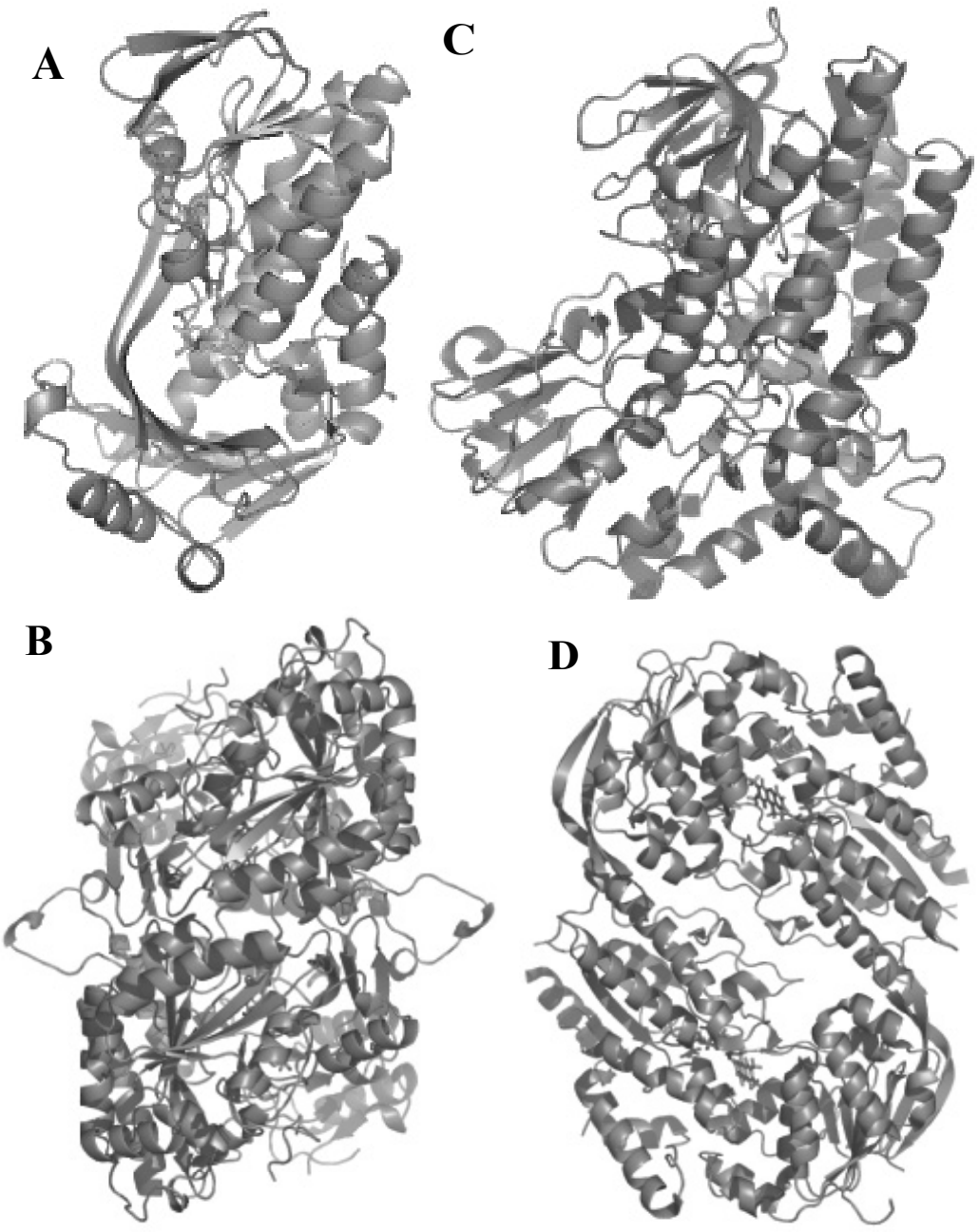

Figure 5. Crystallographic models of **A**, monomeric PHBH, **B**, dimeric VAO, **C**, monomeric PAMO (HAPMO homolog) and **D**, dimeric FprA.

2– Vanillyl Alcohol Oxidase

Vanillyl alcohol oxidase (VAO) was initially isolated from the ascomycete *Penicillium simplicissimum*[128]. The enzyme is an intracellular FAD-dependent aromatic alcohol oxidase performing the conversion of vanillyl alcohol into vanillin using dioxygen as electron acceptor[129,130]. Unlike most flavoproteins, VAO contains a covalently bound FAD cofactor[131]. VAO is known to be active on a wide range of 4-hydroxybenzylic compounds performing oxidation, hydroxylation, oxidative demethylation, oxidative deamination and oxidative desaturation reactions[132]. The hydroxylation reactions are of particular interest as VAO hydroxylates these substrates stereospecifically[133,134]. In solution VAO is in equilibrium between the dimeric (130 kDa) and octameric form (520 kDa), the octamer being the most abundant species[135]. However, urea unfolding shifts the equilibrium towards an active dimer and mercuration induces oligomeric changes in favor of the dimer[135,136]. Native ESI-MS on VAO has revealed that the stability of the VAO octamer is dependent on the pH but not on the ionic strength. When decreasing the pH from 7.7 to 5.1 the octamer is nearly completely converted into dimer (**Fig. 6**). These data reflect known solution-phase properties[135]. Mattevi *et al.*[131] solved the crystal structure of VAO (**Fig. 5B**) confirming FAD tethering to the His422 of each monomeric subunit. Sequence homology alignments and crystal structure comparison with homologous proteins have shown that VAO belongs to a novel widespread family of oxidoreductases sharing a conserved FAD binding domain[130]. Interestingly in about 35% of the flavoproteins found in this family a conserved histidine is found, which is demonstrated or predicted to be flavinylated.

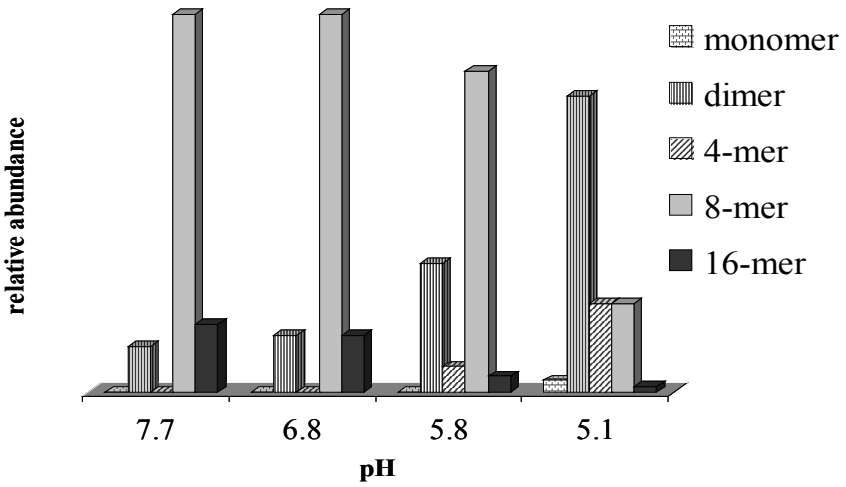

Figure 6. Bar representation of the detected abundance of the electrosprayed oligomeric protein assembly ions as a function of the pH [Adapted with permission from *Ref.*[100]].

3– 4-Hydroxyacetophenone monooxygenase

4-Hydroxyacetophenone monooxygenase (HAPMO) is a Baeyer-Villiger monooxygenase (BVMO), which converts 4-hydroxyacetophenone into 4-hydroxyphenyl acetate[137]. BVMOs oxygenate substrates through a Baeyer-Villiger reaction, thus introduce an oxygen atom between, for example, an aromatic ring and a ketone group. HAPMO is a so-called type I BVMO. These enzymes contain FAD as cofactor and use NADPH as source of electrons, while Type II BVMOs contain FMN and use NADH[138]. Type I BVMOs contain two Rossman-folds securing the binding of the ADP moieties of FAD and NADPH[139]. HAPMO from *Pseudomonas fluorescens ACB* is a 145 kDa homodimeric BVMO interacting noncovalently with one FAD per monomer. This enzyme is able to convert a wide range of aromatic ketones into the corresponding esters or lactones and, in the absence of a suitable substrate, the enzyme can act as an NADPH-oxidase. Recently, an X-ray structure of the type I BVMO phenylacetone monooxygenase (PAMO) from the thermophilic bacterium *Thermobifida fusca* has become available[140] (**Fig. 5C**). This enzyme has 30% sequence identity with HAPMO and is expected to be homologous from a structural point of view. PAMO exhibits a two-domain architecture resembling that of disulfide oxidoreductases[141] and is, in contrast to HAPMO, monomeric. It is thought that the N-terminal domain of HAPMO, which is not present in PAMO, is involved in determining the quaternary structure of the enzyme[137].

4– Flavoprotein oxidoreductase FprA

FprA from *Mycobacterium tuberculosis* is a putative microbial flavoprotein oxidoreductase. A few years ago, the genome of a virulent laboratory strain of *M. tuberculosis* has been completely sequenced[142]. In this strain there are no genes encoding enzymes from ferredoxin-NADP reductases family, electron relays between redox systems[143]. However, the genome revealed a gene sequence, *fprA*, encoding a putative flavoprotein oxidoreductase FprA[142]. The *fprA* gene has been cloned and overexpressed in *Escherichia coli*[125,144]. FprA has been found to tightly but noncovalently interact with FAD and to use NADPH or NADH to reduce ferredoxins and cytochrome *c*[144]. It is thought that FprA is involved in iron metabolism and/or electron transfer to cytochrome P450 systems. Recently, the X-ray structure of FprA in complex with $NADP^+$ has been determined at atomic resolution[125] (**Fig. 5D**). Although the crystallographic model suggests that FprA is a dimer, size-exclusion chromatography data have shown that FprA is a monomeric protein[144] and ESI-MS has confirmed that the enzyme is a 49.5 kDa monomer. The overall structure of FprA is very similar to proteins belonging to the family of glutathione reductase[145].

F) Outline of this thesis

The research reported in this thesis focuses on the application of native mass spectrometry methods to the analysis of noncovalent protein assemblies. This relatively new structural biology tool provides information about protein quaternary structures, stoichiometries, ligand and cofactor binding and stability of protein assemblies. These data are often complementary to the data obtained by established structural biology techniques such as X-ray crystallography, NMR, small-angle X-ray scattering and electron microscopy. In this work were studied oligomerization behavior, cofactor binding and cooperativity effects, protein stability and cofactor modifications of four flavoproteins by (native) ESI-MS, with the aim to reveal their structure-function relationships of these proteins.

Chapter 2 focuses on the importance of the mass spectrometry parameters to successfully detect noncovalent high molecular weight assemblies. High-pressure optimization and fine voltage tuning are prerequisites for the efficient transmission and analysis of large protein ions. To illustrate this phenomenon, the two flavoproteins PHBH and VAO were studied under native conditions by nano-ESI-MS.

In **Chapter 3**, we have investigated the cooperative effect of FAD cofactor binding and protein oligomerization by native nano-ESI-MS. The apoform of VAO H61T mutant is dimeric. Upon the noncovalent binding of FAD octamerization of the protein is induced strongly suggesting a cooperative effect of FAD binding and octamerization.

Chapter 4 shows that ESI-MS is a highly valuable technique for the study of enzyme action mechanisms. The interactions of reduced and oxidized pyridine nucleotide with HAPMO were studied by native nano-ESI-MS. The results showed that the pyridine nucleotide remains bound to the enzyme during the complete catalytic cycle. Thermal inactivation and size-exclusion chromatography data showed that this continued interaction stabilizes the enzyme to a great extent.

The input of mass spectrometry to protein X-ray crystallography data is illustrated in **Chapter 5**. Tandem ESI-MS experiments established that the flavoenzyme FprA can enzymatically modify $NADP^+$ into NADPO. This NADPH derivative had never been identified before.

Finally, the results described in this thesis are summarized and discussed in **Chapter 6**.

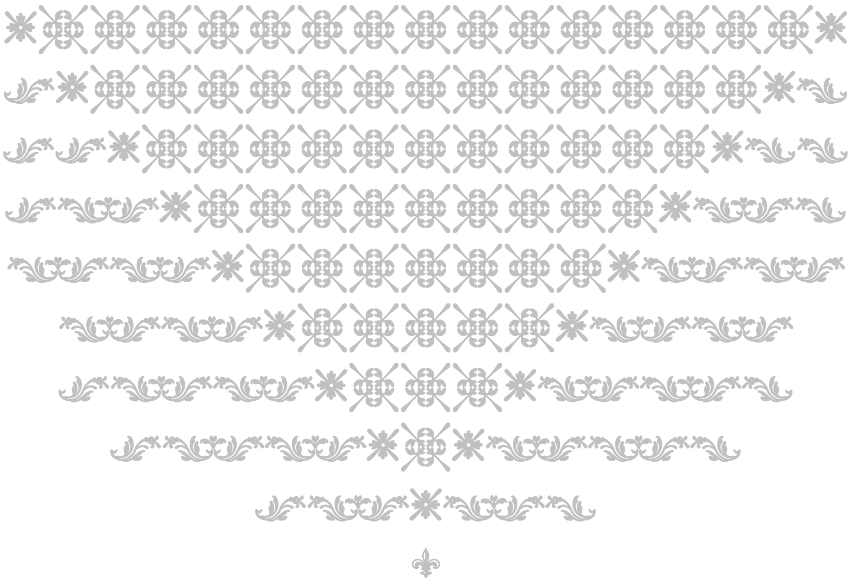

Chapter 2

The effect of the source pressure on the abundance of ions of noncovalent protein assemblies in an electrospray ionization orthogonal time-of-flight instrument.

« *M. Warner:* *What does your work enable researchers to do they weren't able to do before?*

J. Fenn: ***Well, in homely terms, we learned how to make elephants fly, as it were.***»

JOHN B. FENN

Professor Emeritus of Chemical Engineering
Recipient of the 2002 Nobel Prize in Chemistry

Nora Tahallah, Martijn W Pinkse
Claudia S Maier, Albert JR Heck

Adapted from *Rapid Commun Mass Spectrom.* 2001;15(8):596-601

Abstract

The effect of elevating the pressure in the interface region of an electrospray ionization orthogonal time-of-flight mass spectrometer on the ion intensity of different noncovalent protein assemblies has been investigated. Elevating the pressure in the interface region generally led to an enhanced detection of high m/z ions. The optimum pressure was found to be dependent on the m/z value of the ions. This pressure effect should be carefully addressed when relating ion abundance in the mass spectra to solution phase abundance of noncovalent protein assemblies.

Electrospray ionization (ESI)[46] allows the phase transfer from solution- into gas-phase of biomacromolecular systems, which makes them amendable for mass spectrometric analysis[146,147]. This relatively gentle phase transfer from the solution- to the gas-phase has enabled the intact detection by mass spectrometry of larger multi-protein assemblies including intact ribosomes, small viruses and large functional oligomers[39,100,148-154]. Several recent examples have revealed that biologically relevant parameters concerning these multi-protein complexes may nowadays be investigated by mass spectrometry including protein complex topology, protein folding, protein-protein interactions and stability of protein assemblies[33,37,155-157].

In this report we describe the mass spectrometry analysis of the assemblies of two flavoproteins, *p*-hydroxybenzoate hydroxylase and vanillyl alcohol oxidase, using an electrospray ionization orthogonal time-of-flight instrument. We show that these high molecular weight noncovalent protein complexes can only be studied by significantly raising the pressures in the ESI source region. It was found that optimal pressure conditions are different for different ionic species. We compare our results with relevant previously published data on this phenomenon and conclude that this pressure effect should be carefully addressed when relating ion abundance in mass spectra to solution-phase abundance of noncovalent protein assemblies.

Experimental

Instrument description. Electrospray ionization mass spectra were acquired using a commercially available Micromass LC-T electrospray ionization orthogonal time-of-flight mass spectrometer. A schematic picture of the instrument is shown in **Figure 7**.

Briefly, ions are produced and introduced into the mass spectrometer via the Z-spray nanospray ionization source using an initial skimmer with a 0.4 mm aperture. The ions pass two independently pumped hexapole RF-lenses. After entering the time-of-flight (ToF) analyzer region the ion beam is focused by several lenses. The pusher then pulses a section of the beam towards the reflectron. Three turbomolecular pumps provide independent pumping for the two RF-hexapole regions and the ToF-analyzer. Source pumping and turbomolecular backing are provided by a direct drive rotary pump. Three different gauges may be used to read out the pressure in the different regions of the instrument. A first Pirani gauge (G1) is located in the line between the source and the rotary pump. A specifically fitted second Pirani gauge reads out the pressure in the first RF-hexapole (G2) and finally an active inverted magnetron gauge monitors the pressure in the ToF-analyzer. Using standard conditions, the measured pressures in the different regions for G1,

G2 and G3 are 2.0, 2.5 10^{-3} and 5.2 10^{-7} mbar, respectively. In the experiments described below, the pressure in the interface region was varied by reducing the pumping efficiency of the rotary pump by adjusting a specifically fitted speedi-valve (see **Fig. 7**).

Nano-electrospray needles were made from borosilicate glass capillaries (Kwik-Fil™, World precision Instruments Inc., Sarasota, FL, USA) on a P-97 puller (Sutter Instrument Co., Novato, CA, USA). The needles were coated with a thin gold layer (~500 Å) using an Edwards Scancoat six Pinrani 501 sputter coater (Edwards High Vacuum International, Crawley, UK).

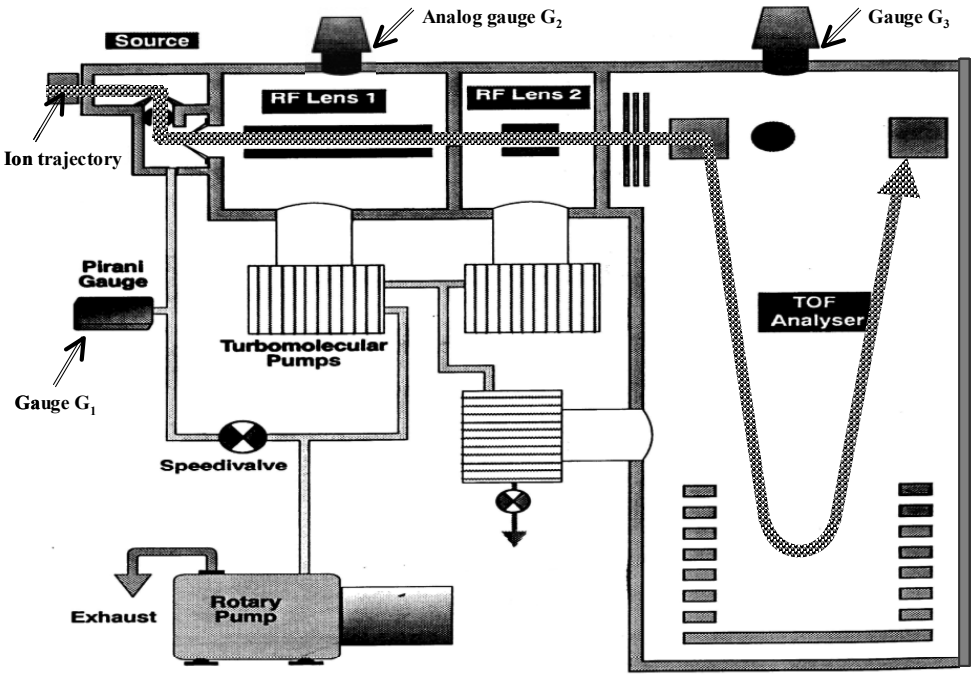

Figure 7. Schematic overview of the LC-T orthogonal electrospray ionization time-of-flight mass spectrometer. The three different gauges used to monitor the pressures in the instrument are indicated by G1, G2 and G3.

Materials. The C116S mutant of PHBH was expressed and isolated as described previously[113]. The expression and purification of the H61T mutant of VAO was performed as described before[88,101]. Complete removal of FAD could be readily achieved by gel permeation of holo-H61T. Absorption measurements at 439 nm verified that the FAD content in the apoprotein was less than 0.1%. FAD sodium salt was obtained from Sigma (Zwijndrecht, The Netherlands).

Results

ESI mass spectra of the noncovalent dimer of PHBH from Pseudomonas fluorescens. 4-hydroxybenzoate hydroxylase (PHBH – EC 1.14.13.2) is considered to be the archetype of flavoprotein monooxygenases, a model enzyme to study the redesign of flavoprotein aromatic hydroxylases into efficient dehalogenases[158]. This enzyme is a noncovalent flavin adenine dinucleotide (FAD)-dependent monooxygenase catalyzing the conversion of 4-hydroxybenzoate into 3,4-dihydroxybenzoate. The protein is active as a homodimer with an estimated dissociation constant of less than 0.25 μM and possibly even in the nanomolar range[159]. Each monomeric subunit is built up of 394 amino acids and functions catalytically independently.

The C116S mutant, which is more resistant towards oxidation artifacts than the wild type, was used in the present experiments and has a monomeric molecular weight of 44 305 Da. A solution of 1 μM C116S PHBH (monomer concentration) dissolved in aqueous 50 mM ammonium acetate, pH = 6.7 was used for the electrospray measurements. Typical spray conditions were needle voltage 1500 V and cone voltage 90 V. Using standard pressure settings, no ions could be detected. It should be noted that under standard pressure settings, ESI mass spectra could be obtained of the large denatured (*i.e.* dissolved in water/acetonitrile/formic acid) proteins PHBH and VAO whereby only ions of the monomer subunits were observed, appearing at much lower *m/z* values in the mass spectra.

The ESI spectrum, obtained at the elevated pressures of 4, 3.5 x 10^{-3} and 6 x 10^{-7} mbar (measured by G1, G2 and G3, respectively), is shown in **Figure 8A**. Four different ion signals were observed corresponding to the 16+ to 19+ charged molecular ions for the noncovalent dimer of PHBH (molecular mass of ~90 kDa). The exclusive observation of the noncovalent dimer was expected as PHBH has a high dimerization constant at pH = 7. Using a single nanospray needle and leaving all experimental parameters, except the pressure, constant the total ion current was monitored. In this run only the four different ions mentioned above were detected. **Figure 8B** shows the total ion current obtained for the 1 μM PHBH solution versus the pressure in the interface region. A strong reproducible variation in ion intensity was observed as a function of the pressure in the interface region. **Figure 8C** shows a plot of the detected total ion current versus the pressure. For the detection of the ions originating from the dimeric PHBH species an optimum in ion intensity was found at the operating pressures of 4, 3.5 x 10^{-3} and 6 x 10^{-7} mbar monitored by G1, G2 and G3, respectively. However, at higher pressures, the measured ion signals broaden significantly. An optimum in peak resolution, albeit not in peak intensity, was observed at pressures slightly below the values quoted above.

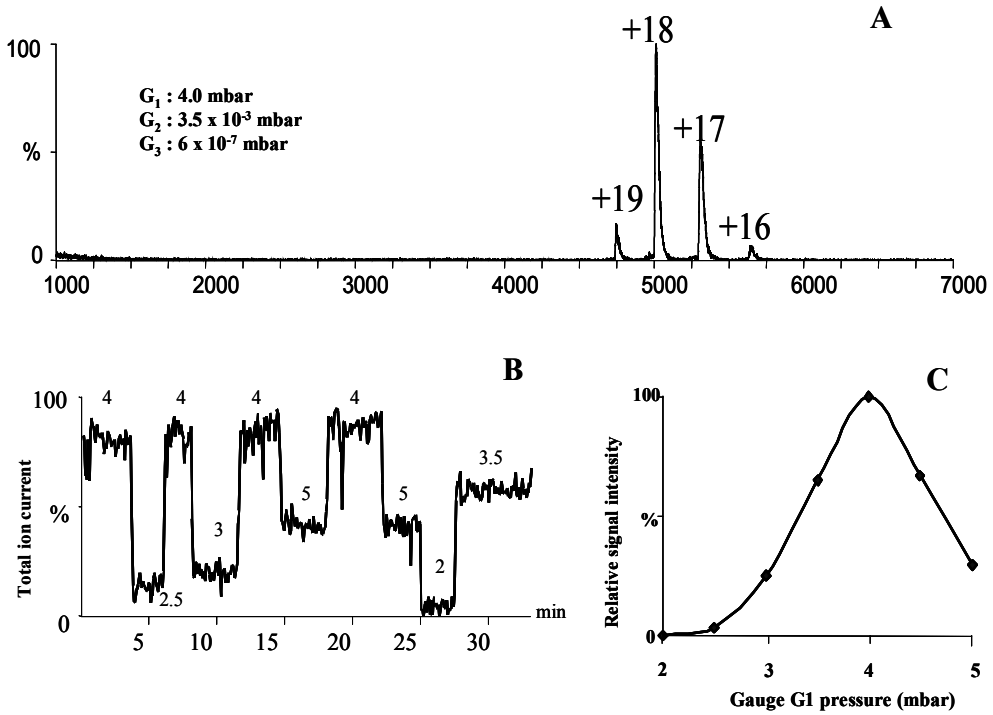

Figure 8. A, Electrospray ionization mass spectrum of PHBH sprayed from a 50 mM ammonium acetate solution, pH = 6.7, at a PHBH monomer concentration of 1 μM. The pressure read-outs for G1, G2 and G3 were 4, 3.5 x 10^{-3} and 6 x 10^{-7} mbar, respectively. **B**, Total ion current of the ions observed in the spectrum of PHBH as a function of the pressure in the electrospray source interface as determined in the rf-only region. **C**, Plot of the total ion current versus the pressure in the electrospray source interface as determined in the rf-only region, revealing a maximum at a G1 pressure of 4 mbar (G2 ≡ 3.5 x 10^{-3} and G3 ≡ 6 x 10^{-7} mbar).

ESI mass spectra of protein assemblies of VAO from Penicillium simplicissimum. Wild type vanillyl alcohol oxidase (VAO – EC 1.1.3.38) catalyzes the oxidation of a wide variety of phenolic compounds, using 8α-(N^3-histidyl)-FAD as a covalently bound prosthetic group[128,133,160]. VAO is the prototype of a novel family of widely distributed oxidoreductases sharing a conserved FAD-binding domain[130,131]. The VAO monomer is built up of 560 amino acids and exhibits a calculated average mass of 63 691 Da including the covalently linked FAD[161].

Previously, we showed that the biologically active octamer protein assembly of VAO, exhibiting a molecular mass of over 0.5 million Dalton, could be detected by mass spectrometry[100]. For the present study the H61T apomutant of vanillyl alcohol oxidase (without covalent FAD) was

selected. A solution of 5 μM apo-H61T-VAO (monomer concentration) dissolved in aqueous 50 mM ammonium acetate, pH = 6.7 was used for the electrospray experiments. Additionally, FAD was added to this sample to a concentration of ~4 μM, below the level of VAO saturation, therefore, the solution should contain some apoprotein of the H61T mutant but also some H61T-VAO tightly but noncovalently bound to FAD (the binding constant of FAD to apo-H61T-VAO is ~1.8 μM[101]). Typical spray conditions were needle voltage 1500 V and cone voltage 110 V. Again, using standard pressure conditions no ions could be detected.

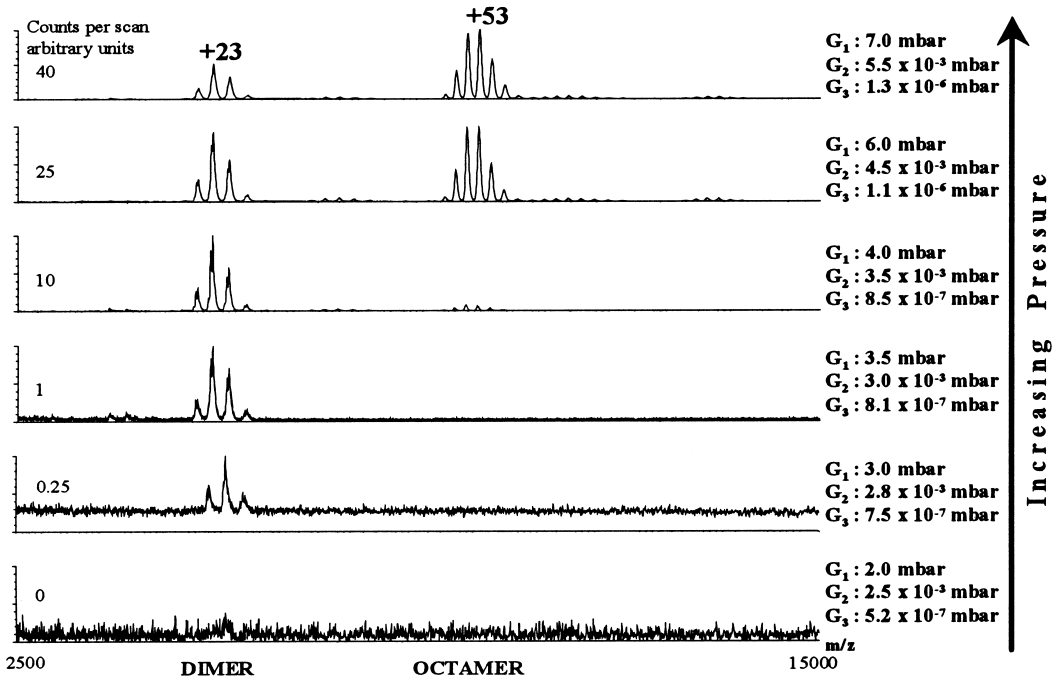

Figure 9. Electrospray ionization mass spectra of a solution containing 5 μM apo-H61T-VAO (monomer concentration) and 4 μM FAD, dissolved in 50 mM ammonium acetate, pH 6.7 measured at different source pressures. The most abundant ions originate from the dimer (*m/z* ~5 000) and the octamer (*m/z* ~10 000). The pressure read-outs for G1, G2 and G3 are given for each spectrum on the right. The number of ion counts per scan (arbitrary units) is given for each mass spectrum on the left.

Figure 9 shows nano-ESI spectra of this sample taken at various pressures with, at the bottom of **Figure 9**, the spectrum obtained under standard pressure conditions and, on the left, the number of ion counts per scan (arbitrary units) for each depicted spectrum. In the mass spectra of **Figure 9** ions are observed of different oligomeric states of the H61T-VAO. The most abundant

ions originate from the dimer (at *m/z* values of ~5 000) and the octamer (at *m/z* values of ~10 000), which are known to be the most stable solution species for this protein. The dimer has a molecular mass of ~125 kDa and the octamer of ~500 kDa. Some fine structure can be observed in the dimer region originating from the apo-H61T-VAO with 0, 1 and 2 FAD molecules bound. The fine structure for the FAD binding is most clearly observed at medium source pressures of 4, 3.5 x 10^{-3} and 6.8 x 10^{-7} mbar. At higher pressures, the ion peaks broaden as was also observed for PHBH. The exact role of the noncovalent FAD binding on the oligomerization state of the H61T-VAO will be the subject of another paper[91]. Obviously, the appearance of the spectra is significantly influenced by the variation in the pressure.

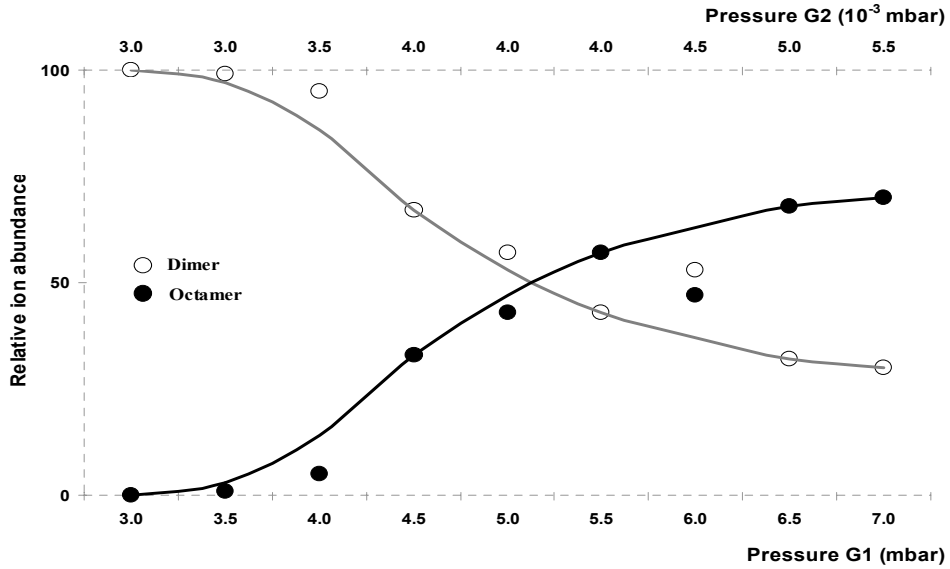

Figure 10. Relative abundance of dimer and octamer ions observed in the nano-ESI mass spectra of a solution containing 5 μM apo-H61T-VAO (monomer concentration) and 4 μM FAD, dissolved in 50 mM ammonium acetate, pH 6.7, measured at different source pressures.

It is evident that the total ion current continuously increases with increasing source pressures. More interesting is the observation that the ratio of detected dimer to octamer ions changes quite dramatically when varying the pressures. **Figure 10** shows the relative abundance of the dimer and octamer ions as detected in the ESI mass spectra versus the source pressure. Although, both the dimer and octamer ion intensities increase continuously with increasing the source pressures, the signal originating from the octamer increases more rapidly leading to the observation that the octamer ions are most abundant near the experimentally highest achievable

pressures. On the current instrument the vacuum is interlocked by the G1 gauge at a pressure of ~9.5 mbar.

Discussion and Conclusion

The phase transfer of noncovalent macromolecular complexes from solution into gas-phase is not straightforward as the formed isolated ionic complexes may suffer from several destabilizing effects such as charge repulsion, loss of hydrophobic interactions, counter ions and solvent molecules adduction. Additionally, the flight through and the detection of larger macromolecular ions exhibiting high mass-to-charge (*m/z*) ratios are in mass spectrometry generally less efficient than for smaller, lower *m/z*, ions. Coupling of a continuous electrospray ionization source with time-of-flight mass spectrometry is done most efficiently by using an orthogonal set-up[39,162,163]. As described by Krutchinsky *et al.*[39] larger ions (*e.g.* with molecular mass of several kiloDaltons) may acquire kinetic energies of 1 000 eV in the electrospray supersonic jet/declustering process, which will negatively affect the efficient orthogonal extraction into a time-of-flight region. To overcome this problem, a quadrupole or hexapole is often introduced in front of the time-of-flight mass analyzer, which can act as a collisional damping interface[39]. Elevating the pressure in this region has been shown to enhance the detection efficiency of larger noncovalent assemblies significantly[39,100,155,157]. Therefore our findings that high *m/z* ions may be detected more efficiently by increasing the pressures in the RF-hexapoles are not novel and may be explained by the collisional cooling effect described by Krutchinsky *et al.* However, in this study, we have investigated in more detail the effect the pressure in the interface region has on the abundance of different ionic protein assemblies each exhibiting different chemical properties, molecular masses and *m/z* values.

New is the finding that on the used instrument (a slightly modified Micromass LC-T) the effect the elevated source pressure has on the detection of ions varies depending on the nature (*e.g.* size, mass and charge) of the ionic species. Changing the source pressures results therefore in an *m/z* discriminative effect in the ion detection. Such an *m/z*-dependent collisional cooling effect may not be that surprising as different *m/z* ions will have different kinetic energies when entering the mass spectrometer. Ions of different *m/z* will also be decelerated differently in the high-pressure region of the RF-hexapoles as they possess different speeds (kinetic energies) and collisional cross-sections. It is not clear at present whether the observed *m/z*-dependent pressure effect is general or unique for the equipment used. We have been able to observe similar *m/z*-dependent effects on our two LC-T and on our Q-ToF-1 instruments. It should also be noted that we do not observe any significant pressure effect for ions with values below ~1500, except peak broadening at elevated pressures. For comparison, we mention that Krutchinsky *et al.* have reported data on an equimolar mixture of peptides and proteins ranging in molecular mass between

1 and 400 kDa. From the limited set of data presented, acquired on a home-built electrospray orthogonal time-of-flight instrument, it seems their instrument is possibly less hampered by the discriminative *m/z* effect reported here. The main differences, between their instrument and the presently described LC-T, are in the source region ('Z-spray' versus 'in-line spray' and variation in the pressures in the differential stages of the source region). Increasing the pressure in the source region also affects the desolvation of ions. Significant peak broadening was observed at the higher source pressures. The broadened peaks could be narrowed by increasing the cone voltage indicating that at lower cone voltages and high source pressures the desolvation was insufficient. High cone voltages may promote dissociation/fragmentation. A careful adjustment of the pressure and the cone voltage, which can be different for different protein assemblies, will lead to the best results.

Finally, a note of caution: raising the pressures in the source region of an electrospray ionization orthogonal time-of-flight instrument may affect different ionic complexes differently. Therefore, we believe that this pressure effect should be carefully addressed when relating ion abundance in mass spectra to solution-phase abundance. Using the present instrumentation, the determination of oligomerization or binding constants of large noncovalent complexes, solely from mass spectrometric data, is therefore not straightforward.

Acknowledgements

We like to thank Kees Versluis for technical assistance. We thank Willem van Berkel (Wageningen University) for help in preparation of the flavoproteins. The present work was made possible by support from the Center for Biomolecular Genetics and by the "Nederlandse Organisatie voor Wetenschappelijk Onderzoek" (NWO: Dutch NSF) grant #99508 for NT.

Chapter 3

Cofactor-dependent assembly of the flavoenzyme vanillyl alcohol oxidase.

« The reason that some portraits don't look true to life is that some models make no effort to resemble their pictures. »
SALVADOR DALI

Nora Tahallah, Robert HH van den Heuvel
Willy AM van den Berg, Claudia S Maier
Willem JH van Berkel, Albert JR Heck
Adapted from *J Biol Chem.* 2002 Sep 27;277(39):36425-32.

Abstract

The oligomerization of the flavoprotein vanillyl alcohol oxidase (VAO) and its site-directed mutant H61T was studied by mass spectrometry. Native VAO has a covalently bound FAD and forms primarily octameric assemblies of 507 kDa. H61T is purified as an FAD free apoprotein and mainly exists as a dimeric species of 126 kDa. Binding of FAD to apo-H61T rapidly restores enzyme activity and induces octamerization, although association of H61T dimers seems not to be crucial for enzyme activity. Reconstitution of H61T with the cofactor analog 5'-ADP also promotes octamerization. FMN on the other hand, interacts with apo-H61T without stimulating dimer association. These results are in line with observations made for several other flavoenzymes, which contain a Rossmann-fold. Members of the VAO flavoprotein family do not contain a Rossmann-fold, but do share two conserved loops that are responsible for binding the pyrophosphate moiety of FAD. Therefore, the observed FAD-induced oligomerization might be general for this family. We speculate that upon FAD binding, small conformational changes in the ADP-binding pocket of the dimeric VAO species are transmitted to the protein surface, promoting oligomerization.

Riboflavin (Vitamin B2) derivatives such as FAD and FMN are essential components of all living organisms serving as cofactors for numerous proteins with diverse functions ranging from electron transport, redox catalysis, oxygen activation and light emission to DNA repair[84]. For most reported flavoproteins the flavin cofactor is noncovalently bound, although ~10% of the human cellular FAD is covalently linked to enzymes like monoamine oxidase and succinate dehydrogenase[86,90]. Many noncovalent flavoproteins can be reversibly dissociated into their constituents the apoprotein and flavin prosthetic group[164-166]. Reconstitution of the holoprotein with either artificial[84,167,168], enzymatically modified[169] or isotopically enriched flavin analogues[164,166,170] then allows to gain insight into the role of the protein in redox catalysis.

For several flavoenzymes, binding of the FAD cofactor induces subunit association and improves the resistance of the protein to thermal and chemical denaturation. For glucose oxidase[171], *D*-amino-acid oxidase[172] and lipoamide dehydrogenase[173-175], it was shown that rapid FAD binding to the monomeric apoprotein is followed by relatively slow dimerization and regain of catalytic activity. For bacterial butyryl-CoA dehydrogenase, on the other hand, it was revealed that optimal reconstitution of tetrameric holoenzyme from dimeric apoenzyme and FAD requires the presence of CoA ligands[176].

Little is known about the role of flavin binding in the assembly of covalent flavoenzymes[177]. Covalent flavinylation mostly occurs via a histidine residue, but enzymes with cysteinyl-flavin, tyrosyl-flavin and threonyl-flavin have been described as well[90]. Vanillyl alcohol oxidase (VAO) from *Penicillium simplicissimum* is a covalent flavoprotein whereby the FAD is bound via a so-called 8α-(N^3-histidyl)-FAD linkage[131]. VAO is active with a wide variety of phenolic compounds[132,133] but the biological function of the enzyme is unclear. Upon growth on 4-methoxymethylphenol, VAO is abundantly expressed in the fungus, which might suggest that the main physiological role of the enzyme is the conversion of this compound into 4-hydroxybenzaldehyde[129]. VAO is primarily a homooctamer of ~0.5 million Da[128,135] with each monomer subunit being composed of two domains[131]. The larger domain binds the FAD in an extended conformation whereas the isoalloxazine ring of the flavin is covalently attached to the His422 of the cap domain[131,161]. Sequence comparisons have revealed that VAO belongs to a novel class of widely distributed oxidoreductases sharing a conserved FAD-binding domain[130].

The functional role of the covalent protein-flavin linkage in VAO has been addressed recently[88] by site-directed mutagenesis. From the properties of His-422 mutants, evidence was obtained that the covalent linkage between His-422 of the apoprotein and FAD is important for

VAO catalysis by raising the redox potential of the flavin. All three mutants H422A, H422C and H422T tightly bound the FAD in a noncovalent mode but the change in redox properties resulted in a marked decrease in the rate of substrate-mediated flavin reduction. The mechanism of flavinylation of VAO was addressed by creation of the design point mutation His-61→Thr[101]. In this mutant enzyme, the covalent linkage between His-422 and the flavin is not formed whereas the enzyme is still able to bind FAD and perform catalysis. Structural analysis of both apo- and holoforms of H61T indicated that binding of FAD to the apoprotein does not induce major structural rearrangements suggesting that covalent flavinylation is an autocatalytical process in which His-61 is crucially involved in activating His-422. As for the wild type enzyme the apoform of H61T is present as a homooctamer in the crystalline state[101]. However, preliminary gel-filtration studies have indicated that in solution the mutant enzyme may easily dissociate into dimers.

In this report we use primarily mass spectrometry to probe the influence of cofactor binding on the oligomerization state of VAO. With the development of new ionization techniques such as matrix-assisted laser desorption ionization[44] and electrospray ionization[46] and the coupling of these to time-of-flight analyzers, the detectable mass range of macromolecular systems by mass spectrometry has been enhanced extensively[146,147]. Moreover, the relatively gentle phase transfer from solution- to gas-phase, realized especially by electrospray ionization, has allowed the intact detection by mass spectrometry of larger multiprotein assemblies[148,150-152]. Several recent examples[37,73,156,178-180] have revealed that biologically relevant parameters concerning multiprotein assemblies may now be investigated by mass spectrometry and examples include protein complex topology, protein-ligand and protein-protein binding constants and protein complex stability. Biomolecular mass spectrometry combines mass resolution, high sensitivity and an enlarged mass-to-charge (*m/z*) range and allows the identification of multiple species in a mixture.

In an earlier report[100], we showed that the wild type VAO multimer is amenable to detailed investigation by nano-electrospray ionization-mass spectrometry. Here we compare wild type VAO and the single point mutant H61T. In the mutant enzyme, the FAD cofactor is no longer covalently bound and the protein can be prepared in its FAD-free apoform. The apoprotein has a moderate affinity for FAD and 5'-ADP[101] providing the unique opportunity to address by mass spectrometry the role of cofactor binding in the supramolecular assembly of a covalent flavoprotein.

Experimental

Chemicals. FAD, FMN and 5'-ADP were obtained from Sigma and used without further purification. Ion-exchange and gel-filtration chromatography resins were from Amersham

Biosciences. CHT ceramic hydroxyapatite was from BioRad. All other chemicals were from Merck and the purest grade available.

Proteins. Wild type VAO[130,161] and mutant H61T VAO[101] were expressed and purified as described previously. Proteins stored in 100 mM potassium phosphate, pH 7.2, were desalted using ultrafiltration units (ultrafree-0.5 Centrifugal Filter Device, Millipore Corporation, Bedford, ENG) with a cut-off of 5 000 Da.

Preparation of apo-VAO. The apoform of H61T VAO was prepared by hydroxyapatite chromatography. 4 mg of H61T VAO in 200 mM potassium phosphate buffer containing 200 μM FAD was applied onto a 1-ml hydroxyapatite column pre-equilibrated in 200 mM phosphate buffer, pH 7.2. Protein-bound FAD was removed by washing the column with 10 column volumes of starting buffer. The apoprotein was eluted from the column with 15 column volumes of 600 mM phosphate buffer, pH 7.2 and concentrated to 4 mg/ml by ultrafiltration (Ultrafree 4, 30 kDa). The FAD content of the apoprotein was < 0.1% as evidenced by absorption spectral analysis. The molar absorption coefficient of apo-H61T VAO was determined at 280 nm by comparison of the absorbance of apoenzyme, holoenzyme and free FAD in 50 mM ammonium acetate, pH 6.8.

Analytical methods. Absorption spectra were recorded on a Hewlett Packard HP 8453 diode array spectrophotometer. Fluorescence spectra were recorded on a Varian Eclipse instrument. All spectrometers were equipped with thermostat cell holders. All spectra were obtained at 25 °C.

Reconstitution kinetics. Reconstitution of holo-H61T from apo-H61T and FAD was performed at 0 and 25°C in 50 mM ammonium acetate, pH 6.8. The apoenzyme and FAD concentrations were 3 and 100 μM, respectively. At time intervals, the reconstitution reaction was monitored by adding an aliquot of the incubation mixture into the assay mixture. The activity of H61T was determined by measuring absorption changes at 296 nm (ε_{296} = 5.5 $mM^{-1}.cm^{-1}$) due to the hydroxylation of eugenol into coniferyl alcohol at pH 7.5[181].

Fluorescence studies. Protein tryptophan fluorescence emission spectra were recorded from 310 to 560 nm using an excitation wavelength of 295 nm. A spectral bandwidth of 5 nm was used in all fluorescence experiments. Binding of FAD to apo-H61T VAO was monitored by the decrease of protein fluorescence at 340 nm. In the titration studies, after each addition, the sample was incubated for 4 min in the dark before measuring the emission intensity.

Nano-electrospray Mass Spectrometry. For nano-electrospray mass spectrometry experiments, enzyme samples were prepared in aqueous 50 mM ammonium acetate solutions. For

measurements under denaturing conditions, these protein solutions were 1:1 diluted in acetonitrile, containing 1% formic acid. VAO samples were introduced into an LC-T nano-electrospray ionization orthogonal time-of-flight mass spectrometer (Micromass, Manchester, UK) operating in positive ion mode. Source pressure conditions in the LC-T mass spectrometer and nano-electrospray voltages were set for optimal transmission of the larger multimer protein assemblies as described previously[40]. Spraying conditions are as follows: needle voltages 1450-1650 V, cone voltages 45-100 V and source temperature 85°C. In the experiments measuring the protein assemblies, the pressure in the interface region was adjusted by reducing the pumping capacity of the rotary pump by closing the valve. Borosilicate glass capillaries (Kwik-Fil™, World Precision Instruments Inc., Sarasota, FL) were used on a P-97 puller (Sutter Instrument Co., Novato, CA) to prepare the nano-electrospray needles. They were subsequently coated with a thin gold layer (~500 Å) using an Edwards Scancoat six Pirani 501 sputter coater (Edwards High Vacuum International, Crawley, UK).

Size-exclusion Chromatography. Size-exclusion chromatography was performed with a Superdex-200 HR 10/30 column connected to an Åkta chromatography system, essentially as described previously[135]. All experiments were performed in 50 mM ammonium acetate, pH 6.8. 3 μM of apo-H61T (or wild type VAO) were incubated at room temperature in the absence or presence of cofactor analogs (30 μM of FAD, 5'-ADP or FMN). At different time intervals, 200 μl aliquots from the incubation mixtures were injected on the column and eluted at a flow rate of 0.7 ml/min. Detection was at 220 nm. Relative abundance of the dimer and octamer species was calculated from the peak areas. To derive the relative abundance of the octamer and dimer, these peak areas were scaled (corrected for the number of subunits) by dividing the area of the octamer by 8 and that of the dimer by 2.

Results

Preparation of apo-VAO. The noncovalent and relatively weak binding of FAD to H61T VAO[101] allowed a novel gentle procedure of preparing the apoenzyme. By binding the H61T mutant to hydroxyapatite, the FAD could easily and quantitatively be removed by washing the column with 200 mM potassium phosphate buffer, pH 7.5. Subsequently, the apoenzyme was stripped from the column by increasing the buffer concentration to 600 mM. This method of apoenzyme preparation is very simple, can be performed at small and large scale and gives almost quantitative yields. The absorption spectrum of apo-H61T in 50 mM ammonium acetate, pH 6.8, showed a maximum at 280 nm and no significant absorbance in the visible region revealing that the FAD is indeed absent (**Fig. 11A**). The molar absorption coefficient at 280 nm was ε_{280}=140 ± 1 $mM^{-1}.cm^{-1}$. For comparison the absorption spectrum of wild type VAO in 50 mM ammonium acetate, pH 6.8 is also shown in **Figure 11A**.

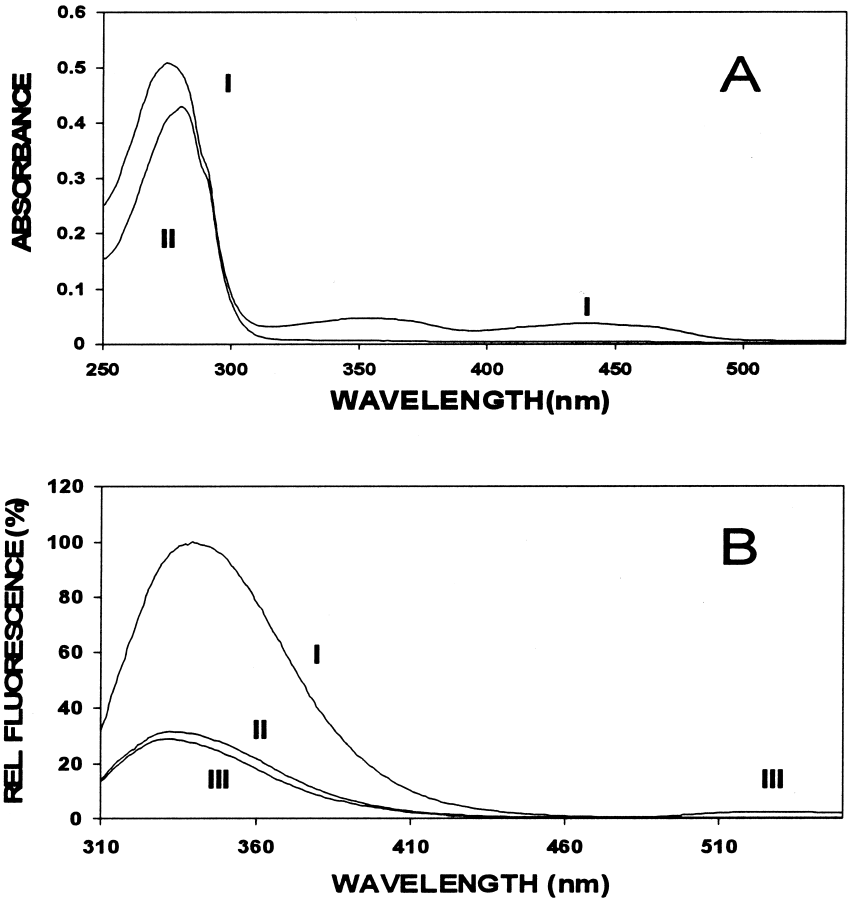

Figure 11. Absorption and tryptophan fluorescence properties of wild type VAO and apo-H61 VAO in 50 mM ammonium acetate, pH 6.8. **A**, absorption spectrum of 3 μM wild type VAO (I) and apo-H61T (II). **B**, tryptophan fluorescence emission spectra of 3 μM apo-H61T (I), wild type VAO (II) and apo-H61T in presence of 30 μM FAD (III).

Reconstitution studies. In an earlier study, the dissociation constant of the complex between apo-H61T VAO and FAD in 50 mM phosphate buffer, pH 7.5, was estimated to be 1.8 μM[101]. In view of the mass spectrometry studies described below, it was of interest to obtain insight in the kinetic and thermodynamic properties of the apoenzyme-FAD complex in 50 mM ammonium acetate, pH 6.8. Reconstitution of apo-H61T by FAD as monitored by activity measurements was a relatively fast process. When 3 μM apoenzyme were incubated at 25°C with 100 μM FAD, the enzyme activity reached a maximum within 1 min. When excess of FAD (50

μM) was added to the assay mixture, the maximum activity approximated the activity of H61T holoenzyme[101]. At 0°C, the reconstitution reaction was slower and took about 5 min to complete. Again, under these conditions the activity reached the level of the H61T holoenzyme when the assay was performed in the presence of 50 μM FAD. **Figure 11B** shows the tryptophan fluorescence emission spectrum of apo-H61T upon excitation at 295 nm. The relative quantum yield of the tryptophan fluorescence of apo-H61T is much higher than that of wild type VAO and holo-H61T (**Fig. 11B**). Furthermore, the maximum of fluorescence emission of apo-H61T VAO is at 340 nm whereas the emission maxima of wild type VAO and holo-H61T are centered around 325 nm. In line with the data from activity experiments, binding of FAD to apo-H61T was a relatively fast process. When 3 μM apo-H61T were incubated at 25°C with a 10-fold excess of FAD, the fluorescence emission at 340 nm was quenched by about 80% and reached a constant value within 30 s. At 0°C, the same level of fluorescence quenching was observed but the reaction took approximately 5 min to complete.

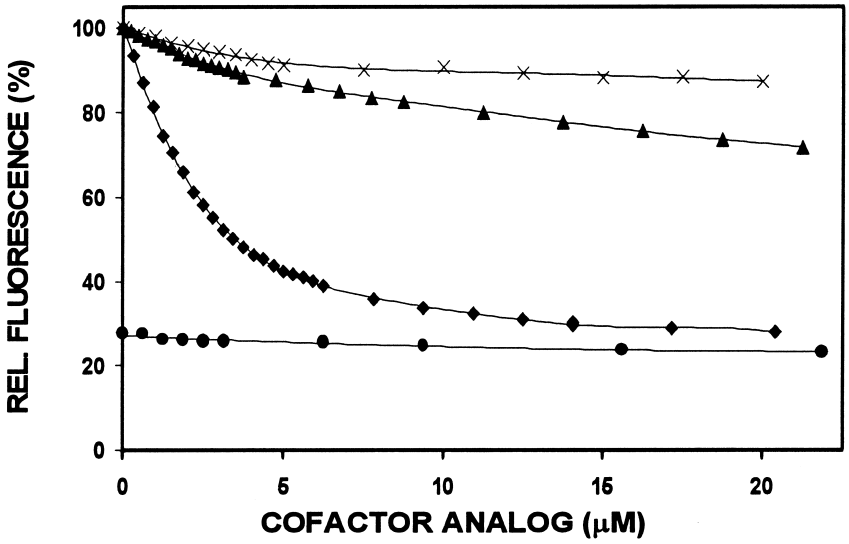

Figure 12. Tryptophan fluorescence emission of apo-H61T VAO with cofactor analogs was measured in arbitrary units. Upon the addition of FAD to 3 μM apo-H61T in 50 mM ammonium acetate, pH 6.8 (♦) fluorescence emission was observed at 340 nm upon excitation at 295 nm. Titrations with FMN (▲) and 5'-ADP (X) are also presented. As a control, wild type VAO enzyme was titrated with FAD (●).

The dissociation constant of the complex apo-H61T-FAD was determined by fluorescence titration experiments. Titration of 3 μM apo-H61T by FAD resulted in a strong decrease of tryptophan fluorescence emission at 340 nm (**Fig. 12**). From the titration data, a dissociation

constant K_d = 0.38 ± 0.04 μM and a relative quantum yield Q = 20 ± 2% with respect to apo-H61T were estimated for the apoenzyme-FAD complex. This is slightly tighter binding than previously reported[101], which might be due to the different buffer system. Titration of apo-H61T with 5'-ADP did not result in a strong fluorescence decrease (**Fig. 12**). Nevertheless, the fluorescence quenching data support an earlier conclusion[101] that 5'-ADP binds to apo-H61T with a similar affinity as FAD. When apo-H61T was titrated with FMN, a clear change in protein fluorescence emission was observed (**Fig. 12**). However, the fluorescence quenching did not reach a constant value suggesting that FMN binds far more weakly to apo-H61T than FAD and 5'-ADP.

Exact mass determination of wild type VAO and H61T. Initially, to check the quality of the recombinant VAO proteins the molecular masses of the protein monomers were determined. To that end, the protein of interest was dissolved in a denaturing acidic solution (50% acetonitrile, 1% formic acid). Under these highly acidic conditions, quaternary structures are most often disassembled; proteins tend to denature and the relatively highly charged ions originating from the protein monomers are observed in the mass spectra. From these nano-electrospray mass spectra the mass of the protein monomer can be assessed. From such data the average molecular weight of the wild type VAO monomer was determined to be 63 561 ± 3 Da. Translation of the gene-sequence published by Benen *et al.*[161] leads to a protein mass of 62 915 Da, excluding the covalently bound FAD. When including the mass of FAD, the measured and expected masses are in agreement when it is assumed that the N-terminal methionine has been post-translationally removed. The average molecular mass of the apoform of the VAO H61T variant was determined to be 62 742 ± 2 Da. The experimental mass difference between the wild type and the apo-VAO H61T mutant is as expected when the single mutation and the covalently bound FAD are taken into account and, again, assuming that the initiator methionine is processed in the apo-VAO H61T mutant. Analysis of tryptic digests by matrix-assisted laser desorption ionization time-of-flight proved indeed the truncation of the methionine in both the wild type and the apo-VAO H61T mutant (data not shown). Additionally, our mass spectrometric data confirmed that no residual covalent FAD was present in the apoprotein[101].

Evaluation of the quaternary structures of VAO assemblies. In order to establish the stoichiometry of the VAO assemblies, mass spectra of the proteins were recorded whereby the proteins were now nano-electrosprayed from pseudo-physiological solutions, *i.e.* aqueous 50 mM ammonium acetate buffered solutions, pH 6.8. We have shown previously[40] that, using electrospray time-of-flight mass spectrometry, the detection of large noncovalent assemblies (exhibiting very high *m/z* values) could be significantly enhanced by optimizing the background pressures in the different regions of the mass spectrometer. In the case of the VAO assemblies studied here, raising the pressure is even indispensable to detect ions originating from the assemblies. In **Figure 13A**, the nano-electrospray ionization mass spectrum of wild type VAO is

shown, when sprayed from a 50 mM ammonium acetate buffer, pH 6.8, at a protein monomer concentration of 4 μM. As reported previously[100], under these conditions, wild type VAO is almost exclusively an octamer. From the crystal structure (inset **Fig. 13A**) it is well established that the VAO octamer can be described as a tetramer of dimers[131]. The exact mass of the large octamer assembly turned out to be more difficult to determine. The average mass was 508 700 ± 350 Da. In the mass spectra of the wild type enzyme, only very small ion signals originating from dimeric species were observed (less than 4% of the total ion current).

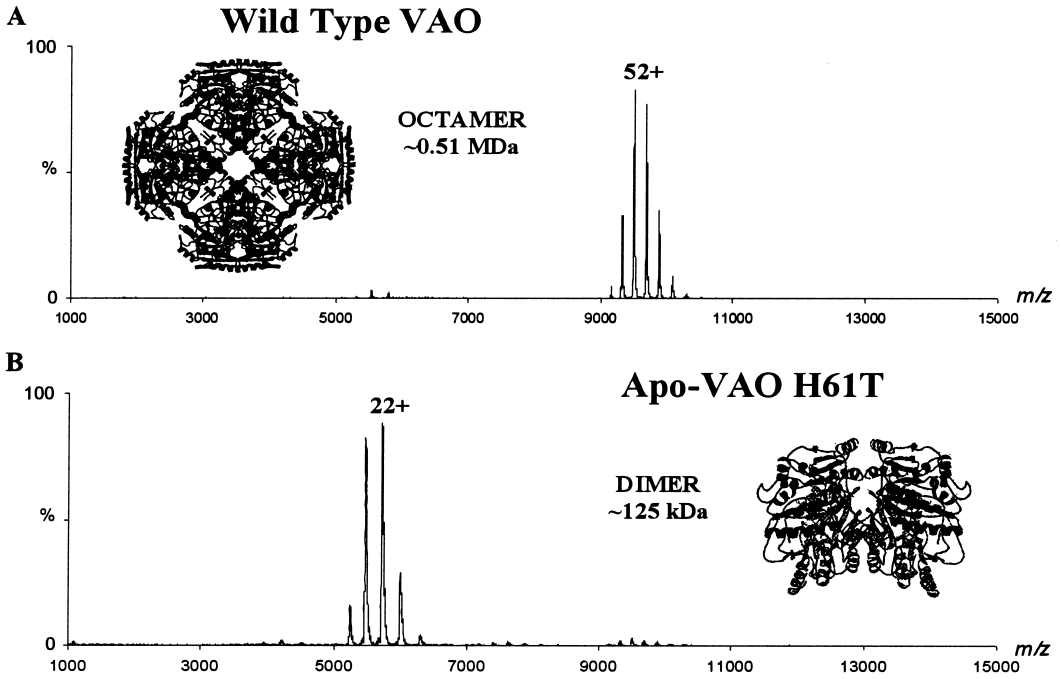

Figure 13. Nano-electrospray mass spectra of wild type VAO and H61T mutant. **A**, 4 μM wild type VAO in 50 mM ammonium acetate, pH 6.8. **B**, 4 μM apo-VAO H61T in 50 mM ammonium acetate, pH 6.8. All experimental conditions were identical.

The nano-electrospray ionization mass spectrum of the apo-VAO H61T mutant, sprayed under exactly the same experimental conditions and protein monomer concentration, is shown in **Figure 13B**. In sharp contrast to the top spectrum, this mass spectrum is dominated by ions that originate exclusively from the dimer. From the spectrum in **Figure 13B**, the average mass of the dimer was determined to be 125 575 ± 26 Da. Tetramer and octamer could be detected as well but these ions contributed only with less than 3% to the total ion current. The finding that apo-VAO

H61T prefers almost exclusively a dimeric structure seems to be in disagreement with previous crystallographic data, which revealed that the apo-H61T variant was octameric. However, the experimental conditions whereby the protein crystals were grown are somewhat different from the current conditions (100 mM sodium acetate, pH 5.1 and an enzyme concentration of 12 mg/ml, which roughly corresponds to a protein monomer concentration of 200 μM[101]).

Cofactor-induced oligomerization of apo-VAO H61T. In analogy to the spectroscopic studies described above, we prepared for mass spectrometric analyses mixtures of apo-VAO H61T at a monomer concentration of 3 μM with increasing concentrations of FAD. In line with the data depicted in **Figure 13B**, apo-VAO H61T mass spectrum, **Figure 14A**, shows a largely dimeric apoprotein. Mass spectra obtained when spraying a solution containing an equimolar concentration of apo-H61T monomer and FAD (both 3 μM) showed several remarkable changes (**Fig. 14B**). First, originating from the VAO octameric assemblies, ion signals in the *m/z* ~10 000 Da region appeared. Second, in both *m/z* ~5 500 and ~10 000 Da regions, binding of one or more FAD molecules to the dimer and the octamer were observed as satellite peaks.

When the concentration of FAD was raised 10-fold to yield saturating conditions[101], the mass spectrum of the resulting apo-H61T-FAD mixture clearly revealed that the dimer binds primarily two FAD molecules (**Fig. 14C**). Moreover, even more intense peaks in the *m/z* ~10 000 Da region are observed in this spectrum. Mass spectra taken from solutions containing apoprotein/cofactor ratios of 1:0, 1:0.5, 1:1, 1:2, 1:4 and 1:10 were all in line with the observations shown in **Figure 14** displaying some illustrative examples. Closer examination of the data shown in **Figure 14**, **B** and **C**, revealed that both H61T VAO dimer and octamer showed extensive fine structure, originating from dimeric and octameric species with different amounts of FAD bound molecules. This is remarkable as the FAD molecules have a molecular weight that is only ~0.15% of the mass of the octamer assembly. Thus almost uniquely, mass spectrometry allows the distinction between species containing different amounts of FAD when the instrument mass resolution is sufficiently high and the sample homogeneous. **Table II** lists the most pronounced measured *m/z* values for both dimer and octamer ion species depicted in **Figure 14B**. To calibrate these mass spectra at these high *m/z* ranges accurately, measurements with separate needles, one containing the sample of interest (3 μM H61T VAO and 3 μM FAD) and one containing an aqueous CsI solution, were performed one after the other, using the CsI clusters as calibrant ions.

Mass resolution ($M/\Delta m$) can be determined by measuring the peak width of the ion signals of a single component. For the CsI cluster ions these widths were ~2.5 and 5 Thomson (Th), or Da as the charge is 1, at full width medium height (FWMH or Δm) at *m/z* 5 000 and 10 000, respectively. For the protein assembly ions the widths in *m/z* were measured to be 10 Th for the dimer and 8 Th for the octamer. Taking into account the average number of charges these widths

in Th converted to an FWMH of 240 and 430 Da for the dimer and octamer ions, respectively. For these ions the experimentally measured mass resolution ($M/\Delta m$) is therefore 525 and 1 200 for the dimer and octamer ions, respectively. These data show that the instrumental mass resolution is not the limiting factor, neither is the natural width of the isotope envelope of these ions (which is below 50 Da).

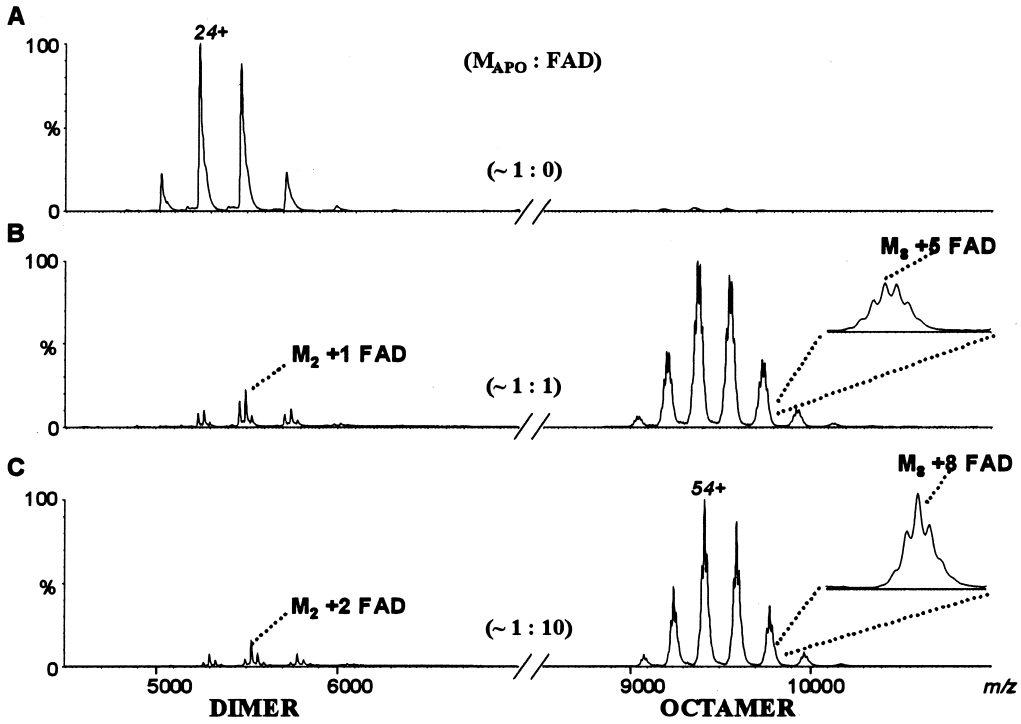

Figure 14. Nano-electrospray mass spectra of 3 μM apo-VAO H61T in 50 mM ammonium acetate, pH 6.8 with added FAD at protein/cofactor ratios of **A**, 1:0, **B**, 1:1 and **C**, 1:10.

Additionally, the data in **Table II** reveal that the measured masses of the dimer complexes are off by ~80 Da, whereas the octamer complexes are off by on average 200 Da (both to higher mass), which is less than 0.05%. The observed peak broadening and the mass deviation observed for the ions of the protein assemblies are most likely due to binding of some ions (such as alkali metal ions) and/or small neutrals to the protein complexes.

It is quite accepted to deconvolute electrospray spectra to produce so-called "zero-charge" mass spectra on a molecular mass scale using maximum entropy analysis[182].

Table II. Ion signals observed in apo-H61T VAO-FAD (1:1) mixture ESI spectrum, displayed in **Figure 13B** and deduced molecular masses for octameric and dimeric assemblies of the enzyme with different number of cofactors (n).

		m/z (z)			n	Average Mass[a] (Da)	Expected Mass(Da)	Δmass (Da)	Δmass (%)
	55	54	53	52					
Octamer +n FAD[b]	9 189	9 359	9 536	9 719	4	505 341 (±14)	505 076	+ 265	0.05
	9 202	9 373	9 549	9 733	5	506 065 (±23)	505 861	+ 204	0.04
	9 216	9 386	9 563	9 748	6	506 809 (±35)	506 646	+ 163	0.03
		m/z (z)			n	Average Mass[a] (Da)	Expected Mass (Da)	Δ mass (Da)	Δ (%)
	25	24	23	22					
Dimer +n FAD[c]	5 023	5 233	5 461	5 709	0	125 575 (±26)	125 484	+ 91	0.07
	5 053	5 265	5 494	5 744	1	126 340 (±40)	126 269	+ 71	0.06
	5 086	5 297	5 528	5 780	2	127 121 (±18)	127 054	+ 67	0.05

[a] *Average mass calculated by averaging the determined mass of each different charge state z of each complex. Individual peak width is* [b] *8 Th or ~430 Da at FWMH and* [c] *10 Th or ~240 Da at FWMH.*

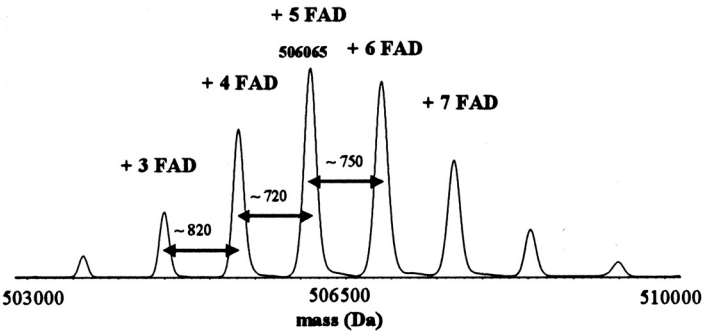

Figure 15. Deconvoluted neutral mass spectrum of the octameric VAO species using maximum entropy analysis. The number of bound cofactors is indicated.

The software maximum entropy is believed to provide probabilistic quantification so that the reliability of features in the spectrum can be ascertained. Because maximum entropy is truthful to the experimental data, the results tend to have improved resolution and signal-to-noise ratio. The deconvoluted spectrum for the octamer ions displayed in **Figure 14B** is shown in **Figure 15**. In this deconvoluted mass spectrum the species containing a different number of FAD molecules were indeed well separated by on average 785 Da (mass of one FAD molecule). Therefore, these

neutral masses deconvoluted mass spectra provide a very elegant way to separate distinct quaternary assemblies although care has to be taken in interpreting the results given that the outcome of the deconvolution is dependent on the chosen parameters.

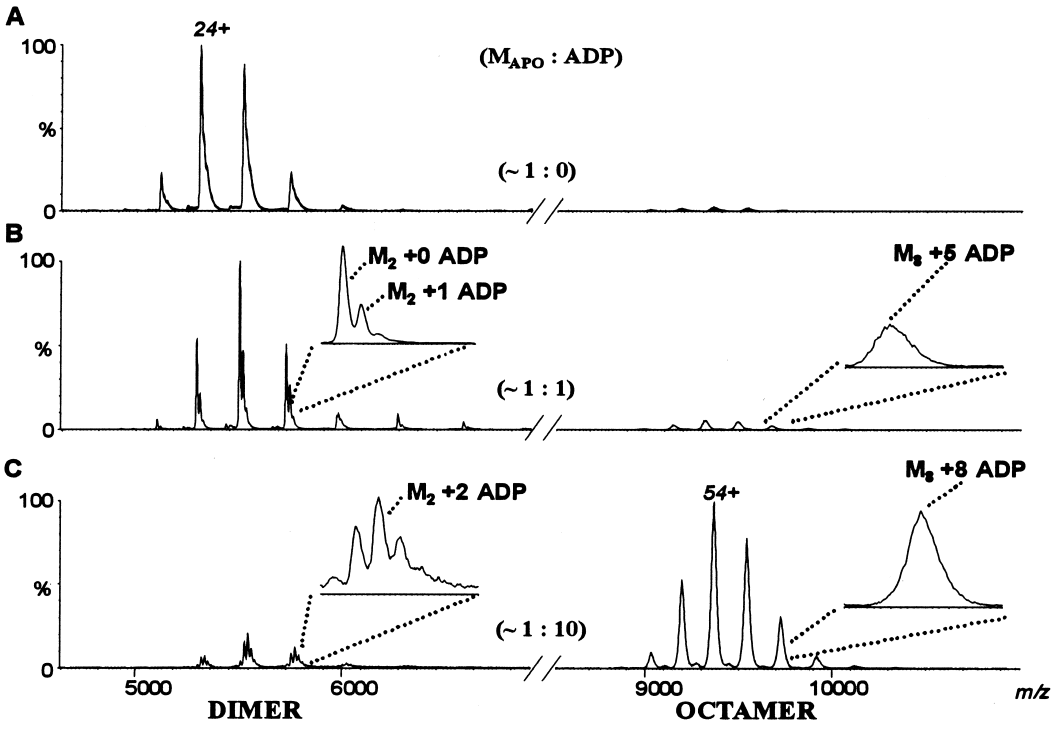

Figure 16. Nano-electrospray mass spectra of 3 μM apo-VAO H61T, in 50 mM ammonium acetate, pH 6.8 with added 5'-ADP at protein/cofactor ratios of **A**, 1:0, **B**, 1:1 and **C**, 1:10.

Figure 16, **A**-**C**, shows the nano-electrospray mass spectra of apo-VAO H61T mixed with 5'-ADP in ratios of 1:0, 1:1 and 1:10, respectively. The results obtained are remarkably similar to those found in the case of FAD as noncovalent cofactor. Again, octamerization of apo-H61T is strongly induced by the binding of the 5'-ADP cofactor analog. The mass spectra of the solutions containing 5'-ADP revealed, similarly to the FAD experiments, clear binding of 5'-ADP to the dimeric entities and, less obviously, to the octameric species. The substructure and mass shift observed for the octamer ions provide evidence of 5'-ADP binding but, most likely due to the lower molecular weight of the 5'-ADP moiety, it is more difficult to distinguish octamer ions containing one or more 5'-ADP molecules. Binding of FMN to apo-H61T was studied in a similar manner. **Figure 17**, **A**-**C**, shows the nano-electrospray mass spectra of apo-VAO H61T mixed

with FMN in ratios of 1:0, 1:1 and 1:10, respectively. In sharp contrast to the addition of FAD or 5'-ADP, the presence of FMN hardly induced formation of octamer. Even for higher FMN concentrations (up to a protein/cofactor ratio of 1:25) no octamerization of apo-H61T was observed in the mass spectra. However, it cannot be excluded from our data that FMN binds to the dimeric complex considering the ion signals broadening. Especially in the spectra obtained at a ratio of 1:10 (**Fig. 17C**), satellite peaks did appear that suggested binding of FMN to the dimer. This observation is in agreement with the observation that FMN induces changes in the tryptophan fluorescence emission of apo-H61T VAO.

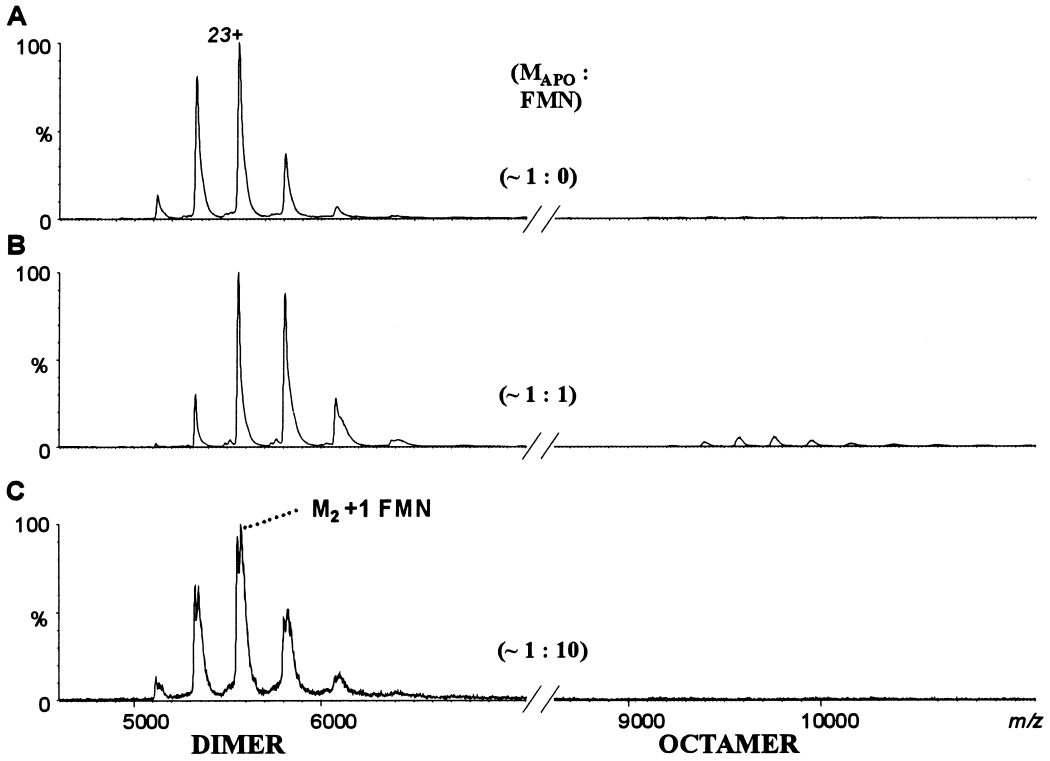

Figure 17. Nano-electrospray mass spectra of 3 μM apo-VAO H61T, in 50 mM ammonium acetate, pH 6.8 with added FMN at protein/cofactor ratios of **A**, 1:0, **B**, 1:1 and **C**, 1:10.

In solution protein assembly is often dependent on the ionic strength and/or type of salt[183]. In all the above reported data the ammonium acetate concentration was 50 mM. To investigate whether buffer salt concentrations affect the dimer/octamer equilibrium, we recorded mass spectra from solutions with ammonium acetate concentrations ranging from 5 mM to 1 000 mM. All data

indicated that the dimer-octamer equilibrium is only marginally shifted towards the octamer at higher salt concentrations (data not shown).

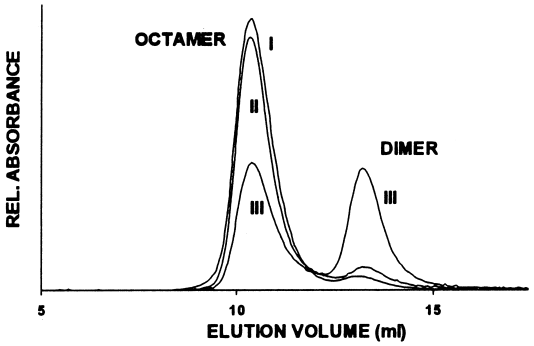

Figure 18. Size-exclusion chromatography profiles in 50 mM ammonium acetate, pH 6.8 of **I**, 3 μM wild type VAO and of apo-H61T in presence of **II**, 30 μM 5'-ADP and **III**, 30 μM FMN. Absorbance was measured at 220 nm.

Table III. Normalized octamer/dimer ratios observed by size-exclusion chromatography for wild type VAO, apo-H61T and apo-H61T in presence of cofactor analogs.

Enzyme	Octamer[#]	Dimer[#]
Wild type VAO	86 ± 5	14 ± 5
Apo-H61T	15 ± 5	85 ± 5
Apo-H61T + FAD	78 ± 10	22 ± 10
Apo-H61T + 5'-ADP	81 ± 5	19 ± 5
Apo-H61T + FMN	13 ± 9	87 ± 9

[#] *Each data point results from three independent experiments.*

Protein assembly probed by gel-filtration. In order to compare the mass spectrometric results with data obtained in solution, size-exclusion chromatography was performed on VAO also using ammonium acetate as buffer salt. When 3 μM wild type VAO was incubated for 2 hours at room temperature in 50 mM ammonium acetate, pH 6.8, the enzyme was for ~86% present in its octameric form and for 14% in its dimeric form (**Fig. 18**; **Table III**). Under similar experimental conditions, apo-H61T was mainly in the dimeric form (**Table III**). When apo-H61T was incubated for 2 hours with excess FAD, the octamer/dimer equilibrium clearly shifted towards the octameric form (**Table III**). A similar shift in the dimer/octamer ratio was observed when apo-H61T was incubated with 5'-ADP (**Fig. 18**; **Table III**). In contrast, nearly no effect on the dimer/octamer ratio of H61T was observed when the mutant was incubated with FMN (**Fig. 18**; **Table III**). These results show that the size-exclusion chromatography data are in qualitative agreement with the data obtained by mass spectrometry.

Earlier urea unfolding studies indicated that the dimeric form of wild type VAO is nearly as active as the octameric form[136]. The rapid reconstitution of holo-H61T from its constituents apo-H61T and FAD did not allow the discrimination between the activities of dimeric and octameric holo-H61T. Nevertheless, our gel-filtration data suggested that the FAD-induced oligomerization of apo-H61T is a relatively fast process. When 3 μM of apo-H61T was mixed with 30 μM FAD and immediately injected onto the Superdex column, more than 60% of the enzyme eluted in the

octameric form (compared to 10% octamer for 3 μM apo-H61T). This confirms that FAD binding to apo-H61T rapidly shifts the equilibrium between dimeric and octameric species towards the octameric state.

Discussion

In this study we have probed the influence of cofactor binding on the assembly of VAO in different solutions as determined by relative changes in ion intensities in the corresponding mass spectra and for comparison by gel-filtration. Before discussing the results, we believe it is necessary to address some of the factors that may influence the relative ion signal intensities of the various observed protein assemblies. It is now well established that mass spectrometry may be used to detect even weakly bound noncovalent complexes of protein assemblies even when they are very large and high in mass as the ones described here.

We have been able to detect ions in the mass spectra corresponding to the dimeric as well as the octameric assemblies of the protein VAO. Detection of these ions by mass spectrometry depends heavily on the experimental conditions (mass spectrometer source and analyzer conditions such as voltages, pressures and temperature) and the nature of the sprayed solutions (temperature, pH and organic solvent content). We optimized the instrument parameters to optimally detect the octameric species (see "Experimental" and *Ref.*[40]). The pressure in the front-end region of the mass spectrometer was specifically raised as far as the pumping system allowed, which led to the best transmission and detection of the octamer ions. In general in mass spectrometry, it has to be assumed that high mass ions will most likely be negatively discriminated. This discrimination occurs during the ionization event, the transmission through the instrument and upon making impact on the detector (usually smaller proteins "fly" better than larger proteins). The higher mass ions attain relatively less charges per entity and have lower velocities through the instrument. Therefore we believe that the relative abundance of the VAO octamer ions in the mass spectra is underestimated when compared with the relative abundance of these species in solution. It is clear that ion abundances observed in mass spectra cannot directly be translated to the species abundances in solution. For this purpose we have optimized the conditions for the high mass ions and kept all experimental conditions constant throughout this work. Trends observed in the mass spectra can then be qualitatively interpreted.

For cofactor-induced stabilization of protein assemblies, the absence of any significant dimeric species in the mass spectra of wild type VAO is a clear indication that the native enzyme is indeed most stable as the octameric assembly of 508.7 kDa (**Fig. 13A**). Similarly, the absence of any significant octameric species in the mass spectra of apo-VAO H61T suggests that, in solution and at relatively low ionic strength and protein concentration, the apoprotein adopts mainly the

dimeric conformation (**Fig. 13B**). This is in qualitative agreement with the present gel-filtration data but in disagreement with earlier results obtained from X-ray crystallography[101]. The fact that apo-H61T crystallizes as an octamer might therefore be explained by the high protein concentration and different incubation conditions used. Interestingly, binding of FAD to apo-H61T can be unequivocally demonstrated by our nano-electrospray ionization mass spectrometry approach. In the mass spectra, signals were clearly evident for strong and highly specific FAD-apo-VAO interactions given that the principal dimeric component detected from the FAD-saturated solution is the 2FAD-dimer complex. The mass spectral analysis of the reconstitution of the H61T mutant also indicates that binding of FAD gradually but largely shifts the dimer/octamer equilibrium in favor of the octameric species. Activity and fluorescence studies showed that the reconstitution of apo-VAO H61T with FAD is a fast process. From the full recovery of enzyme activity and the established equilibrium between dimeric and octameric species we conclude that, in analogy to wild type VAO[136], the activity of the dimeric form of the holo-H61T mutant must be comparable with the octameric form. However, because octamerization is also relatively fast, the present data do not allow the discrimination between the rate of FAD binding and the rate of octamerization.

Fraaije *et al*.[101] reported that 5'-ADP was a strong competitive inhibitor of the H61T mutant enzyme while FMN did not reveal any inhibitory effect. With the observed binding of 5'-ADP to the dimeric form of apo-H61T and the oligomerization provoked by the presence of this cofactor analog, our mass spectral data clearly showed that the adenosine diphosphate moiety of FAD plays an essential role in the formation of the octameric structures. Because the crystal structure of the octameric apo-H61T mutant is highly similar to that of wild type VAO[101] and incubation of dimeric apo-H61T with FMN does not stimulate octamerization, we conclude that upon FAD binding, small conformational changes in the ADP-binding pocket of the dimeric species are transmitted to the protein surface, promoting oligomerization. In this respect it is important to note that VAO belongs to a newly recognized family of flavoenzymes[130], which lack the well known Rossmann fold for binding the ADP-moiety of FAD[120,139]. In the Rossmann-fold containing flavoenzymes, ADP and FAD have often similar influence on the oligomerization state of the enzymes whereas FMN has not[174]. For the members of the VAO family only limited data on cofactor binding are available. Nevertheless it is of interest to note, here, that for all VAO homologues with known structure two conserved loops are responsible for binding the pyrophosphate moiety of the FAD[184,185]. Furthermore, in heterotrimeric CO dehydrogenase the flavoprotein moiety can only be reconstituted when the apoprotein is bound to the molybdo-iron-sulfur protein moiety[186], whereas for heterodimeric *p*-cresol methylhydroxylase noncovalent binding of the FAD (and not FMN) to the flavoprotein subunit triggers binding of the cytochrome subunit, which is necessary for subsequent covalent FAD attachment[177].

Acknowledgements

The present work was made possible by the support from the Center for Biomolecular Genetics and the Netherlands Organization for Scientific Research (NWO) grant to AJRH and NT (#99508). We like to thank Kees Versluis and Martijn Pinkse for their precious technical assistance.

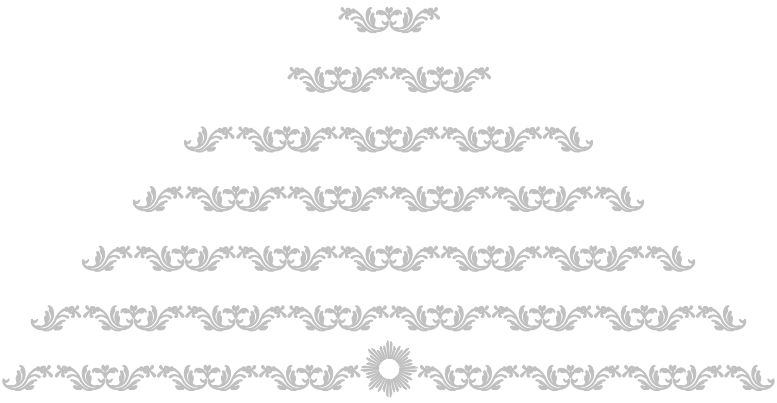

Chapter 4

Coenzyme binding during catalysis is beneficial for the stability of 4-hydroxyacetophenone monooxygenase.

« Stability is not immobility. »
Prince KLEMENS VON METTERNICH

Robert HH van den Heuvel*, Nora Tahallah*
Nanne M Kamerbeek, Marco W Fraaije
Willem JH van Berkel, Dick B Janssen, Albert JR Heck
** Equally contributing authors*
Adapted from *J Biol Chem.* 2005 Sep 16;280(37):32115-21.

Abstract

The NADPH-dependent dimeric flavoenzyme 4-hydroxyacetophenone monooxygenase (HAPMO) catalyzes Baeyer-Villiger oxidations of a wide range of ketones, thereby generating esters or lactones. In the present work, we investigated the binding characteristics of the nicotinamide coenzyme during enzyme catalysis and its structural role in complex with the protein. For this, we used (i) wild type HAPMO, (ii) the Arg339Ala variant, which is active but has a low affinity towards NADPH and (iii) the Arg440Ala variant, which is inactive but has a high affinity towards NADPH. Electrospray ionization mass spectrometry was used as the primary tool to directly observe noncovalent protein-ligand complexes in real-time. These analyses showed that the nicotinamide coenzyme remains bound to HAPMO during the entire catalytic cycle of the NADPH oxidase reaction. This is the first direct evidence of the continued association of the coenzyme to a Baeyer-Villiger monooxygenase. Together with the observations that $NADP^+$ only weakly interacts with oxidized enzyme and that HAPMO is mainly in the reduced form during catalysis we conclude that $NADP^+$ interacts tightly with the reduced form of HAPMO. The association with the coenzyme appeared to be crucial for enzyme stability. The interaction with the coenzyme analog 3-aminopyridine adenine dinucleotide phosphate ($AADP^+$) strongly enhances the thermal stability of wild type HAPMO. This coenzyme-induced stabilization may also be important for related enzymes.

The interaction of proteins with small molecules such as ligands and cofactors often coincides with an increased stability of the protein due to the coupling of the binding with the unfolding equilibrium[83,107,187,188]. Thus apart from their catalytic role cofactors may also have a structural role. The importance of cofactor binding for protein stability is revealed for several flavoproteins[83]. The common polymorphism 677C>T in methylenetetrahydrofolate reductase causing the single point mutation Ala222Val reduces the affinity of the enzyme for the FAD cofactor and results in a lower thermal stability[98,99]. For the octameric protein vanillyl alcohol oxidase it was demonstrated that cofactor binding influences the quaternary architecture of the enzyme[91]. The His61Thr mutant is purified as apoenzyme and mainly exists as a dimeric species. Binding of FAD to the enzyme restores the octameric conformation[91,101]. Similarly, for lipoamide dehydrogenase it was shown that FAD binding increases the protein melting temperature from 35ºC to 80ºC[174]. Coenzymes such as $NAD(P)^+$ and NAD(P)H can have, besides their function in electron transfer, also a structural role. Several liver and pectoral muscle enzymes are substantially protected by $NAD(P)^+$ against heat and proteolysis by trypsin[189]. Phosphite dehydrogenase[190] is stabilized by NAD^+ and DNA ligases[191] become more compact upon anchoring NAD^+ coenzyme. In the present work, we have studied the noncovalent interactions between the oxidized or reduced nicotinamide coenzyme ($NADP^+$ or NADPH) and the flavoenzyme 4-hydroxyacetophenone monooxygenase (HAPMO). HAPMO from *Pseudomonas fluorescens ACB* is a Baeyer-Villiger monooxygenase (BVMO), which converts a wide range of ketones into the corresponding esters or lactones[137]. The enzyme is also able to perform enantioselective sulfoxidations[192]. In recent years, BVMOs have received increasing attention since they represent a promising alternative for chemical oxidation reactions allowing highly selective oxygen insertion reactions[193,194].

HAPMO is a so-called type I BVMO. These enzymes contain FAD as cofactor and use NADPH as source of electrons while type II BVMOs contain FMN and use NADH[138]. Type I BVMOs contain two Rossman-folds, which are involved in binding of the ADP moieties of FAD and NADPH[139]. Together with bacterial N-hydroxylating monooxygenases and eukaryotic flavin-containing monooxygenases type I BVMOs form a newly identified superfamily of flavoprotein monooxygenases[195], which is distinct from the family of flavoprotein aromatic hydroxylases. Recently, the crystal structure of phenylacetone monooxygenase from *Thermobifida fusca* was solved[140]. This first structure of a type I BVMO revealed a two-domain architecture and highlighted the importance of an active site arginine, which seems critically involved in substrate oxygenation. Replacement of this conserved arginine in HAPMO (Arg440Ala) does not impair NADPH binding but results in complete enzyme inactivation[196]. From site-directed mutagenesis it was also established that Arg339 and Lys439 are involved in determining the coenzyme specificity

of HAPMO. The Arg339Ala mutant showed a largely decreased affinity for NADPH as judged from kinetic analysis and binding experiments. Saturation mutagenesis of Lys439 suggested that this residue is involved in the binding of the 2'-phosphate of NADPH and allowed to change the coenzyme specificity of HAPMO in favor of NADH[196].

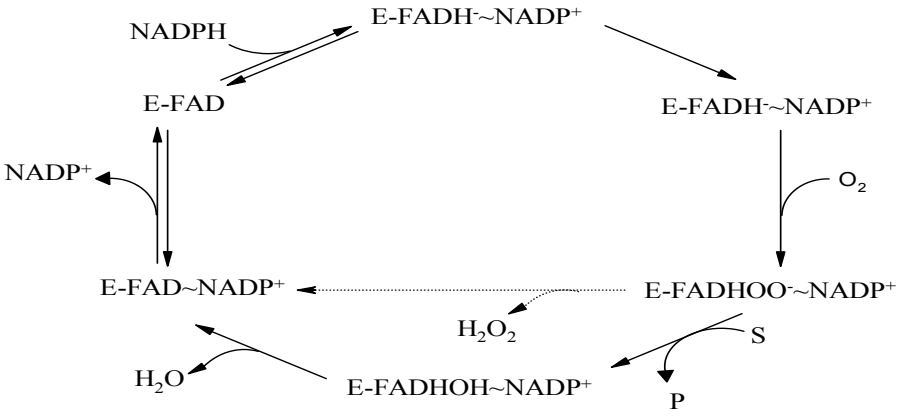

Scheme 1. Proposed mechanism of action for HAPMO. The mechanism is based on the kinetic analysis of both cyclohexanone monooxygenase[197] and HAPMO. S and P indicate substrate and product, respectively. In the experiments described in this article no ketone substrate was present. Under these conditions, the peroxyflavin intermediate slowly decays to form hydrogen peroxide while releasing $NADP^+$ acting as an NADPH oxidase (inner cycle).

Scheme 1 shows the proposed mechanism of action of BVMOs[197]. After flavin reduction by NADPH and reaction with oxygen, the generated flavin C4a-peroxide attacks the carbonyl carbon of the substrate. After product formation, water is released from the resulting hydroxyflavin regenerating the oxidized enzyme. For cyclohexanone monooxygenase there is evidence derived from kinetic studies that the initially formed $NADP^+$ remains bound during the substrate oxygenation process. In fact, release of $NADP^+$ from the reoxidized enzyme is the last step to complete the catalytic cycle and is the rate-determining step in catalysis[197]. A similar kinetic mechanism has been proposed for pig liver flavin-containing monooxygenase[198] suggesting that continued association of coenzyme is a recurrent theme for this class of monooxygenases to regulate enzyme activity. It has also been found for these monooxygenases that when no suitable substrate is present the flavin C4a-peroxide will slowly decay to form hydrogen peroxide while releasing $NADP^+$ (**Scheme 1**) thereby acting as an NADPH oxidase. The observed oxidase activity of HAPMO in the absence of an aromatic substrate is 0.1 s^{-1} [137], which may suggest that also with HAPMO $NADP^+$ remains bound throughout the oxidative half-reaction.

The interaction of the above mentioned flavin-containing monooxygenases with $NADP^+$ might be beneficial for the enzyme from a structural point of view. To study this in details, we selected HAPMO and two HAPMO mutants (Arg339Ala and Arg440Ala) and used electrospray ionization mass spectrometry and size-exclusion chromatography as principal tools to monitor coenzyme binding and its effect on protein stability. The major advantage of mass spectrometry is that it allows the direct observation of the noncovalent interactions between protein and ligand in real-time even when a stoichiometric heterogeneous mixture is formed[34,46,150]. The data described in this article showed that the nicotinamide coenzyme either in its reduced or oxidized form interacts with HAPMO throughout the catalytic cycle and stabilizes the enzyme to a great extent.

Experimental procedures

Chemicals, protein expression and purification. NADPH, $NADP^+$ and 3-aminopyridine adenine dinucleotide phosphate ($AADP^+$) were obtained from Sigma-Aldrich. The hapE gene from *Pseudomonas fluorescens ACB* encoding HAPMO was expressed in *Escherichia coli* strain TOP10 containing the vector pBADNK/hapE. The two genes encoding the mutant proteins Arg339Ala and Arg440Ala were generated as recently described[196]. For efficient expression *E. coli* cells were grown at 20ºC with 0.002% (w/v) arabinose and 50 mg/ml ampicillin essentially as described before[196]. Purification of wild type HAPMO and Arg339Ala and Arg440Ala variants was performed as reported earlier[137].

Nanoflow electrospray ionization mass spectrometry. Enzyme samples for nanoflow electrospray ionization mass spectrometry experiments were prepared in aqueous 50 mM ammonium acetate, pH 6.8. Wild type, Arg339Ala and Arg440Ala HAPMO were introduced into a nanoflow electrospray ionization orthogonal time-of-flight mass spectrometer (Micromass LCT, Waters) modified for high-mass operation and operating in positive ion mode. For wild type HAPMO and variants, mass determinations were performed under conditions of increased pressure in the source and intermediate pressure regions in the mass spectrometer (Pirani gauge 7 mbar and Penning gauge 1.2 x 10^{-6} mbar)[40,199]. Nanoflow electrospray voltages were optimized for transmission of larger multimer protein assemblies (capillary voltage 1 450-1 650 V and cone voltage 100-125 V). For the mass determinations of NADPH, $NADP^+$ and $AADP^+$ electrospray voltages were optimized for transmission of smaller organic molecules (capillary voltage 1 050-1 150 V and cone voltage 30 V). Borosilicate glass capillaries (Kwik-Fil, World Precision Instruments) were used on a P-97 puller (Sutter Instruments) to prepare the nanoflow electrospray capillaries with an orifice of about 5 mm. The capillaries were subsequently coated with a thin gold layer (~500 Å) using an Edwards Scancoat six Pirani 501 sputter coater (Edwards High Vacuum International). For the kinetic experiments with NADPH an automated chip-based electrospray source (Nanomate, Advion) was used. The automated source was programmed to

aspirate 4 µl of sample into the conductive pipette tip and then to deliver the sample to the inlet side of the electrospray chip. This chip consists of 10x10 nozzles in a silicon wafer and a channel extends from the nozzle to an inlet side at the opposite face of the chip. Electrospray was initiated by applying an electric voltage of 1 850 V, a head pressure of 0.2 psi to the sample in the pipette tip and a cone voltage of 30 V.

Analytical procedures. The enzyme activity of HAPMO was spectrophotometrically determined by monitoring the consumption of NADPH at 340 nm[137] in the absence or presence of 4-hydroxyacetophenone. Consumption of NADPH and formation of $NADP^+$ in the absence of 4-hydroxyacetophenone was also monitored by mass spectrometry. The inhibition constant of $NADP^+$ with respect to NADPH was determined spectrophotometrically with varying concentrations of $NADP^+$. The thermal stability of wild type HAPMO and Arg339Ala and Arg440Ala variants was analyzed by enzyme-inactivation studies and size-exclusion chromatography. 10 µM HAPMO in 50 mM ammonium acetate, pH 6.8 were incubated at 36˚C in the absence or presence of 200 µM FAD or 50 µM $AADP^+$. At various time points, aliquots were taken and analyzed for enzyme activity and hydrodynamical behavior. Analytical size-exclusion chromatography was performed using a Superdex 200 HR 10/30 column (Amersham Biosciences) in 50 mM ammonium acetate, pH 6.8. Aliquots of 100 µl were loaded on the column and eluted at a flow rate of 0.8 ml/min. Apparent molecular masses were determined using a calibration curve made with standards from a molecular weight marker kit (BioRad) containing thyroglobulin (670 kDa), bovine γ-globulin (158 kDa), chicken ovalbumin (44 kDa), equine myoglobin (17 kDa) and vitamin B12 (1.35 kDa).

Results

Quaternary structure of HAPMO variants. Wild type HAPMO is a homodimeric flavoprotein with each monomer containing a tightly noncovalently bound FAD cofactor[137]. To determine accurate masses of wild type, Arg339Ala and Arg440Ala HAPMO and to investigate whether these proteins remain in their native form during ionization, 1 µM of HAPMO variants in 50 mM ammonium acetate, pH 6.8 was analyzed by nanoflow electrospray ionization mass spectrometry (**Fig. 19**). As can be seen from **Figure 19A** ionization of wild type HAPMO revealed two major ion series around *m/z* 4 500 and 6 000 corresponding to molecular masses of 77 610 ± 10 and 145 232 ± 21 Da, respectively (**Table IV**). These species represent the monomeric and dimeric form of HAPMO with the dimeric species being the dominant form. The molecular masses of the monomeric and dimeric forms are in close agreement with the calculated masses including the FAD cofactors. Besides the native species containing two FAD molecules also small amounts of the dimeric apoprotein and dimeric protein with one FAD molecule were observed. Thus, the mass spectrometry data showed the dimeric nature of HAPMO with tight binding of FAD.

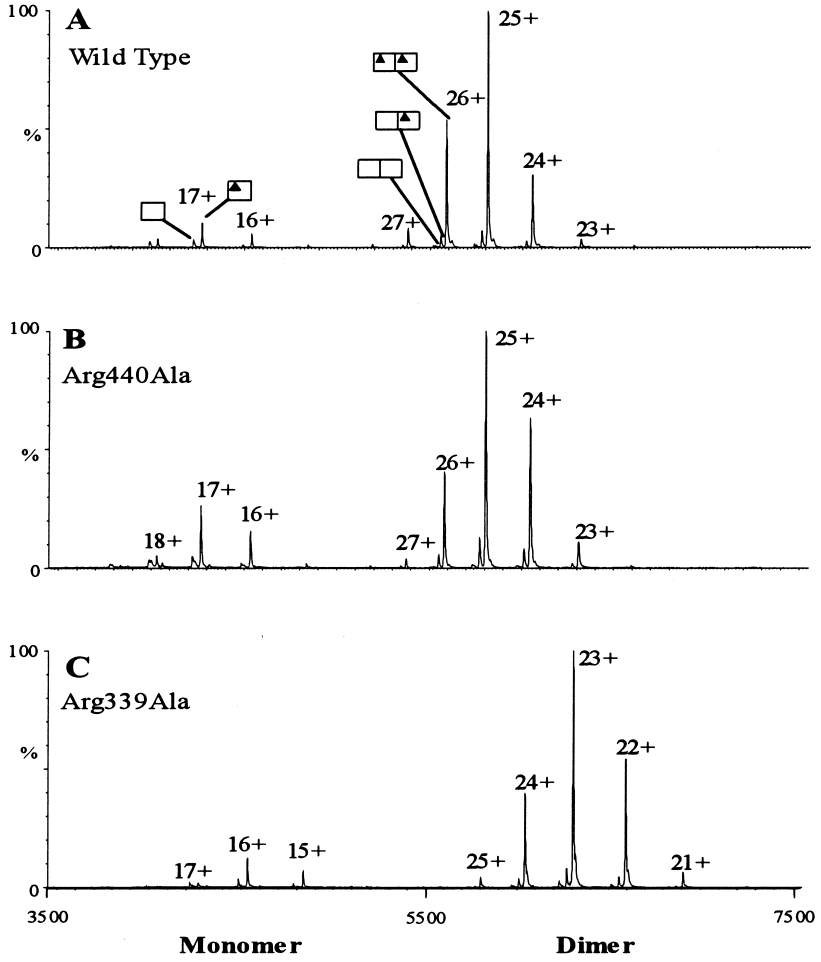

Figure 19. Nanoflow electrospray mass spectra of 1 μM HAPMO variants in 50 mM ammonium acetate, pH 6.8, infused into the nanoflow electrospray source. Spectra were collected in positive ion mode. **A**, wild type, **B**, Arg440Ala and **C**, Arg339Ala. (□) Apomonomer and (▲) one molecule of FAD.

Mass determination of Arg339Ala and Arg440Ala variants revealed molecular masses of 145 103 ± 43 and 145 092 ± 44 Da, respectively. Again, these molecular masses are in close agreement with the calculated masses of the dimers, including two FAD molecules (**Table IV**). The HAPMO mutants were essentially present as holodimers and only minor amounts of holo and apomonomer and apodimer were observed (**Fig. 19B and 19C**). The mass spectrum of Arg440Ala

revealed some more monomeric protein compared to wild type and Arg339Ala HAPMO, which may indicate that in this particular HAPMO variant the interaction between the monomers is somewhat weaker. Interestingly, the Arg339Ala mutant obtained in the electrospray processed fewer charges than wild type and Arg440Ala HAPMO. Whereas Arg339Ala yielded for the dimeric form a series of 21+ to 25+ ions for the dimeric form, both wild type and Arg440Ala yielded series of 23+ to 27+ ions. The observation that Arg339Ala obtains one charge less per monomer may indicate that the side chain of Arg339 is exposed to solvent and is protonated in wild type enzyme or, alternatively, it may reflect that the mutation causes a small conformational difference.

Table IV. Molecular masses deduced from the nanoflow electrospray mass spectra of each dimeric HAPMO variant in complex with FAD.

Enzyme	Species	Cofactor	Average MW (Da)	Calculated mass[a] (Da)
Wild type	Dimer	FAD	145 232 (± 21)	145 222
Arg339Ala	Dimer	FAD	145 103 (± 43)	145 052
Arg440Ala	Dimer	FAD	145 092 (± 44)	145 052

[a] *Mass calculated on the basis of the primary sequence including the cofactor.*

Complex formation between oxidized HAPMO variants and NADP$^+$ or AADP$^+$. In the following, we aimed to obtain more information about the binding of the nicotinamide coenzyme to the HAPMO variants. To study these protein-ligand interactions by mass spectrometry we used NADP$^+$ and the coenzyme analog AADP$^+$. For these studies we could not use NADPH as the reduced coenzyme would slowly react with oxidized HAPMO. AADP$^+$ is a nonreducing coenzyme analog in which the amide function of the nicotinamide moiety is replaced by a primary amine function. This compound has often been used to probe coenzyme binding[200-202].

Mixing 1 μM wild type enzyme with 10 μM NADP$^+$ and subsequent analysis by nanoflow electrospray ionization mass spectrometry did not reveal the presence of a complex between the protein and NADP$^+$. Only at a 5-fold higher concentration of coenzyme some NADP$^+$ binding was observed (< 5% saturation per monomer). Weak binding of NADP$^+$ to the oxidized enzyme was supported by UV-visible absorbance difference spectroscopy. Addition of 1.5 mM NADP$^+$ to 10 μM HAPMO did not influence the absorption properties of the flavin cofactor indicating that NADP$^+$ does not bind, or at least not in the vicinity of, the isoalloxazine ring.

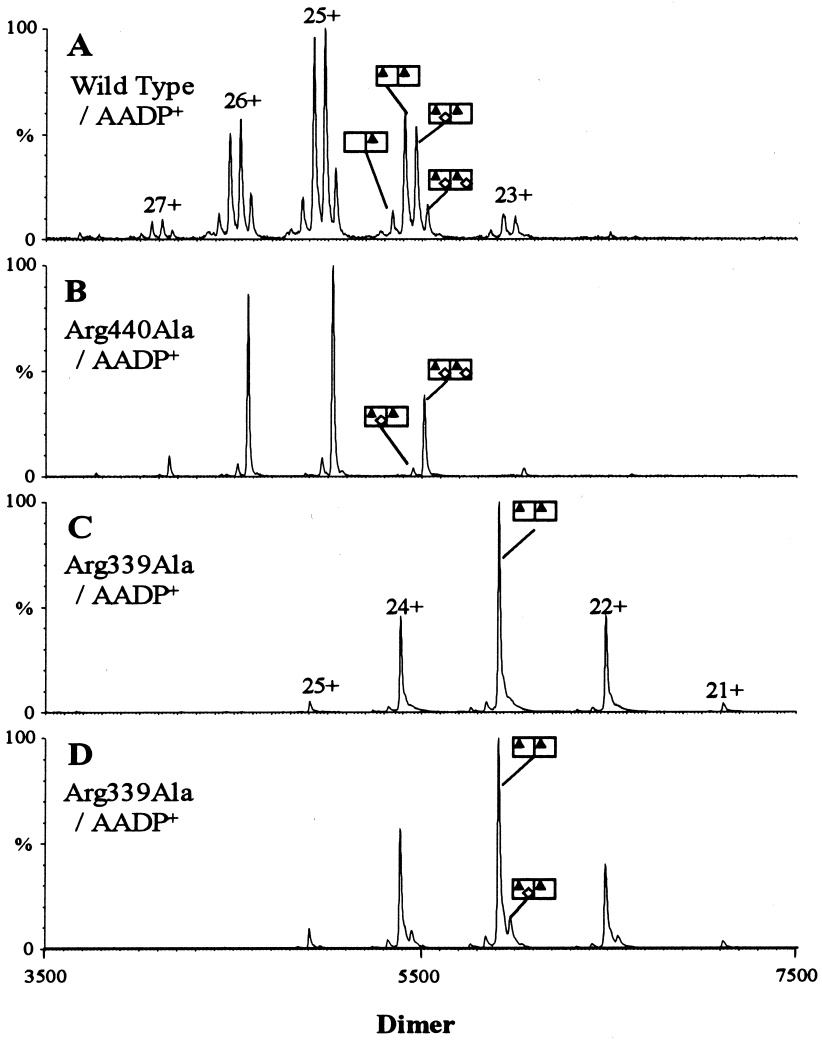

Figure 20. Nanoflow electrospray mass spectra of HAPMO variants in the presence of $AADP^+$. 1 μM enzyme in 50 mM ammonium acetate, pH 6.8 was mixed with $AADP^+$ and infused in the electrospray source. Spectra were collected in positive ion mode. **A**, Wild type enzyme mixed with a stoichiometric amount of $AADP^+$. **B**, Arg440Ala HAPMO mixed with a stoichiometric amount of $AADP^+$. **C**, Arg339Ala HAPMO mixed with a stoichiometric amount of $AADP^+$. **D**, Arg339Ala HAPMO mixed with 10-fold molar excess of $AADP^+$. (□) Apomonomer, (▲) one molecule of FAD and (◇) one molecule of $AADP^+$.

$AADP^+$ is known to tightly bind to wild type HAPMO and Arg440Ala with dissociation constants of 0.4 and 0.1 μM, respectively[196]. Indeed, when we mixed wild type HAPMO (1 μM)

with $AADP^+$ (1 μM) we observed two new ion series in the mass spectrum (**Fig. 20A**). Deconvolution of these two ion series revealed molecular masses of 145 773 and 146 493 Da strongly indicating the presence of dimeric protein in complex with one and two molecules of $AADP^+$. Similarly, the mass spectrum of a mixture between Arg440Ala and $AADP^+$ revealed complexes between the protein and one and two molecules of $AADP^+$ (**Fig. 20B**). **Figure 20** clearly shows that in an equimolar ratio, Arg440Ala was nearly saturated with $AADP^+$ whereas wild type enzyme was saturated for only ~30%. Wild type HAPMO became fully saturated with $AADP^+$ when the enzyme (1 μM) was mixed with a 4-fold excess of $AADP^+$ (4 μM) (data not shown). The mass spectra also suggested that $AADP^+$ stabilizes the quaternary structure of wild type and Arg440Ala HAPMO as no apoprotein was observed when the coenzyme analog was bound. The Arg339Ala mutant, on the other hand, did not display significant binding of $AADP^+$ (**Fig. 20C**). Even at a 10-fold excess of the compound hardly any protein-$AADP^+$ complex was formed (**Fig. 20D**). These results agree well with earlier studies, which indicate that Arg339Ala only weakly interacts with $AADP^+$ [196]. In summary, none of the oxidized HAPMO variants were able to bind specifically to $NADP^+$, however, wild type and Arg440Ala HAPMO, but not Arg339Ala, interacted strongly with the coenzyme analog $AADP^+$.

Complex formation during NADPH oxidation. The interaction between $NADP^+$ and reduced HAPMO has not been yet characterized because of the difficulties of directly observing these complexes. Analysis of the binding of $NADP^+$ to reduced HAPMO by electrospray mass spectrometry is not straightforward as it is difficult to keep anaerobic conditions within the source of the electrospray ionization probe. Therefore, we analyzed the binding of the nicotinamide coenzyme to the enzyme under aerobic conditions in the absence of ketone substrate. By measuring the redox state of the flavin cofactor during enzyme turnover information can be obtained about the rate-limiting step in catalysis. These experiments have shown that under aerobic conditions and in the presence of sufficient NADPH, but in the absence of a ketone substrate, the flavin is mainly in a reduced form in both wild type and Arg440Ala HAPMO (100% and 97%, respectively) whereas in the Arg339Ala variant most of the FAD is in the oxidized form. These results indicate that at least in the wild type enzyme and Arg440Ala variant flavin reduction is relatively fast[196]. As a consequence, the predominant enzyme form present during the reaction of substrate-free HAPMO with NADPH under aerobic conditions may be a complex of a reduced or oxygenated enzyme species and $NADP^+$ (**Scheme 1**, right part of the cycle). This biochemical property allowed us to study the interaction between $NADP^+$ and substrate-free reduced wild type and Arg440Ala HAPMO during turnover by mass spectrometry.

In a typical experiment we mixed 1 μM HAPMO enzyme with excess of NADPH and measured noncovalent protein complex formation and the amounts of NADPH and $NADP^+$ in real-time up to 50 min at room temperature.

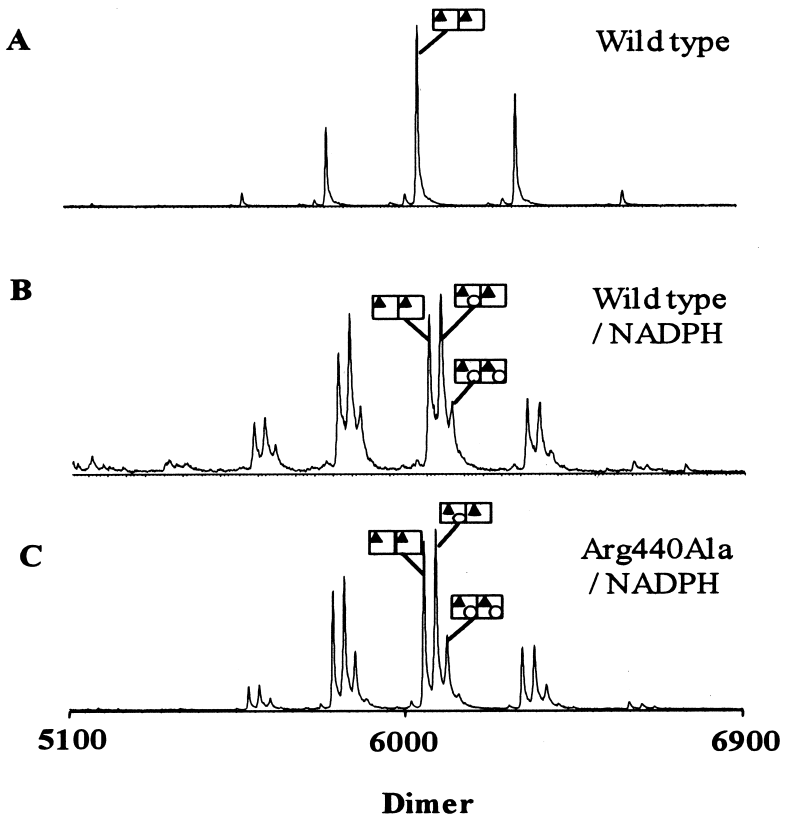

Figure 21. Nanoflow electrospray mass spectra of HAPMO variants during turnover of NADPH. 1 μM enzyme in 50 mM ammonium acetate, pH 6.8, was mixed with 10 μM NADPH and aliquots were taken at different time points and mass spectra were recorded in positive ion mode. **A**, Wild type HAPMO in the absence of NADPH, **B**, Wild type HAPMO in complex with $NADP^+$ after 10 min and **C**, Arg440Ala HAPMO in complex with $NADP^+$ after 10 min. (□) Apomonomer, (▲) one molecule of FAD and (O) one molecule of $NADP^+$.

First, we monitored the mass spectra of wild type HAPMO and Arg440Ala variant during incubation with 10 μM NADPH (**Fig. 21**). Upon mixing with NADPH, the mass spectrum revealed two new ion series, which corresponded to the binding of one and two molecules of the pyridine nucleotide to the dimeric species of wild type and Arg440Ala variants. Full saturation of the wild type enzyme and Arg440Ala variant with NADP(H) was not reached due to the relatively low concentration of NADPH used. Increasing the molar excess may, however, induce nonspecific complex formation. As the enzyme bound flavin is mainly in the reduced or oxygenated state

during steady-state conditions, the species we observed in the mass spectrum most probably reflects the reduced enzyme in complex with $NADP^+$.

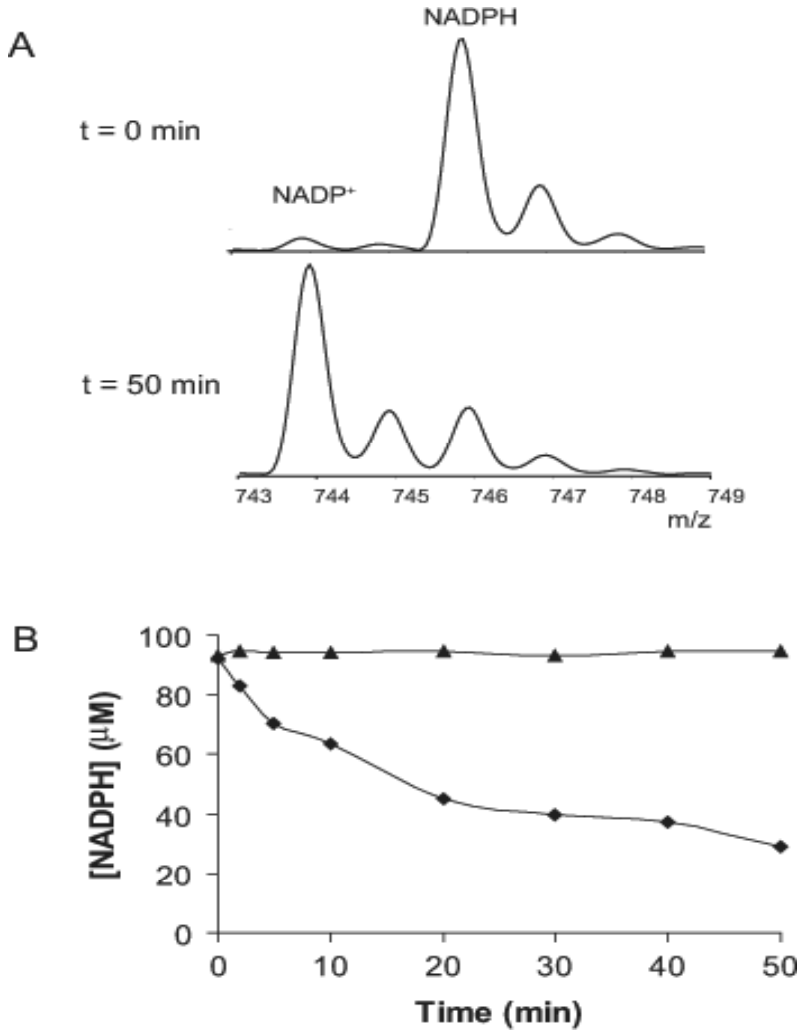

Figure 22. NADPH oxidation by HAPMO variants monitored by nanoflow electrospray mass spectrometry. 1 μM enzyme was mixed with 100 μM NADPH in 50 mM ammonium acetate, pH 6.8 at room temperature and mass spectra were recorded in real-time in positive ion mode. A freshly prepared solution of NADPH contained ~8% of $NADP^+$. **A**, Oxidation of NADPH (746 amu) into $NADP^+$ (744 amu) by wild type HAPMO after 0 and 50 min of incubation and **B**, Progress curve of NADPH oxidation of (♦) Wild type HAPMO and (▲) Arg440Ala HAPMO.

Unfortunately, the high molecular mass of the HAPMO dimer did not allow us to differentiate between reduced, oxygenated or oxidized HAPMO. For Arg339Ala we did not observe any interaction between the protein and the nicotinamide coenzyme.

Second, we analyzed the amounts of $NADP^+$ and NADPH present during the HAPMO-mediated NADPH oxidase reaction. It should be noted here that by electrospray ionization mass spectrometry $NADP^+$ is detected as the M^+ ion (744 amu) as it has already a fixed positive charge in the nicotinamide ring whereas NADPH is detected as the $[M+H]^+$ ion (746 amu)[125,203]. It was found that under the used experimental conditions a freshly prepared solution of NADPH contained ~8% of $NADP^+$ and no further spontaneous oxidation occurred within the time frame of the experiment. The enzyme-mediated oxidation of NADPH to $NADP^+$ was evidenced by the fact that we observed an increase in the amount of $NADP^+$ (744 amu) in time and a decrease in the amount NADPH (746 amu) (**Fig. 22**).

Under the experimental conditions applied wild type HAPMO oxidized about 70% of the added amount of NADPH within 50 min. The fact that the reaction did not reach completion can be attributed to product inhibition by $NADP^+$. The Arg440Ala mutant did not oxidize NADPH[196].

In order to determine whether $NADP^+$ binds to the enzyme during turnover, we measured the inhibition behavior of $NADP^+$ with respect to NADPH. For wild type enzyme it was found that $NADP^+$ behaves as a weak competitive inhibitor with a K_i of 390 μM. The relatively large difference in K_m for NADPH (12 μM)[196] and K_i for $NADP^+$ indicates that the oxidized enzyme is efficient in discriminating between both oxidized and reduced states of the coenzyme. Furthermore, the fact that $NADP^+$ competes with NADPH for binding is in line with the kinetic mechanisms that have been elucidated for sequence related monooxygenases[197]. If a similar mechanism would be operative for HAPMO, $NADP^+$ would dissociate from reoxidized enzyme while being tightly bound to the reduced enzyme.

In summary, the results clearly showed that we can monitor HAPMO-catalyzed oxidation of NADPH into $NADP^+$ by mass spectrometry and that $NADP^+$ forms a stable intermediate complex with reduced and/or oxygenated enzyme, but not with oxidized enzyme. Furthermore during catalysis the nicotinamide coenzyme, either in the reduced or oxidized form, is continuously associated with HAPMO.

Coenzyme binding increases the stability of HAPMO. The observed interaction of the nicotinamide coenzyme with HAPMO during the entire reaction cycle might also be of importance for the enzyme from a structural point of view. Therefore we probed the thermal stability of HAPMO variants in the absence or presence of pyridine nucleotide derivatives.

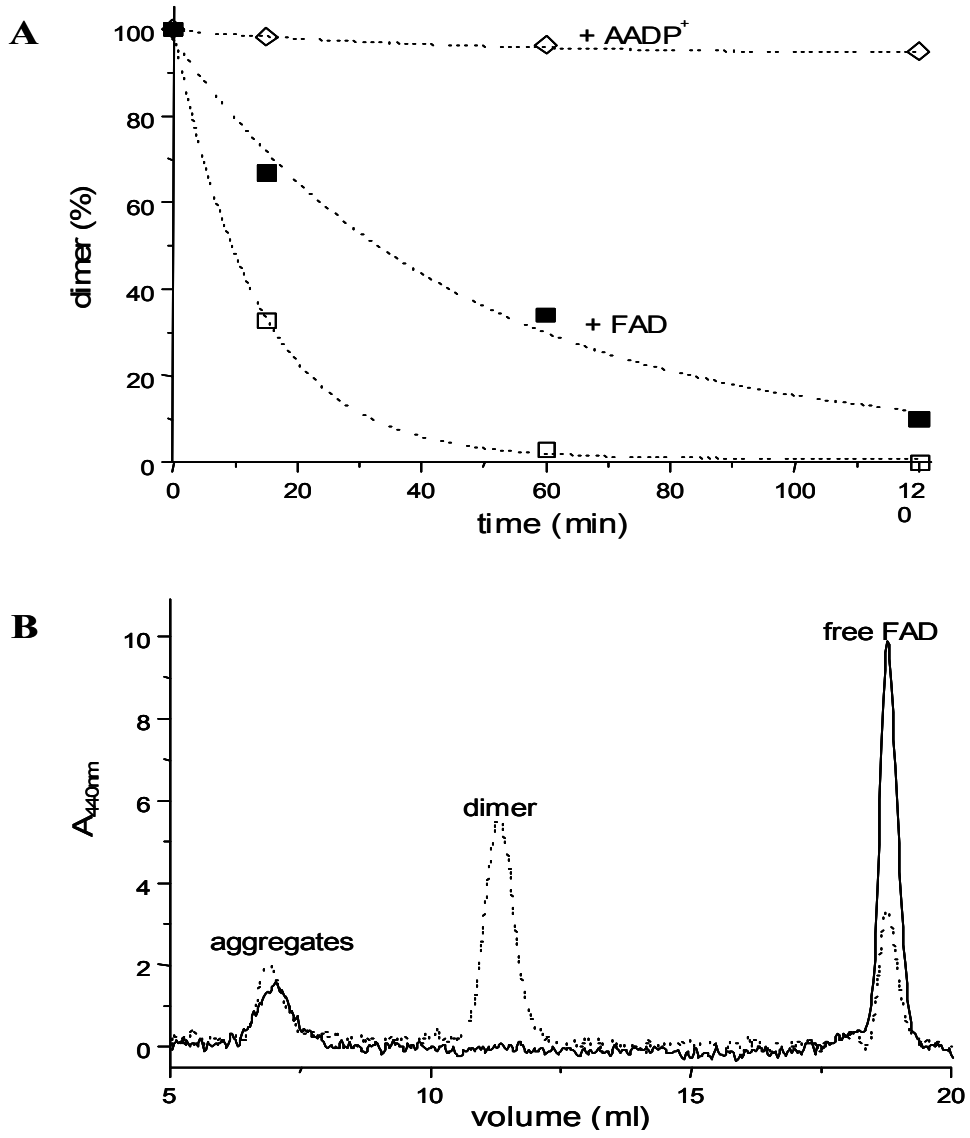

Figure 23. Stability of wild type HAPMO monitored by size-exclusion chromatography. The enzyme (10 μM) was incubated at 36˚C in 50 mM ammonium acetate, pH 6.8 and aliquots were taken at regular time intervals up to 120 min. Subsequently, samples were analyzed with a Superdex 200 HR 10/30 column. **A**, time dependent decay of HAPMO dimers. (□) Free enzyme, (■) in the presence of 200 μM FAD and (◇) in the presence of 50 μM $AADP^+$. **B**, Elution pattern of HAPMO incubated for 120 min at 36°C in the absence (—) or presence (····) of $AADP^+$. The absorption was monitored at 280 and 440 nm. Free FAD, HAPMO dimer and HAPMO aggregates eluted around 18, 11.5 and 7 min, respectively.

When the free wild type enzyme (10 μM) was incubated at 36˚C we observed a rapid loss of enzyme activity, which coincided with the loss of the dimeric structure. After 120 min incubation at 36˚C wild type HAPMO was completely inactivated. By size-exclusion chromatography of the same incubations we observed a loss of quaternary structure (**Fig. 23A**), which accompanied enzyme inactivation. The size-exclusion chromatography data also showed that during the inactivation process protein aggregates are formed and that the FAD cofactor is released (**Fig. 23B**). We have to mention here that it is very likely that most of the aggregates formed were too large and/or heterogeneous to be detected by size-exclusion chromatography. The binding of $AADP^+$ to HAPMO appeared to have a dramatic effect on the denaturation process. Addition of the coenzyme analog clearly stabilized the dimeric holoenzyme as evidenced by size-exclusion chromatography analysis (**Fig. 23A**). In the presence of an excess of free FAD the aggregation process of wild type HAPMO was slowed down to some extent suggesting that release of the cofactor plays a role in the inactivation process (**Fig. 23A**). However, the effect was far less dramatic as compared to $AADP^+$.

To probe whether the stabilizing effect of $AADP^+$ can be related to ligand binding, the same experiments were performed with the HAPMO mutants. Again, a similar stabilizing effect of $AADP^+$ was found for the Arg440Ala variant (data not shown). In line with earlier observations in this article that Arg339Ala interacts only weakly with $AADP^+$, addition of $AADP^+$ had no effect on the stability of Arg339Ala. Thus these results confirm that the HAPMO structure is stabilized by $AADP^+$ binding and that the continued association of the nicotinamide coenzyme enhances enzyme stability.

Discussion

In this study we report the first direct analysis of the noncovalent interaction of a flavin-containing Baeyer-Villiger monooxygenase with its nicotinamide coenzyme during catalysis. This was accomplished by the application of nanoflow electrospray ionization mass spectrometry. In addition, we studied the effect of coenzyme binding on the thermal stability of the enzyme by size-exclusion chromatography.

Complex formation between HAPMO and pyridine nucleotides. For these studies we focused on three HAPMO variants with different biochemical properties. Wild type HAPMO and Arg440Ala interact strongly with NADPH but only wild type enzyme is fully active and Arg339Ala interacts weakly with NADPH but can still perform catalysis at high coenzyme concentrations.

Electrospray ionization mass spectrometry data under native conditions showed that the three HAPMO variants have a dimeric quaternary structure and bind up to two molecules of FAD per dimer. Our data provide strong evidence that the quaternary structures of these three enzyme variants are very similar. The Arg339Ala variant has a slightly different mass spectrum with one charge less per monomer than the two other HAPMO variants. These differences in charge either reflect small conformational differences between the enzyme variants or are directly related to the replacement of Arg339 into Ala thereby removing one potential protonation site during the electrospray process[188,204].

Very recently, the crystal structure of phenylacetone monooxygenase (PAMO), a BVMO from the thermophilic bacterium *Thermobifida fusca*, has become available[140]. This enzyme has 30% sequence identity with HAPMO and is expected to be homologous from a structural point of view. Phenylacetone monooxygenase exhibits a two-domain architecture resembling that of disulfide oxidoreductases[141]. Both the FAD-binding domain and the NADPH-binding domain exhibit the typical dinucleotide-binding fold[120]. Unfortunately no crystallographic model for the enzyme in complex with a pyridine nucleotide is available. On the basis of the crystallographic model of PAMO a structural model of HAPMO has been constructed. In this model residue Arg339 in HAPMO aligns with residue Arg217 in phenylacetone monooxygenase, which has been assigned as a residue for interacting with the adenine part of NADPH. This nicely agrees with the observed effects on coenzyme recognition when this residue is replaced in HAPMO. It also indicates that Arg339 in HAPMO is not involved in monomer-monomer subunit interaction. The published crystallographic model of the related BVMO also suggests that Arg339 in wild type HAPMO is positioned at the surface of the protein and may well be protonated in the electrospray process. The Arg440 residue of HAPMO can also be pinpointed in the PAMO structure and corresponds to Arg337 in this monooxygenase. It is located in the active site and is of crucial importance for catalysis as evidenced by the inability of the HAPMO Arg440Ala variant to perform Baeyer-Villiger reactions. This agrees with the fact that the Arg440Ala variant is still able to bind the coenzyme while it is unable to complete the catalytic cycle. The suggested location of Arg440 in HAPMO would also agree with the observation that the replacement of this residue does not result in a decrease of the number of charges during the electrospray process.

The Michaelis Menten constant of NADPH for wild type HAPMO is relatively low (K_m = 12 μM) suggesting that NADPH interacts strongly with the oxidized enzyme. Our mass spectrometry experiments with wild type enzyme and Arg339Ala and Arg440Ala variants showed that $NADP^+$ does not tightly interact with the oxidized enzyme indicating that HAPMO can differentiate between oxidized and reduced pyridine nucleotides. These data were validated by biochemical inhibition studies, which revealed an inhibition constant of 390 μM for $NADP^+$ for wild type HAPMO. Our studies also revealed tight binding of the coenzyme analog $AADP^+$ to

wild type and Arg440Ala HAPMO but not to Arg339Ala. These results are in agreement with recent biochemical data, being $AADP^+$ a strong competitive inhibitor mimicking NADPH[196]. Apparently the enzyme has evolved a very specific recognition site for binding reduced coenzyme to favor catalysis.

HAPMO catalyzes the conversion of ketones into their corresponding esters or lactones using NADPH as external electron donor (**Scheme 1**). In the absence of a suitable ketone substrate consumption of NADPH by HAPMO results in forming and stabilizing a peroxy-enzyme intermediate containing a bound $NADP^+$ molecule[137]. The consumption of NADPH in the absence of aromatic substrate is slow (k'_{cat} = 0.10 s^{-1}) and relates to the slow decay of the peroxy-enzyme intermediate yielding hydrogen peroxide as product. These results were confirmed by enzyme-monitored-turnover experiments revealing that during catalysis the flavin cofactor in wild type enzyme is mainly in the reduced and/or oxygenated state[196] awaiting binding of a suitable substrate. It has been postulated for sequence related monooxygenases that $NADP^+$ remains bound to the enzyme until the peroxy-enzyme intermediate has been converted[197,205]. This suggests that the enzyme is virtually continuously occupied by the reduced or oxidized coenzyme. Only during the exchange of $NADP^+$ with NADPH the enzyme is in the free form. In order to characterize the noncovalent interactions of the nicotinamide coenzyme to HAPMO during turnover, we followed the reaction of HAPMO variants with NADPH under aerobic conditions in real-time by mass spectrometry. The mass spectra clearly evidenced that HAPMO, when functioning as an NADPH oxidase (**Scheme 1**, inner cycle), is in complex with its coenzyme throughout the whole catalytic cycle. This strongly suggests that we observed binding of $NADP^+$ to a reduced or oxygenated enzyme. This is the first direct observation that coenzyme binds to a BVMO during catalysis.

Stability of HAPMO. The coenzyme analog $AADP^+$ was used to probe the influence of pyridine nucleotides on the stability of HAPMO. Data from size-exclusion chromatography showed that this analog prevents to a great extent aggregation and inactivation of HAPMO variants (wild type and Arg440Ala) that are able to bind this coenzyme analog. This indicates that the effect is not related to the intrinsic properties of the $AADP^+$ molecule as the Arg339Ala mutant showed no difference in stability upon the addition of the coenzyme analog. The stabilizing effect suggests that coenzyme binding induces a more rigid tertiary and/or quaternary structure due to specific noncovalent interactions between coenzyme and its highly specific binding site. The mass spectrometric observation that the binding affinity of FAD is enhanced upon binding of $AADP^+$ to wild type HAPMO and Arg440Ala may also indicate that the enzymes adopt a more rigid structure.

In conclusion, this study establishes the noncovalent interactions between pyridine nucleotides and HAPMO. This is the first direct evidence that the coenzyme remains bound to the

enzyme during catalysis. Binding of the coenzyme also results in a dramatic increase in the stability of the enzyme. Based on the results of this study, it can be expected that most of the time HAPMO will be occupied by a coenzyme when it is in its natural intracellular environment. This indicates that the enzyme is *in vivo* more stable when compared with the isolated enzyme, which might explain the relatively poor stability of many reported isolated coenzyme-dependent enzymes. For example cyclohexanone monooxygenase, a well-studied homologue of HAPMO, has been shown to inactivate quite rapidly at room temperature[206]. The concept of enzyme stabilization by $AADP^+$ binding might be exploited for enzyme purification or storage. The obtained results also show that the electrospray ionization technique is very well suited to detect noncovalent interactions between HAPMO subunits and between HAPMO and ligands and to monitor these interactions in real-time[34,150].

Acknowledgments

We thank Kees Versluis and Pascal Gerbaux for excellent mass spectrometry assistance. N. T. was supported by Netherlands Organization for Scientific Research Grant #99508.

Chapter 5

A covalent modification of $NADP^+$ revealed by the atomic resolution structure of FprA, a *Mycobacterium tuberculosis* oxidoreductase.

« In a lifestyle dictated by the time it takes to cook a hamburger, it is remarkable that the tubercle bacillus - more often associated with the nineteenth century - still claims the title of "captain of all the men of death". »
DOUGLAS B. YOUNG

Roberto T Bossi, Alessandro Aliverti, Debora Raimondi
Federico Fischer, Giuliana Zanetti, Davide Ferrari, Nora Tahallah
Claudia S Maier, Albert JR Heck, Menico Rizzi, Andrea Mattevi
Adapted from *Biochemistry*. 2002 Jul 16;41(28):8807-18.

Abstract

FprA is a mycobacterial oxidoreductase that catalyzes the transfer of reducing equivalents from NADPH to a protein acceptor. We determined the atomic resolution structures of FprA in the oxidized (1.05 Å resolution) and NADPH-reduced (1.25 Å resolution) forms. The comparison of these FprA structures with that of bovine adrenodoxin reductase showed no significant overall differences. Hence, these enzymes, which belong to the structural family of the disulfide oxidoreductases, are structurally conserved in very distant organisms such as mycobacteria and mammals. Despite the conservation of the overall fold, the details of the active site of FprA show some peculiar features. In the oxidized enzyme complex, the bound NADP$^+$ exhibits a covalent modification, which has been identified as an oxygen atom linked through a carbonylic bond to the reactive C4 atom of the nicotinamide ring. Mass spectrometry confirmed this assignment. This NADP$^+$ derivative is likely to form by oxidation of the NADP$^+$ adduct resulting from nucleophilic attack by an active-site water molecule. A Glu-His pair is well positioned to activate the attacking water through a mechanism analogous to that of the catalytic triad in serine proteases. The NADP$^+$ nicotinamide ring exhibits the unusual cis-conformation, which may favor derivative formation. The physiological significance of this reaction is presently unknown. However, it could assist with drug-design studies in that the modified NADP$^+$ could serve as a lead compound for the development of specific inhibitors.

Tuberculosis is still a major cause of mortality in both developing and industrialized countries. It kills about 3 million people every year and its rate is increasing[207]. Among the main factors involved are the high resilience of mycobacteria, poor compliance of patients to treatments, which can result in drug resistant strains and the HIV epidemic. The picture emerges that despite available vaccine and effective drugs new antitubercular agents and therapies are needed. With this in mind, a structural genomics project targeting *Mycobacterium tuberculosis* proteins has been undertaken through a worldwide consortium approach[208].

We have investigated FprA, a *M. tuberculosis* flavoenzyme encoded by gene Rv3106 of the H37Rv strain of the pathogen[142]. This 50 kDa enzyme is able to take two reducing equivalents from NADPH and transfer them to a yet unidentified protein acceptor via the protein-bound FAD cofactor[144]. Plant ferredoxin, bovine adrenodoxin and *Mycobacterium smegmatis* 7Fe ferredoxin can all function as *in vitro* electron acceptors. Although the physiological role of FprA is still unclear insights can be derived from its primary structure. A BLAST search[209] of FprA sequence against the database retrieves, among the highest score proteins, mammalian adrenodoxin reductase (AR) and the yeast protein Arh1p displaying 41% and 30% sequence identity, respectively (**Fig. 24**). The yeast homologue Arh1p acts via a ferredoxin and is crucial for iron homeostasis and in vivo assembly of Fe/S proteins[210]. Inactivation of the gene coding Arh1p has been shown to be lethal[211]. Mammalian AR is part of steroid and vitamin D biosynthesis. It is a mitochondrial flavoenzyme, which transfers electrons from NADPH to cytochrome P450 through the [2Fe-2S]-protein adrenodoxin[212-214]. All these data suggest a relevant role of FprA possibly in Fe metabolism or in cytochrome P450-dependent reactions. While the former process is known to be crucial for mycobacterial infection[215], the latter should also be important since *M. tuberculosis* genome contains 22 genes coding putative cytochrome P450 proteins[142].

Recently, the structures of bovine AR in complex with $NADP^+$, NADPH and adrenodoxin have been solved[216-218]. These structures revealed the binding mode of NADP(H) and FAD and the mainly polar interaction between AR and adrenodoxin. Here we present the crystal structures of FprA in two redox states obtained by cocrystallization of the oxidized enzyme with $NADP^+$ (FprA-NADPO) and by soaking the crystals in an NADPH-containing solution, which yielded the complex between the reduced enzyme and NADPH ($FprA_{red}$-NADPH). The very high resolution of the diffraction data allowed us to analyze in detail these structures. In the oxidized enzyme a novel covalent derivative of the pyridine nucleotide has been found (abbreviated as NADPO; **Fig. 25**) and characterized by mass spectrometry.

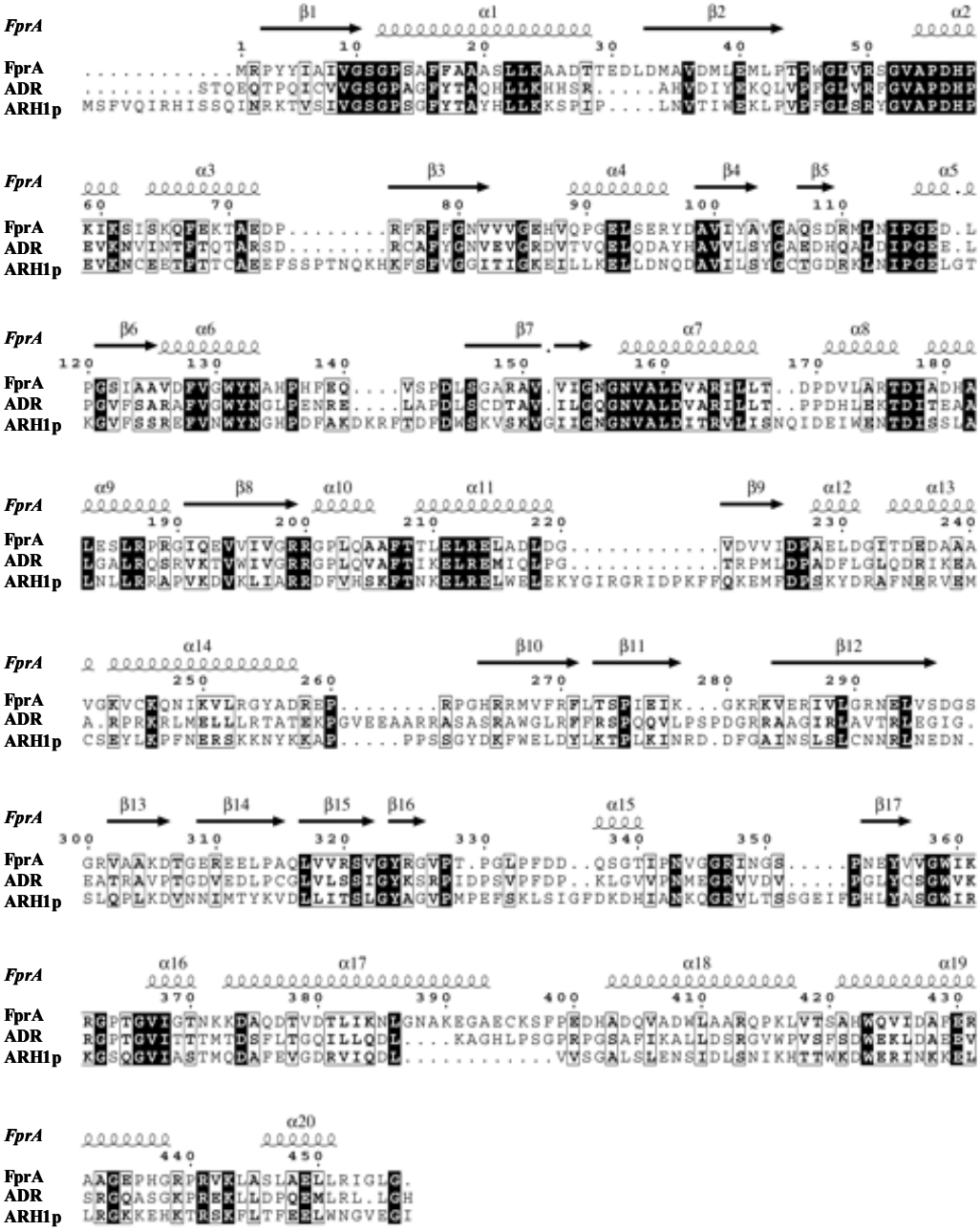

Figure 24. Sequence alignment of *M. tuberculosis* FprA, bovine AR, and yeast Arh1p as calculated with CLUSTALW[219]. The secondary structure elements are for the structure of FprA.

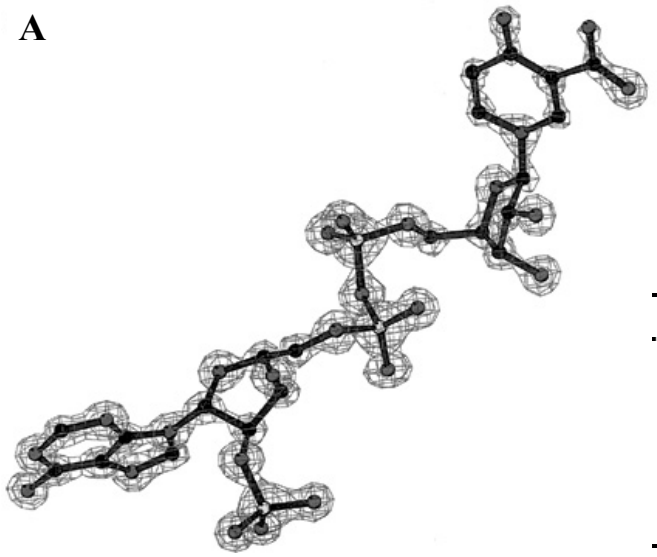

Bond Distances	Monomer A (Å)	Monomer B (Å)
N1-C2	1.41	1.37
C2-C3	1.35	1.37
C3-C4	1.40	1.45
C4-O4	1.27	1.23
C4-C5	1.47	1.45
C5-C6	1.41	1.40
N1-C6	1.38	1.38
C3-C7	1.54	1.52
C7-O7	1.25	1.25
C4-N7	1.31	1.30

Figure 25. Crystallographic data for identification of the modified $NADP^+$. **A**, The final 2Fo-Fc electron density map of the covalently modified $NADP^+$ found in the FprA-NADPO complex. The resolution is 1.05 Å. The contour level is 2σ. **B**, Atomic numbering and crystallographic bond distances of the nicotinamide ring of the $NADP^+$ derivative.

Experimental

Sample preparation and crystallization. Recombinant FprA was overexpressed and purified as described previously[144]. FprA was crystallized at 4°C by the vapor diffusion method in both hanging and sitting drops. Before crystallization, the enzyme was incubated for about 1 hour in a solution containing $NADP^+$. The enzyme solution contained 25 mg FprA/ml, 10 mM Hepes/KOH pH 7.0, 10% (v/v) glycerol, 5 mM dithiothreitol and 0.65 mM $NADP^+$. The well solution consisted of 30% (w/v) poly(ethylene glycol) 4 000, 0.1 M sodium citrate, pH 5.6 and 0.2 M ammonium acetate. Crystals grew in approximately 1 week reaching a maximum size of 0.1 × 0.1 × 1.0 mm^3. They belong to space group $P2_12_12_1$ with unit cell axes a = 69.3 Å, b = 89.2 Å and c = 160.9 Å.

Single-crystal microspectrophotometry and NADPH soaking. UV-visible spectra on FprA were recorded on single crystals at room temperature using a Zeiss MpM800 microspectrophotometer[220]. Crystals were harvested in a stabilizing solution containing 32% (w/v) poly(ethylene glycol) 4 000, 0.1 M sodium citrate pH 5.6, 0.2 M ammonium acetate and 0.65 mM $NADP^+$ and then placed in a quartz cell with a crystal face orthogonal to the incident light beam.

Spectra were measured at different times before and after soaking under aerobic conditions in a stabilizing solution containing 10 mM NADPH instead of $NADP^+$. The microspectrophotometric analysis indicated that FprA crystals are reduced after about 30 min of soaking in NADPH. This soaking protocol was used for the structure determination of the $FprA_{red}$-NADPH complex.

Data collection and processing. For data collection, FprA crystals were cryoprotected in a solution consisting of 30% (w/v) poly(ethylene glycol) 4 000, 0.1 M sodium citrate pH 5.6, 0.2 M ammonium acetate, 20% (v/v) glycerol and 0.65 mM $NADP^+$ and then flash-cooled in a 100 K nitrogen stream. For the NADPH-soaked structure the cryoprotecting solution contained 10 mM NADPH instead of 0.65 mM $NADP^+$. Data were collected at the BW7B beamline of the EMBL/DESY Outstation (Hamburg) using a MAR image plate detector. Data integration was performed by MOSFLM[221] whereas merging and scaling were made using the CCP4 program suite[222]. A summary of the data collection statistics is reported in **Table V**.

Structure determination and refinement. For structure determination data of the FprA-NADPO complex obtained by cocrystallization with $NADP^+$ were used. The structure was solved through molecular replacement using the structure of bovine adrenodoxin reductase (PDB entry 1E1L; *Ref.*[217]) as the search model and the program BEAST[223]. Employment of this program improved the clarity of the solutions found in the molecular replacement calculations indicating the presence of an FprA dimer in the asymmetric unit. The 2-fold noncrystallographic symmetry was exploited to improve the model phases by density modification through the program DM[224]. Native data up to 1.9 Å resolution and DM phases were used to automatically build the model by the ARP/wARP package[225]. For the success of the autobuilding procedure it was essential to down-weight the model phases in the phase combination steps of the DM density modification calculations (for a description of the protocol see *Ref.*[226]). A total of 900 residues (out of 912) were automatically positioned in the electron density using ARP/wARP[225]. This structure was further refined by Refmac5 using standard protocols[227]. All measured reflections up to 1.05 Å resolution were used. Individual anisotropic displacement parameters and hydrogen atoms at their idealized positions have been introduced. Model building was performed with O[228]. No restraints were applied to both FAD and $NADP^+$ to allow detection of any unusual stereochemical feature in these ligands. Ordered water molecules were generated with the program ARP[225] using the criteria that the peaks in 2Fo-Fc and Fo-Fc maps had to be higher than 1.25 and 3.0 σ, respectively and that the water molecules had to be within H-bond distances from a protein or solvent atom. Except for the last refinement cycle, 0.5% of unique reflections were excluded from calculations to perform R-free validation. The model of FprA-NADPO provided the starting coordinates for refinement of the $FprA_{red}$-NADPH structure performed at 1.25 Å resolution. Also for this structure, individual anisotropic displacement parameters and hydrogen atoms at their idealized positions have been introduced. Refinement statistics are summarized in **Table V**. Structure analysis was done using

O[228], PROCHECK[229], ACONIO[230] and programs from the CCP4 package[222]. Figures were produced by MOLSCRIPT[231], BOBSCRIPT[232] and LIGPLOT[233].

Table V. Data collection and refinement statistics.

	FprA-NADPO	$FprA_{red}$-NADPH
space group	$P2_12_12_1$	$P2_12_12_1$
a,b,c (Å)	69.3, 89.2, 160.9	69.5, 89.5, 161.6
resolution limit (Å)	1.05	1.25
total observations	1 170 509	877 990
unique reflections	440 216	275 836
overall completeness (%)	95.8	98.1
completeness outermost shell (%)	95.4	98.1
overall I/σ(I)	5.1	9.1
$I/\sigma(I)$ outermost shell	1.6	2.5
*R*sym (%)[a]	7.1	5.3
R-factor (%)[b]	13.4	12.5
R-free (%)[b]	15.3	14.2
rmsd bond length (Å)[c]	0.015	0.014
rmsd bond angle (deg)[c]	1.747	1.666
Ramachandran plot (%)[d] most favored/additional asymmetric unit[e]	93.9/5.6	93.8/5.6
protein	7104	7006
FAD	106	106
NADP	98	96
water	1864	1422
acetate	44	44

[a] $Rsym = \Sigma_{hkl,i} |I_{hkl,i} - \langle I_{hkl} \rangle| / \Sigma_{hkl,i} I_{hkl,i}$. [b] R-factor = $\Sigma ||Fo| - |Fc|| / \Sigma |Fo|$, where the working and free R-factors are calculated using the working and free reflection sets, respectively. The free reflections (0.5% of the unique reflections) were held aside throughout the refinement and included in the last cycle only. [c] Calculated with Refmac5[227]. [d] As classified by PROCHECK[229]. [e] Number of atoms in the asymmetric unit. Hydrogen atoms are not included. The FprA subunit consists of 456 amino acids. The only missing amino acids are in FprA-NADPO, Pro260, Pro399, Glu400 in monomer A and Glu400 in monomer B and in $FprA_{red}$-NADPH, Pro260 and Glu400 in monomer A and Glu400 in monomer B. Alternate conformations were modeled for 35 residues in FprA-NADPO and 16 residues in $FprA_{red}$-NADPH.

Mass Spectrometry. All mass spectrometry experiments were performed in positive ion mode. The mass analyses were carried out on an LC-T orthogonal time-of-flight instrument equipped with a Z-spray nano-electrospray ion source (Micromass, Manchester, UK). Gold-coated borosilicate glass capillaries were used for sample introduction and prepared as described previously[40].

The capillary and cone voltages were optimized for stable spraying conditions. The source temperature was set at 60°C. For optimal detection of the noncovalently associated species, collisional cooling conditions were employed as described previously[40]. Protein stock solutions (25 mg FprA/ml, 10 mM Hepes/KOH pH 7.0, 10% glycerol and 0.65 mM $NADP^+$) were diluted

directly into 50 mM ammonium acetate, pH 6.8. For determining the molecular mass of the apoprotein, denaturing conditions were used by diluting protein stock solutions in 0.7% formic acid. Sample concentrations were adjusted to 3-25 μM monomer concentration. Deconvolution of the conventional ESI mass spectra of the proteins was performed by maximum entropy process using the MaxEnt program incorporated in the Micromass MassLynx software.

A Q-ToF mass spectrometer also fitted with a Z-spray nano-electrospray ion source (Micromass, Manchester, UK) was used for CID-MS/MS experiments. After optimizing capillary and cone voltages, the resolution of the mass-analyzing quadrupole was set so that the full isotopic envelope of the selected precursor ion was transmitted. Argon was used as collision gas. The collision-offset potentials were typically set to 20-75 V. The calculated monoisotopic masses M_{th} based on the respective chemical formulas are 744.08 u for $NADP^+$ ($C_{21}H_{29}O_{17}N_7P_3$), 759.08 u for the $NADP^+$ derivative ($C_{21}H_{28}O_{18}N_7P_3$), and 785.56 u for FAD ($C_{27}H_{33}O_{15}N_9P_2$).

Results and Discussion

Crystallographic analysis. Growth of FprA crystals was possible only by cocrystallization with $NADP^+$ while crystals of the free enzyme were never obtained. The structure of oxidized FprA has been solved at 1.05 Å resolution in complex with $NADP^+$ (FprA-NADPO). Structure determination has been performed through molecular replacement using bovine AR[216] as search model. Employment of a maximum likelihood scoring function[223] in molecular replacement greatly facilitated structure solution. Soaking in an NADPH-containing mother liquor led to reduction of the crystalline protein ($FprA_{red}$-NADPH complex). We have collected data up to 1.25 Å resolution on an NADPH-soaked crystal and solved this second structure using the atomic coordinates of FprA-NADPO.

The asymmetric unit of FprA crystals contains a protein dimer (2 × 50 kDa) with the two subunits related by a noncrystallographic 2-fold axis (**Fig. 26A**). The electron density (**Fig. 25A**) allowed the positioning of the FAD cofactor, of the NADP ligand and of nearly all 456 residues of each FprA monomer (**Table V**). The refined models have an *R*-factor of 13.4% (*R*-free 15.3%) for FprA-NADPO and of 12.5% (*R*-free 14.2%) for $FprA_{red}$-NADPH (**Table V**).

Overall structure. The FprA monomer consists of two α/β domains with similar topologies (**Fig. 26B**). The FAD-binding domain consists of the N- and C-terminal regions of the enzyme (residues 2-106 and 327-456) whereas the central part of the polypeptide chain (residues 110-323) forms the NADP-binding domain; a small two-stranded β-sheet (residues 107-109 and 324-326) links the two domains. This overall architecture is common to the proteins belonging to the structural family of glutathione reductase[145,234] of which FprA is a member. Both domains of FprA

exhibit a Rossmann fold topology[235] but some variations are present in this scaffold. The FAD-binding domain has a central five-stranded parallel β-sheet surrounded on both sides by α-helices. Although within this family of proteins the crossover between strand 3 and strand 4 is typically an antiparallel β-sheet (the so-called β-meander)[145], in FprA this is replaced by an α-helix (helix 89-96). A six-stranded central β-sheet is present in the NADP-binding domain flanked on one side by α-helices and on the other side by the β-meander.

In the X-ray structure, FprA is present as a dimer (**Fig. 26A**). The intersubunit interactions are not extensive involving only 5.6% (1 138 Å2) of the monomer surface area suggesting that dimerization is probably a result of crystal packing. This notion is supported by gel-filtration studies, which indicate that the enzyme in solution is mainly monomeric[144]. The two crystallographically independent monomers are virtually identical with a root-mean-square deviation (rmsd) of 0.83 Å for 3 447 atom pairs in FprA-NADPO and 0.89 Å for 3 454 pairs in $FprA_{red}$-NADPH. The interactions between FprA and the prosthetic group (**Fig. 27A**) resemble those typically found for FAD binding within the structural family of glutathione reductase[235] with the characteristic N-terminal $\beta\alpha\beta$-unit (residues 3-43) involved in the binding of the cofactor ADP moiety. The isoalloxazine is bound in a planar conformation. The angle between pyrimidine and dimethylbenzene rings is 4° implying a very small tilting of the flavin. The cofactor pyrimidine ring is partly exposed to the solvent while the dimethylbenzene ring is buried in the flavin-binding site. The N-terminus of α-helix 367-393 interacts with the electronegative N1-O2 locus of the flavin and directly binds to O2 with Ile368 N atom. Loop 358-366 covers the active site as a cap interacting with both the flavin and the NADP ligand.

Comparison with Adrenodoxin Reductase. The structure of AR has been solved in different states[216-218], namely in the native form (PDB code 1CJC), cocrystallized with $NADP^+$ (1E1L), soaked with $NADP^+$ or NADPH (1E1K and 1E1M) and in complex with adrenodoxin (1E6E). The overall structures of FprA and AR are highly similar especially in the FAD-binding domain. Superposition of the FAD-binding domain of FprA (monomer A of FprA-NADPO) onto the equivalent domain of AR results in rmsds below 0.85 Å (164 CR pairs) for all AR structures while superposition of the NADP-binding domain produces rmsds below 1.8 Å (212 CR pairs). However, some differences exist in the domain orientations. This aspect was investigated by calculating the rotation angle required to optimally superimpose the NADP-binding domain of FprA onto that of AR, starting with the FAD-binding domains superimposed. The smallest value (4.5°) resulted from the superposition between FprA and AR cocrystallized with $NADP^+$. The corresponding angle was 6° for AR soaked in NADP(H) and 8.3° for AR in complex with adrenodoxin. This analysis indicated that FprA and AR differ in that FprA domains adopt a slightly more “open” orientation relatively to the AR structures.

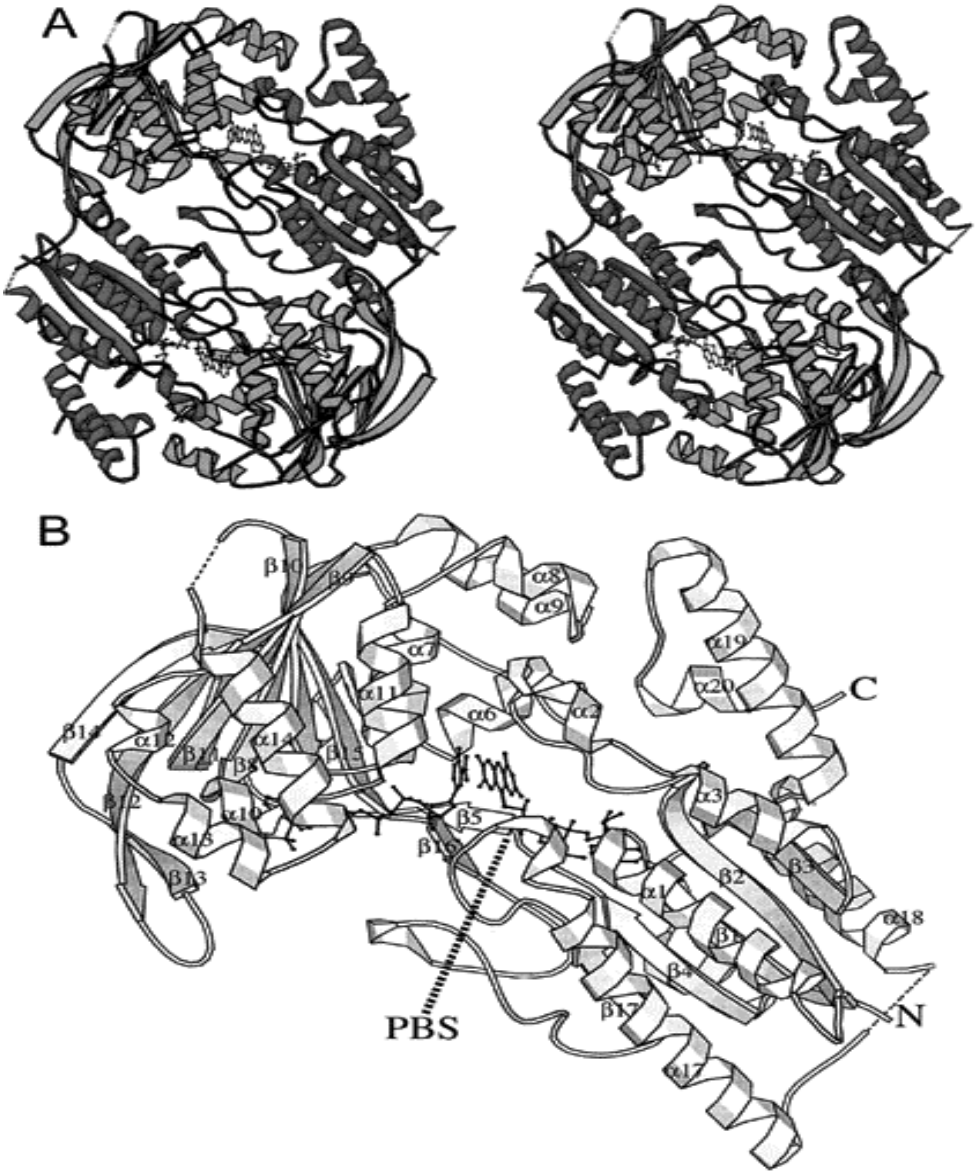

Figure 26. Three-dimensional structure of FprA. **A**, Stereoview of the FprA dimer. The noncrystallographic 2-fold axis is perpendicular to the plane of the drawing. The modified $NADP^+$ ligand is black. The dashed lines connect residues at the borders of disordered regions of the protein. **B**, FprA monomer. Secondary structures are labeled as in **Figure 24**. The letters "N" and "C" indicate the N-terminal and C-terminal residues, respectively. The putative binding site for the protein partner is labeled as "PBS". It is located in a cleft between the FAD-binding and NADP-binding domains.

The binding site for adrenodoxin in AR is formed by a shallow cleft (**Fig. 26B**), which is located between the FAD-binding and NADP-binding domains[218]. Several charged residues on the cleft surface take part in the interaction with the protein partner. It is noticeable that many of these amino acids are conserved in FprA (Lys24, Arg213, Lys246, Arg362, and Asp374), consistent with the observation that FprA binds bovine adrenodoxin and possesses NADPH-adrenodoxin oxidoreductase activity[144]. A search of the *M. tuberculosis* genome revealed no genes coding proteins that have clear homology to adrenodoxin. Thus, the similarity between AR and FprA in the binding site is likely to reflect conservation in the electrostatic nature of the interaction with their respective protein partners, which, however, may be structurally dissimilar.

NADP+ Derivative. The NADP ligand binds in an extended conformation in a solvent-accessible position being in contact with many ordered water molecules (**Fig. 26** and **27B**). As usual for this kind of nucleotide-binding fold[120,235,236], the substrate ADP moiety is accommodated within the NADP-binding domain. The nicotinamide ring is bound at the domain interface between the FAD isoalloxazine ring and Asn157 with the substrate amide group H-bonded to the side chain of Glu211. The nicotinamide is essentially parallel to the flavin (**Fig. 28A**) with an angle between the two rings of 9°. The reactive C4 atom of $NADP^+$ is at 3.27 Å from N5 of FAD in monomer A and at 3.31 Å in monomer B. An unexpected feature, emerged during refinement, was an additional electron density present on the nicotinamide ring of both monomers of FprA-NADPO (**Fig. 25A**). The detailed investigation of the electron density and the environment of the ligand led us to the conclusion that the additional density represents an extra oxygen atom linked through a carbonylic bond to the C4 atom of $NADP^+$ (**Fig. 25B**).

There are many data in support of this interpretation.

(i) The planarity of the nicotinamide ring was assessed by calculating the angle α_N between the planes N1-C2-C6 and C2-C3-C6 and the angle α_C between the planes C2-C3-C6 and C3-C4-C5. These parameters are useful to quantitatively assess the "out-of-plane" position of the N1 and C4 atoms of the ring, respectively[237]. The resulted values were $\alpha_N = 2.6°$ and $\alpha_C = 0.6°$ for monomer A and $\alpha_N = 0.3°$ and $\alpha_C = 1.5°$ for monomer B. These values indicate that the nicotinamide ring is almost perfectly planar and support the notion that the C4 atom has trigonal planar configuration.

(ii) The position of the extra atom was defined by refining without setting any restraint on distances and angles on $NADP^+$. The result of these calculations was the placement of this atom at 1.27 Å from C4 in monomer A and 1.23 Å in monomer B (**Fig. 25B**). These values are in perfect agreement with the presence of a carbonylic oxygen bound to C4.

(iii) The extra atom is within H-bond distance from two water molecules and the nitrogen atom of the amide moiety of nicotinamide. The latter H-bond is made possible by the *cis* conformation of the amide of the FprA-bound $NADP^+$ (*i.e.* the oxygen points towards the ribose, see **Fig. 25A** and **27B**).

(iv) The shape of the electron density for the extra atom, contoured at different levels, is in good agreement with it being an oxygen. This assignment could be made thanks to the atomic resolution of the X-ray analysis, which allowed us to distinguish between oxygen and nitrogen atoms for all Asn and Gln amide moieties of the protein. The *B*-factor of the oxygen atom is 16.6 $Å^2$ in monomer A and 11.7 $Å^2$ in monomer B. These values do not differ from the *B*-factors of the other atoms of the nicotinamide ring implying that the $NADP^+$ derivative is bound with full occupancy to both subunits of the crystalline enzyme. Taken together, these data strongly indicate that the modified $NADP^+$ is a quinonic compound as depicted in **Figure 25B** (this compound has been named NADPO).

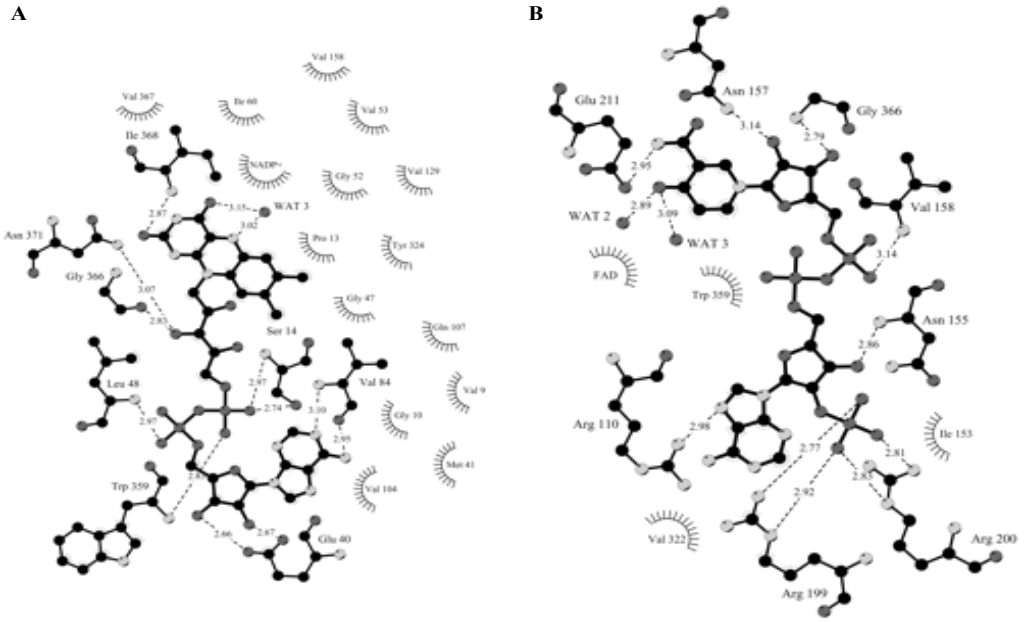

Figure 27. Schematic representation of the binding of **A**, FAD and **B**, modified $NADP^+$ to monomer A of FprA-NADPO. H-bonds are shown as black-broken lines. Distances are in Å. Shading around atoms and residue labels indicates involvement in van der Waals contacts. Atoms are color coded as follows: black, carbon; dark gray, oxygen and phosphorus; light gray, nitrogen.

The active site of FprA is a highly polar environment with basic and acidic residues as well as several water molecules. All these elements have ordered conformations and set up an intricate network of hydrogen bonds. In this milieu, a central role is fulfilled by two water molecules, which in monomer A have been designated water2 and water3 (**Fig. 28A**). They are both H-bonded to the oxygen atom of NADPO being on different sides of the nicotinamide plane (**Fig. 28A**). They also

interact with several active site residues and water3 is bound to the N5 and O4 atoms of FAD (**Fig. 27A, 28A** and **28B**).

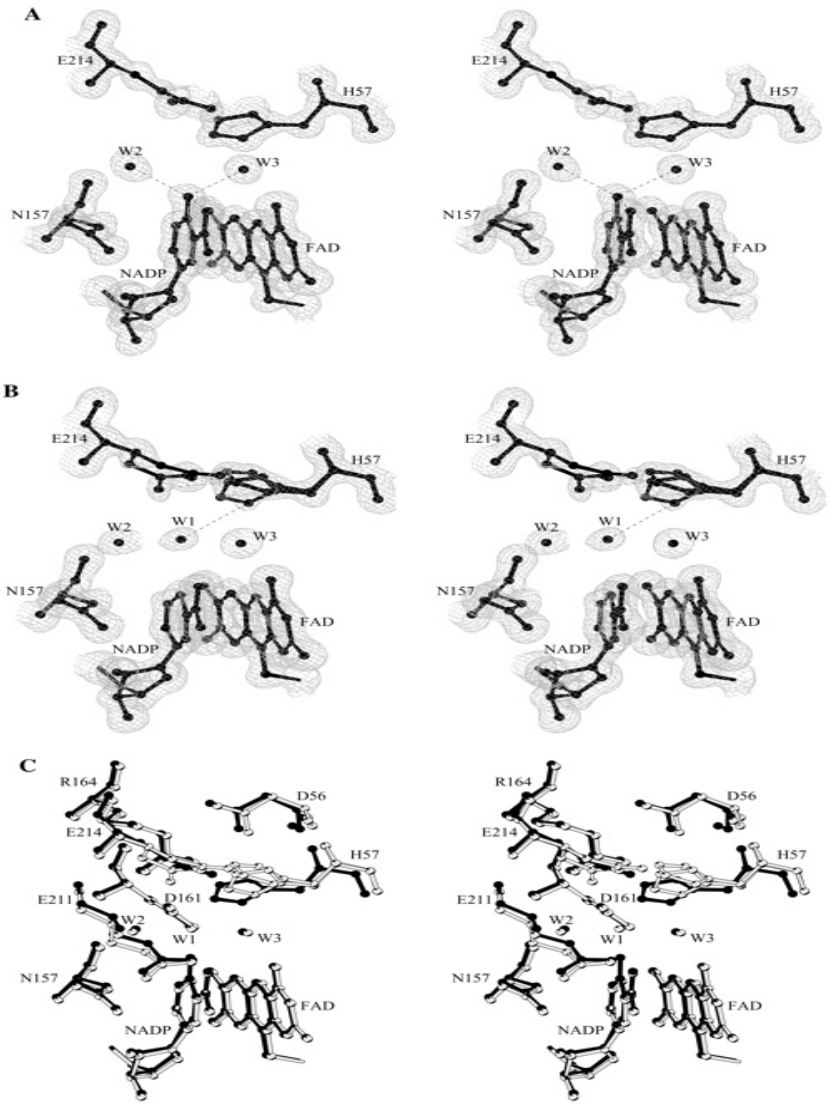

Figure 28. Active site of FprA monomer A. The orientation is the same as that in **Figure 26**. H-bonds are outlined by dashed lines. Water molecules are labeled by "W". Water molecules *B*-factor values are W2 = 16.2 Å^2 and W3 = 9.9 Å^2 for FprA-NADPO; W1 = 24.1 Å^2, W2 = 22.0 Å^2 and W3 = 13.4 Å^2 for FprA$_{red}$-NADPH. **A**, Stereo diagram of the electron density of the modified nicotinamide ring and neighboring

residues (contoured at 1σ) in the FprA-NADPO complex. **B**, Stereo diagram of the active site of $FprA_{red}$-NADPH structure. His57 and Glu214 have alternate conformations (see text). **C**, Superposition of the active site residues of FprA-NADPO (black) and $FprA_{red}$-NADPH (light gray) structures.

Characterization by Mass Spectrometry. In electrospray ionization mass spectrometry (ESI-MS) proteins are detected as multi-protonated species. Initial mass spectrometry experiments on FprA incubated with $NADP^+$ were performed under pseudo-physiological conditions (50 mM ammonium acetate, pH 6.8) allowing direct observation of functional multi-component protein complexes[100]. The mass spectrum displayed an intensive charge state distribution comprising four abundant ions carrying 16-13 protons with the 15-fold protonated ion at *m*/*z* 3405 predominating. To facilitate interpretation we deconvoluted the conventional ESI mass spectrum to the so-called "zero-charge" mass spectrum allowing direct extraction of the molecular mass of the analyzed species (**Fig. 29A**). Centroiding the mass peak of the transformed mass spectrum gave an average mass of 51 040 ± 10 Da corresponding to the ternary complex consisting of the FprA monomer, FAD and $NADP^+$. Unfortunately the mass determination was not sufficient to distinguish if $NADP^+$ or its derivative was present.

To obtain the molecular masses of the apoprotein and the individual ligands, we transferred the protein stock solution into 0.7% formic acid. Under these conditions the protein should denature releasing noncovalent ligands. ESI mass spectra acquired from denaturing solutions were dramatically different from that obtained in near physiological solutions exhibiting a broad charge state distribution of highly protonated protein ions located below *m*/*z* 1 600. The "zero-charge" mass spectrum obtained after deconvolution is depicted in **Figure 29A**. The obtained molecular mass of the apo-FprA monomer was 49 477 ± 5 Da in good agreement with the expected average mass of FprA derived from the gene sequence after adding the residue mass for the initiation methionine (average M_{th} = 49 472.3 Da).

Besides the apoprotein ions, molecular ions at *m*/*z* 744.1, 760.3 and 786.1 were present in the lower *m*/*z* range indicating the presence of $NADP^+$, the proposed $NADP^+$ derivative and FAD, respectively. Interestingly, $NADP^+$ is detected as an M^+ ion because of its pre-existing fixed positive charge on the nicotinamide moiety whereas the other two cofactors are detected as the commonly observed $[M+H]^+$ ions.

Collisionally induced dissociation (MS/MS) experiments yield structure-specific fragment ions that allow assessing the compound identity. For example, MS/MS experiments on the selected $[M+H]^+$ ion of FAD at *m*/*z* 786 resulted in three fragment ions at *m*/*z* 136, 348 and 439 representing the adenine, the adenosine 5'-monophosphate and the riboflavin 5-monophosphate moiety, respectively.

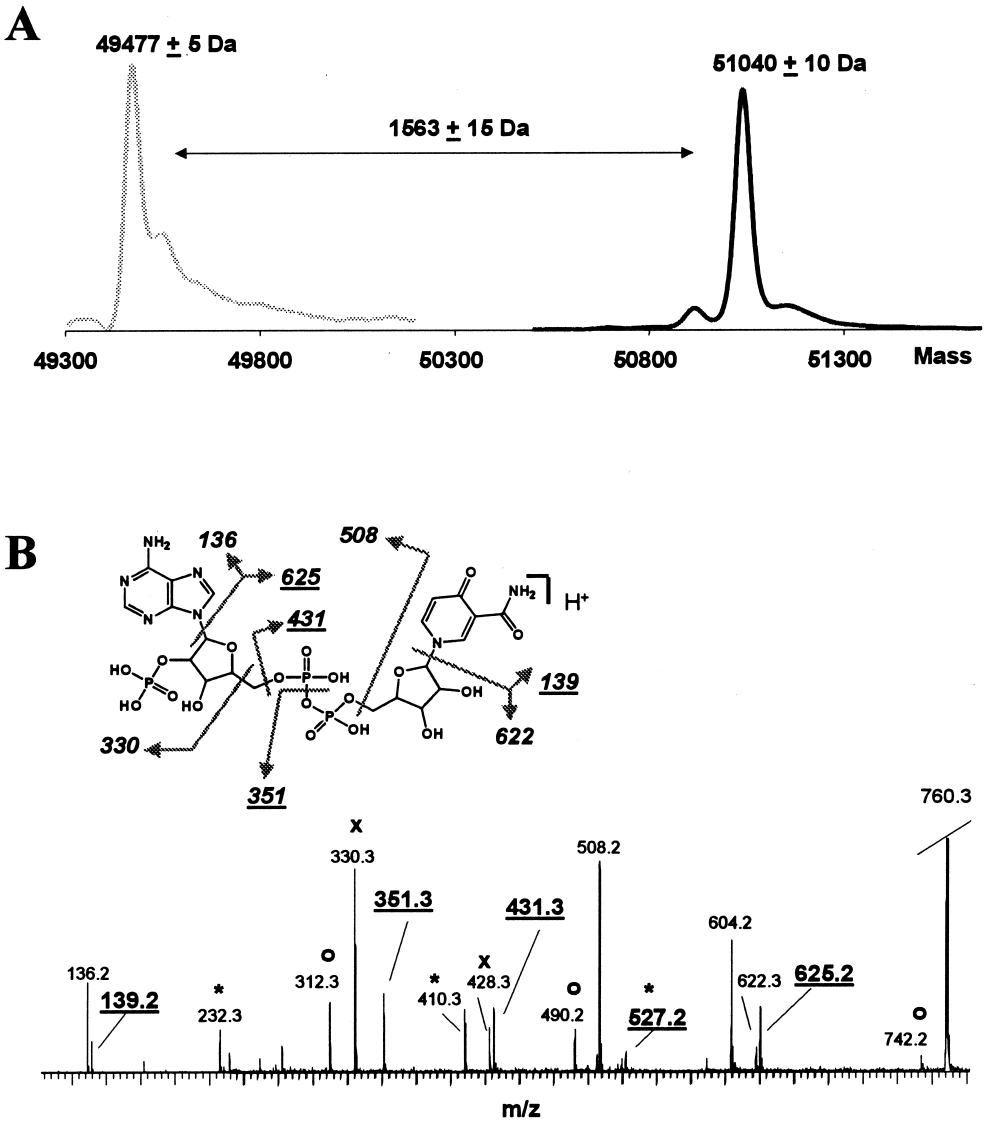

Figure 29. A, Comparison of the deconvoluted mass spectrum obtained for the apoform of FprA (gray line, M_r = 49 477 ± 5 Da) and the FprA-NADPO holoprotein (black line, M_r = 51 040 ± 10 Da). **B**, Fragment ions spectrum and fragmentation scheme of the $NADP^+$ derivative (MH^+ 760.3). The underlined fragment ions are indicative of the $NADP^+$ derivative. Fragment ions marked with *****, **x**, and **o** originate from low-energy fragmentation pathways and refer to the loss of H_3PO_4 (Δm = 98 u), HPO_3 (Δm = 80 u) and H_2O (Δm = 18 u), respectively.

Thus these structure-specific fragment ions unequivocally confirmed the original assignment of the *m*/*z* 786 ion as the molecular ion of FAD. In a similar fashion we used MS/MS to identify the ion at *m*/*z* 760, the proposed molecular ion of NADPO. For this purpose we compared the fragment ions of the parent ion at *m*/*z* 760 with the fragment ions that resulted from MS/MS of the parent ion at *m*/*z* 744, the M^+ ion of $NADP^+$. Several structure-specific fragment ions were observed beside fragment ions that originated from low energy fragmentation pathways such as the loss of H_3PO_4 (Δm 98 u), HPO_3 (Δm 80 u) and H_2O (Δm 18 u). The structure-specific fragment ions of NADPO are depicted in **Figure 29B**.

The fragment ions at *m*/*z* 136, 330, 508 and 622 were also observed for $NADP^+$ while the fragment ions at *m*/*z* 139, 351, 431 and 625 were specific for the $NADP^+$ derivative. The observation of the fragment ions at *m*/*z* 351 and 139 allowed the assignment of the derivative to the nicotinamide moiety. It is noteworthy that the *m*/*z* values of all observed derivative-specific fragment ions were consistent with the covalent modification being due to a carbonylic oxygen. Most importantly, the mass spectrometry analysis unambiguously showed that formation of the covalent adduct occurs in solution and is, therefore, not an artifact of the crystallization process.

NADPH-Soaked FprA. Soaking of the crystals in an NADPH-containing solution resulted in the reduction of the crystalline enzyme as indicated by the loss of the crystal yellow color. To investigate the reactivity of the crystalline enzyme we subjected the crystals to microspectrophotometry analysis[220]. UV-visible absorption spectra of an FprA crystal are shown in **Figure 30**. Upon soaking in NADPH under aerobic conditions the height of the typical absorption peak at 452 nm of the enzyme-bound oxidized cofactor[144] decreases coupled to increased absorption at longer wavelengths. These features suggest that NADPH soaking leads to cofactor reduction with FAD mainly in the semiquinone one-electron reduced form. In the NADPH-soaked structure the conformation of the nicotinamide ring deviates from planarity (α_N = 4.8° and α_C = 7.8° for monomer A and α_N = 5.1° and α_C = 4.8° for monomer B). This geometry supports the presence in the crystals of the reduced form of the ligand[237], which therefore has been modeled as NADPH. This interpretation is in agreement with solution studies, which have shown that aerobic incubation of FprA with excess NADPH leads to accumulation of the neutral semiquinone form of FAD and formation of a stable complex between the protein and the reduced substrate[144].

The overall structures of FprA-NADPO and $FprA_{red}$-NADPH are essentially identical with an rmsd of 0.29 Å for 6 894 atoms. However, enzyme reduction is associated with a few differences in the active site. A first observation concerns the flavin conformation. The angle between pyrimidine and dimethylbenzene rings in $FprA_{red}$-NADPH is 7.9°. This value, although small, is twice the corresponding angle observed in the oxidized enzyme and indicates a slight bent

in the reduced cofactor conformation. A more significant difference with respect to FprA-NADPO was found in the NADP ligand. Namely, the additional electron density on the C4 atom was not present in the $FprA_{red}$-NADPH structure (**Fig. 28B**). Rather, a peak of electron density was found in proximity of the C4 atom but not continuous with its density. This peak was identified as a water molecule located at 3.39 Å from the C4 atom of NADPH and involved in several bifurcated H-bonds with active site residues. This water molecule has been found in monomer A but not in chain B of $FprA_{red}$-NADPH although the extra oxygen covalently bound to C4 was absent also in monomer B. This unique water molecule of $FprA_{red}$-NADPH has been named water1. The absence of the NADP covalent modification does not alter the conformation of the ligand, which is indistinguishable from that found in the oxidized enzyme.

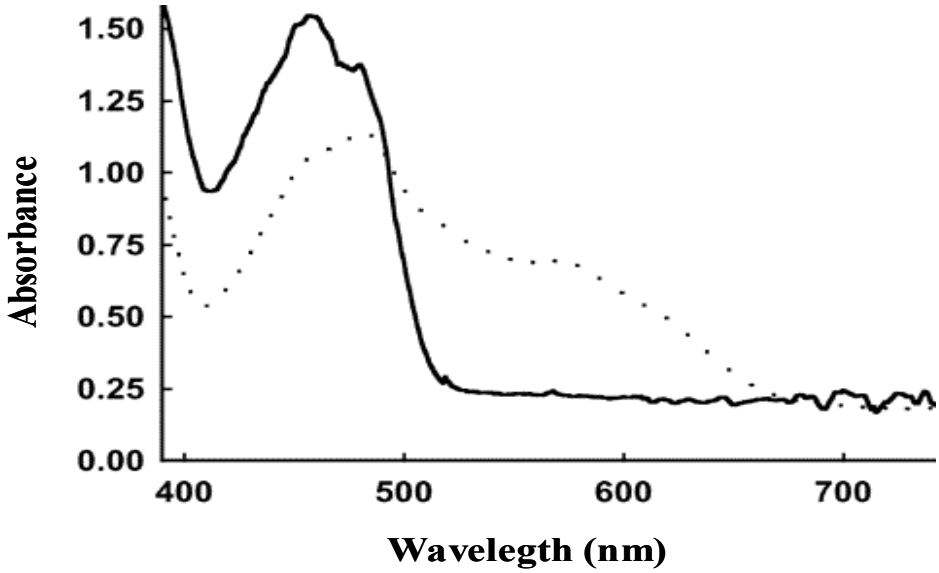

Figure 30. Microspectrophotometric analysis of FprA crystals. Polarized absorption spectra were recorded on an oriented crystal with the electric vector of the linearly polarized light parallel to the *a* crystal axis. The spectrum of the oxidized crystal is shown in solid line while the dashed line is the spectrum recorded on the same crystal after 30 min of soaking in 10 mM NADPH under aerobic conditions.

Some interesting differences between FprA-NADPO and $FprA_{red}$-NADPH concern two active site residues, His57 and Glu214. These side chains are positioned above FAD and $NADP^+$ with their side chains H-bonded to each other (**Fig. 28**). In subunit A of the $FprA_{red}$-NADPH structure, these residues display an electron density consistent with a double conformation. In these two alternate conformations His57 and Glu214 are displaced by ~1 Å away from the nicotinamide ring relatively to the conformation found in FprA-NADPO (**Fig. 28C**). This

displacement creates a space that is filled by water1. In one of the alternate conformations of His57, the N_δ atom is within H-bond distance from this water molecule while the N_ϵ atom is H-bonded to the side chain of Glu214. The shifted conformations of His57 and Glu214 are not present in subunit B of $FprA_{red}$-NADPH where they adopt the same conformation present in the oxidized protein. This is likely due to the different crystal contacts. In subunit A, these two active site residues are far from a symmetry related protein molecule. They have the freedom to move and adopt double conformations allowing water1 to place itself in the active site. On the contrary in monomer B, a symmetry related molecule is in contact with these residues being at ~4.5 Å from them. Therefore, in monomer B, crystal packing interactions seem to prevent the conformational changes observed in monomer A. However, the presence of unmodified NADPH in both subunits of the $FprA_{red}$-NADPH complex indicates that the exchange of NADPO for NADPH in the crystal lattice can occur. The relative positioning of the nicotinamide and flavin rings observed in the two FprA complexes is perfectly suited for the hydride transfer reaction thought to underlie the NADPH-dependent oxidation of FAD[144]. Such a steric relation between the substrate and the cofactor is very similar to that found in the structures of AR and several other NAD-(P)H-dependent flavoproteins[217,236] in which a hydride transfer mechanism is known to occur.

Mechanism of NADP+ Modification. The geometry of the active site observed in the $FprA_{red}$-NADPH structure suggests a possible mechanism for formation of the NADPO compound found in the oxidized enzyme (**Fig. 31**). With reference to monomer A of $FprA_{red}$-NADPH, Glu214, His57 and water1 appear to form a sort of catalytic triad[238]. In one of the alternate conformations the side-chain oxygens of Glu214 are H-bonded to the N_ϵ atom of His57 while the N_δ atom of the histidine is within H-bond distance from water1 (**Fig. 28B**). This geometry is reminiscent of the catalytic triad of serine proteases[238] with water1 fulfilling the role of the serine $O\gamma$ atom in proteases. Thus the interaction of Glu214 with the imidazole group should increase the basicity of His57, which in turn would become more prone to accept a proton from water1. The final result would be a transient salt bridge between Glu214 and the positively charged His57 and a hydroxyl ion in place of water1. This ion can carry out a nucleophilic attack on the C4 atom of $NADP^+$ yielding a covalent adduct with a hydroxyl group introduced on the substrate. The subsequent step would be hydride transfer from C4 of the hydroxylated NADPH to N5 of FAD coupled to proton release from the -C4-OH group of the hydroxylated NADPH. The ultimate result of these reactions is the modified $NADP^+$ as seen in the FprA-NADPO structure.

Several observations support the proposed mechanism. Water1 lays slightly out of the nicotinamide plane on the side opposite to that facing the flavin. Thus, the hydroxyl group resulting from the nucleophilic attack by the water would point away from the cofactor. Conversely, the C4-bound hydrogen atom of the hydroxylated NADPH would point towards the flavin as required for the postulated hydride transfer reaction (**Fig. 31**). Another point is the

geometry of the "FprA triad". It is known that in the classical triads the carboxylate-imidazole interaction has usually a favorable geometry while the H-bond between imidazole and the Ser Oγ is often strained[238]. This decreases the energy of this bond and favors the proton-relay process. In FprA this is actually the observed situation. The interaction between Glu214 and His57 is well in agreement with ideal H-bond geometry whereas the pair His57-water1 is interacting through a much more distorted H-bond (distance N_{δ}-water1 = 3.28 Å, angle C_{β}-N_{δ}-water1 = 59°).

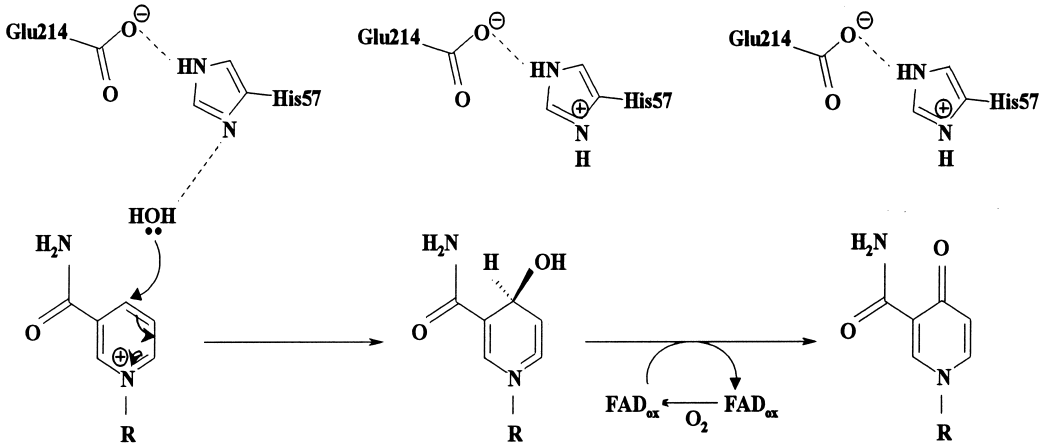

Figure 31. Proposed mechanism for $NADP^+$ derivative formation. The water molecule performing the nucleophilic attack is proposed to correspond to water1 found in the $FprA_{red}$-NADPH structure (see **Fig. 28B**).

For $NADP^+$ modification to occur, the C4 atom of the FprA-bound $NADP^+$ must have an electrophilic character. The neighboring electron-deficient oxidized flavin should exert a polarizing effect on the reactive carbon atom of $NADP^+$ making it more prone to a nucleophilic attack. An additional effect might be due to the *cis* conformation of the nicotinamide ring, which places the amide nitrogen at 2.65 Å from the extra oxygen atom of NADPO. The presence of this intramolecular H-bond interaction may stabilize the derivative thereby facilitating its formation. The *cis* conformation of the FprA-bound $NADP^+$ is unusual since, in most NADP-binding proteins, the *trans* conformation is found[239]. To our knowledge, the $NADP^+$ derivative of FprA has not been found in other enzyme structures. The crystallographic and mass spectrometry data show that the derivative forms upon incubation of the oxidized protein with $NADP^+$. Whether derivative formation can occur in the cellular environment and whether it has any physiological role are subjects for future studies.

Acknowledgements

The protein crystallography group of the University of Pavia is member of the *Mycobacterium tuberculosis* Structural Genomics Consortium whose support is gratefully acknowledged. We thank the EMBL/DESY staff for assistance during data collection. This work was supported by grants from the Ministero della Università e Ricerca Scientifica e Tecnologica ("Biologia strutturale e dinamica di proteine redox" and "Caratterizzazione funzionale, strutturale e genetica della glutammil-tRNA riduttasi di *M. tuberculosis*"), the European Union ("Quality of Life and Management of Living Resources", Contract QLK2-2000-01761) and the Netherlands Organization for Scientific Research (NWO #99508).

Data deposition: coordinates of *M. tuberculosis* FprA structures in the oxidized and reduced form have been deposited in the Protein Data Bank[240] with the accession codes 1LQT and 1LQU, respectively.

Chapter 6

Summarizing Discussion

«Health is the silence of molecules, cells, tissues and organs.»
R. LUISE KRAUTH-SIEGEL
& R. HEINER SCHIRMER

With the advent of the 'soft' electrospray ionization technique in the late 1980's, the mass range of species amendable to mass spectrometric analysis has been increased immensely. Nowadays, noncovalent species with masses well over one million Dalton can be transferred intact from the solution-phase into the gas-phase, which brings the technique to the level of intact protein oligomers and functional machineries. This has led to the birth of a new field in biomolecular mass spectrometry, the so-called native mass spectrometry, which focuses on the analysis of intact proteins and protein complexes under pseudo-physiological conditions. Thus, native mass spectrometry is a relatively new player in the field of structural biology, which can provide information about protein tertiary and quaternary structure, stoichiometries, ligand or cofactor binding, cooperative effects and stability and dynamics of protein assemblies. These data are mostly complementary to established structural biology techniques such as NMR, X-ray crystallography, small-angle X-ray scattering (SAXS) and electron microscopy. In this work we aimed to obtain structure-function relationships of the four flavin-containing proteins PHBH, VAO, HAPMO and FprA by using native mass spectrometry tools. For this we focused on oligomerization behavior, cofactor binding, cooperativity effects, protein stability and cofactor modification. As is clear from **Table I** in the introductory chapter relatively few studies have described the functional characterization of flavoproteins by native ESI-MS methods.

Nano-ESI-MS of the noncovalent protein assemblies PHBH and VAO

Chapter 2 describes in detail the importance of nano-ESI-MS parameters to successfully detect noncovalent high molecular weight assemblies. High-pressure optimization and fine voltage tuning appeared to be prerequisites for efficient transmission and analysis of large protein ions. To illustrate this phenomenon, we analyzed the two flavoproteins PHBH and VAO under pseudo-physiological conditions. Our findings that highOur findings that high *m/z* ions are detected more efficiently at higher pressures can be explained by the previously described collisional cooling effect[39]. New is the finding that on our instrument (a slightly modified Micromass LC-T) the effect of the elevated pressure varies depending on the nature (size, *m/z*…) of the analyzed ionic species. Changing the source pressures results in an *m/z* discriminative effect in ion detection; different *m/z* ions will be decelerated differently, owing to their different velocities (kinetic energies) and collisional cross-sections. It is not clear, at present, whether the observed *m/z*-dependent pressure effect is general or unique for the equipment used. We observed similar *m/z*-dependent effects on two LC-Ts and one Q-ToF-1 instrument. Conversely, we did not observe any significant pressure effect for ions with values below *m/z* 1 500, but peak broadening. This peak broadening is probably due to the unfocusing of the ion beam of low *m/z* ions. One has to be careful as high cone

voltages are beneficial for desolvating and cooling of large *m/z* ions, they may promote dissociation/fragmentation of low *m/z* ions. Thus, a careful adjustment of the pressure and the cone voltage, possibly different for each protein assembly and mass spectrometer, will give the best result.

Cooperativity effect of cofactor binding and VAO oligomerization

The knowledge about the nano-ESI-MS parameters gained in chapter 2 was used to investigate structure-function relationships of the target flavoproteins. In chapter 3 we studied the cooperative effect of FAD cofactor binding on VAO oligomerization. Under native conditions, wild type VAO was almost exclusively detected as an octameric species. In sharp contrast, apo-VAO H61T measured under the same experimental conditions was exclusively detected as a dimer. With a 10-fold molar excess of FAD, the mass spectrum of VAO H61T clearly revealed the presence of dimeric and octameric species. Whereas the dimer was saturated with 2 molecules of FAD, the octamer was an ensemble of species containing up to 8 molecules of FAD. These results strongly suggest a cooperative effect of FAD binding and octamerization. Addition of 5'-ADP to apo-H61T revealed, similar to the experiments with FAD, a strongly induced octamerization and interaction of 5'-ADP to both dimeric and octameric species. In sharp contrast to FAD or 5'-ADP, FMN did not induce formation of the octamer. The ESI-MS data were validated by size-exclusion chromatography; holo-H61T VAO was mainly present as octamer, whereas apo-H61T was mainly present as dimer. This work shows that native ESI-MS is a very powerful method to study cooperativity effects in proteins. In fact, the ability to distinguish between different oligomeric species containing different amounts of FAD is an almost unique property of this mass spectrometry method.

First direct evidence of continued binding of NADP(H) to HAPMO and its influence on enzyme stability

In chapter 4 we described a study towards the binding charactistics of the nicotinamide coenzyme during the HAPMO catalytic cycle with the aim to gain mechanistic insight. In addition, we studied the structural role of the coenzyme. For the HAPMO homologue cyclohexanone monooxygenase, there is evidence from kinetic studies that the initially formed $NADP^+$ remains bound to the enzyme during the substrate oxygenation process[197]. This suggests that, durig catalysis, the enzyme is virtually continuously occupied by the reduced or oxidized coenzyme. Our real-time ESI mass spectra clearly showed that HAPMO, when functioning as an NADPH oxidase, is in complex with its coenzyme throughout the whole catalytic cycle. This is the first direct evidence of the continued association of the coenzyme to a Baeyer-Villiger monooxygenase. Our results also provide evidence that $NADP^+$ interacts tightly with reduced enzyme, but not with

oxidized enzyme. The association with coenzyme appeared to be crucial for enzyme stability. We proposed that this coenzyme-induced stabilization might also be important for related enzymes. This may also explain the relatively poor stability of many reported isolated coenzyme-dependent enzymes. These real-time nano-ESI-MS measurements are also applicable to other enzymes to obtain information about their mechanism of action.

FprA can produce NADPO

In chapter 5 the determination of the atomic resolution structure of FprA in the oxidized and NADPH-reduced state by X-ray crystallography is reported. Our contribution has been the identification/verification of an enzymatically modified coenzyme by ESI-MS. The most interesting feature of the FprA crystallographic structure was the covalent modification of $NADP^+$. The X-ray data suggested an oxygen atom linked to the reactive C4 atom of the nicotinamide ring. The deconvoluted mass spectrum of native FprA-$NADP^+$ complex revealed a ternary FprA-FAD-$NADP^+$ complex. Unfortunately, the resolution was insufficient to distinguish if $NADP^+$ or its oxygenated derivative was present. Under denaturing conditions, the mass spectrum displayed, besides the FprA apoprotein, peaks corresponding to $NADP^+$, the proposed $NADP^+$ derivative and FAD. Data comparison of collisionally induced dissociation (MS/MS) on the proposed $NADP^+$ derivative and on $NADP^+$ revealed several common, structure-specific fragments as well as fragments specific for the $NADP^+$ derivative, allowing the assignment of the modification to the nicotinamide moiety consistent with a carbonylic oxygen at position C4. The MS analysis unambiguously showed that the covalent adduct is present in solution and, therefore, it is not an artifact of the crystallization process. To our knowledge, this $NADP^+$ derivative produced by FprA has not been detected in other enzymes. The physiological significance of this reaction is presently unknown. However, it could assist drug-design studies, as the modified $NADP^+$ is a potential lead compound for the development of specific inhibitors. Whether the derivative formation can occur in the cellular environment and whether it has any physiological role are subjects for future studies. Very recently, such a modified $NADP^+$ derivative, $NADP(OH)_2$, was identified in an alcohol dehydrogenase[203] using a similar approach as in our project.

Concluding remarks

The data reported in this thesis show that native mass spectrometry is a valuable tool in structural biology to investigate quaternary structures of homogeneous protein complexes, ligand modifications or binding and cooperative effects of ligand binding. Thus, native mass spectrometry can be used to study structure-function relationships of proteins, providing data that are largely complementary to classical structural biology techniques and biochemical assays. In this thesis we focused on homogeneous protein complexes, often oligomers in complex with

cofactors. We have to keep in mind, however, that protein complexes can be far more complex containing various different proteins, nucleic acids and additional smaller molecules. Since a few years native mass spectrometry can also be used to study such assemblies. The most impressive example to data is the analysis of ribosome complexes, consisting of proteins and RNA[241]. A great challenge in the coming years is to obtain structure-function relationships of large heterogeneous protein assemblies by native mass spectrometry tools. These assemblies are often dynamic entities with transient binding partners and with complex regulation and mechanism of action. Mass spectrometry will be especially suited to analyze these assemblies, as classical structural biology techniques are often limited in mass range, cannot analyze an ensemble of species or require larger amounts of protein. To reach these aims several technological advances are made or have to be made in the near future. An important aspect is the detection of large *m/z* ions. At present, the flight through and the detection of larger macromolecular ions exhibiting high *m/z* ratios are in mass spectrometry generally less efficient than of smaller lower *m/z* ions. In order to routinely analyze larger assemblies an increase in sensitivity and/or efficiency is needed. Current developments in this area include cryo-detectors that allow detection of large molecules without loss of sensitivity in the high mass region and improved time-of-flight analyzers for increased resolution and sensivity in the high mass region.

Fascinating developments that allow the extraction of even more information from ionized protein species include ion mobility-mass spectrometry hybrids and tandem mass spectrometry of large proteins ions. Ion mobility spectrometry provides insights into gas-phase ion conformations. In such a set-up protein ions are pulsed into an ion mobility device and separated based on their ability to traverse the drift cell under the influence of a weak electrostatic field. The mobility of an ion is a function of mass, charge and physical size and shape. Ion mobility coupled to mass spectrometry thus combines separation on the basis of size and shape and *m/z*. Tandem mass spectrometry, on the other hand, can provide information about stoichiometry, molecular architecture and binding energies of the interacting partners (see also Chapter 1). Other current developments include size-exclusion chromatography coupled to mass spectrometry and mass spectrometry-electron microscopy combinations. Both combinations will increase the applications of native mass spectrometry to analyze protein assemblies.

The kinetic experiments in this thesis are performed at a minute timescale, thus by far not sufficient to study single enzyme turnover. Some research groups have already coupled rapid mixing devices with a mass spectrometry to study enzyme mechanism of action, however, to date the amounts of enzyme needed for these experiments go beyond the amounts one can obtain of most non-commercial enzymes. A promising approach to miniaturize these devices would be the use of microfluidics. Such a development would enlarge the scope of mass spectrometry to study enzyme kinetics enormously.

References

1. Cramer P, Bushnell DA, Kornberg RD. Structural basis of transcription: RNA polymerase II at 2.8 angstrom resolution. *Science* 2001;292(5523):1863-1876.
2. Janin J, Wodak SJ. Protein modules and protein-protein interaction. Introduction. *Adv Protein Chem* 2002;61:1-8.
3. Schwikowski B, Uetz P, Fields S. A network of protein-protein interactions in yeast. *Nat Biotechnol* 2000;18(12):1257-1261.
4. Macheroux P. UV-visible spectroscopy as a tool to study flavoproteins. *Methods Mol Biol* 1999;131:1-7.
5. Ghisla S, Massey V, Lhoste JM, Mayhew SG. Fluorescence and optical characteristics of reduced flavines and flavoproteins. *Biochemistry* 1974;13(3):589-597.
6. Ghisla S, Massey V. Mechanisms of flavoprotein-catalyzed reactions. *Eur J Biochem* 1989;181(1):1-17.
7. Van Berkel WJ, Benen JA, Eppink MH, Fraaije MW. Flavoprotein kinetics. *Methods Mol Biol* 1999;131:61-85.
8. Reed J, Kinzel V. Near- and far-ultraviolet circular dichroism of the catalytic subunit of adenosine cyclic 5'-monophosphate dependent protein kinase. *Biochemistry* 1984;23(7):1357-1362.
9. Apiyo D, Wittung-Stafshede P. Presence of the cofactor speeds up folding of *Desulfovibrio desulfuricans* flavodoxin. *Protein Sci* 2002;11(5):1129-1135.
10. Greenfield NJ. Application of circular dichroism in protein and peptide. *Trends Anal Chem* 1999;18(4):236-244.
11. Vanoni MA, Curti B, Zanetti G. Glutamate synthase. In: *Chemistry and Biochemistry of Flavoenzymes III*. Muller F, ed. Florida, USA. Boca Raton, CRC Press, 1992:309-317.
12. Santoro MM, Bolen DW. Unfolding free energy changes determined by the linear extrapolation method. 1. Unfolding of phenylmethanesulfonyl alpha-chymotrypsin using different denaturants. *Biochemistry* 1988;27(21):8063-8068.
13. McClain DL, Binfet JP, Oakley MG. Evaluation of the energetic contribution of interhelical Coulombic interactions for coiled coil helix orientation specificity. *J Mol Biol* 2001;313(2):371-383.
14. Mayhew SG, Tollin G. General properties of flavodoxins. In: *Chemistry and Biochemistry of Flavoenzymes III*. Muller F, ed. Florida, USA. Boca Raton, CRC press, 1992:389-426.
15. Munro AW, Lindsay JG, Coggins JR, Kelly SM, Price NC. Analysis of the structural stability of the multidomain enzyme flavocytochrome P-450 BM3. *Biochim Biophys Acta* 1996;1296(2):127-137.
16. Berry A, Scrutton NS, Perham RN. Switching kinetic mechanism and putative proton donor by directed mutagenesis of glutathione reductase. *Biochemistry* 1989;28(3):1264-1269.
17. Van Den Berg PAW, Van Hoek A, Visser J, Walentas CD, Perham RN. Time-resolved flavin fluorescence quenching in *E.coli* glutahione reductase. In: *Flavins and Flavoproteins XII*. Stevenson KJ, Massey V, Williams CH, Jr., eds. Calgary, Alberta, Canada. University of Calgary Press, 1997:697-701.
18. Doyle ML. Characterization of binding interactions by isothermal titration calorimetry. *Curr Opin Biotechnol* 1997;8(1):31-35.
19. Jelesarov I, Bosshard HR. Isothermal titration calorimetry and differential scanning calorimetry as complementary tools to investigate the energetics of biomolecular recognition. *J Mol Recognit* 1999;12(1):3-18.
20. Leavitt S, Freire E. Direct measurement of protein binding energetics by isothermal titration calorimetry. *Curr Opin Struct Biol* 2001;11(5):560-566.
21. Velazquez-Campoy A, Leavitt SA, Freire E. Characterization of protein-protein interactions by isothermal titration calorimetry. *Methods Mol Biol* 2004;261:35-54.
22. Cole JL, Hansen JC. Analytical ultracentrifugation as a contemporary biomolecular research tool. *J Biomol Tech* 1999;10(4):163-176.
23. Laue TM, Stafford WF, 3rd. Modern applications of analytical ultracentrifugation. *Annu Rev Biophys Biomol Struct* 1999;28:75-100.
24. Liu J, Shire SJ. Analytical ultracentrifugation in the pharmaceutical industry. *J Pharm Sci* 1999;88(12):1237-1241.
25. Taylor IA, Eccleston JF, Rittinger K. Sedimentation equilibrium studies. *Methods Mol Biol* 2004;261:119-136.
26. Bottcher B, Wynne SA, Crowther RA. Determination of the fold of the core protein of hepatitis B virus by electron cryomicroscopy. *Nature* 1997;386(6620):88-91.

27. Zuiderweg ER. Mapping protein-protein interactions in solution by NMR spectroscopy. *Biochemistry* 2002;41(1):1-7.
28. Vervoort J, Muller F, Lee J, Van Den Berg WA, Moonen CT. Identifications of the true carbon-13 nuclear magnetic resonance spectrum of the stable intermediate II in bacterial luciferase. *Biochemistry* 1986;25(24):8062-8067.
29. Clore GM, Gronenborn AM. New methods of structure refinement for macromolecular structure determination by NMR. *Proc Natl Acad Sci* 1998;95(11):5891-5898.
30. Aebersold R, Mann M. Mass spectrometry-based proteomics. *Nature* 2003;422(6928):198-207.
31. Gavin AC, Bosche M, Krause R, Grandi P, Marzioch M, Bauer A, Schultz J, Rick JM, Michon AM, Cruciat CM, Remor M, Hofert C, Schelder M, Brajenovic M, Ruffner H, Merino A, Klein K, Hudak M, Dickson D, Rudi T, Gnau V, Bauch A, Bastuck S, Huhse B, Leutwein C, Heurtier MA, Copley RR, Edelmann A, Querfurth E, Rybin V, Drewes G, Raida M, Bouwmeester T, Bork P, Seraphin B, Kuster B, Neubauer G, Superti-Furga G. Functional organization of the yeast proteome by systematic analysis of protein complexes. *Nature* 2002;415(6868):141-147.
32. Alberts B. The cell as a collection of protein machines: preparing the next generation of molecular biologists. *Cell* 1998;92(3):291-294.
33. Loo JA. Electrospray ionization mass spectrometry: a technology for studying noncovalent macromolecular complexes. *Int J Mass spectrom* 2000;200(1-3):175-186.
34. Heck AJ, Van Den Heuvel RH. Investigation of intact protein complexes by mass spectrometry. *Mass Spectrom Rev* 2004;23(5):368-389.
35. Sobott F, Robinson CV. Protein complexes gain momentum. *Curr Opin Struct Biol* 2002;12(6):729-734.
36. Van den Heuvel RH, Heck AJ. Native protein mass spectrometry: from intact oligomers to functional machineries. *Curr Opin Chem Biol* 2004;8(5):519-526.
37. Fitzgerald MC, Chernushevich I, Standing KG, Whitman CP, Kent SB. Probing the oligomeric structure of an enzyme by electrospray ionization time-of-flight mass spectrometry. *Proc Natl Acad Sci* 1996;93(14):6851-6856.
38. Sobott F, Hernandez H, McCammon MG, Tito MA, Robinson CV. A tandem mass spectrometer for improved transmission and analysis of large macromolecular assemblies. *Anal Chem* 2002;74(6):1402-1407.
39. Krutchinsky AN, Chernushevich IV, Spicer VL, Ens W, Standing KG. Collisional damping interface for an electrospray time-of-flight mass spectrometer. *J Am Soc Mass Spectrom* 1998;9(6):569-579.
40. Tahallah N, Pinkse MW, Maier CS, Heck AJ. The effect of the source pressure on the abundance of ions of noncovalent protein assemblies in an electrospray ionization orthogonal time-of-flight instrument. *Rapid Commun Mass Spectrom* 2001;15(8):596-601.
41. Chernushevich IV, Thomson BA. Collisional cooling of large ions in electrospray mass spectrometry. *Anal Chem* 2004;76(6):1754-1760.
42. Ayed A, Krutchinsky AN, Ens W, Standing KG, Duckworth HW. Quantitative evaluation of protein-protein and ligand-protein equilibria of a large allosteric enzyme by electrospray ionization time-of-flight mass spectrometry. *Rapid Commun Mass Spectrom* 1998;12(7):339-344.
43. Van Den Heuvel* RH, Tahallah* N, Kamerbeek NM, Fraaije MW, Van Berkel WJ, Janssen DB, Heck AJ. Coenzyme binding during catalysis is beneficial for the stability of 4-hydroxyacetophenone monooxygenase. *J Biol Chem* 2005;280(37):32115 - 32121. **Equally contributing authors.*
44. Karas M, Hillenkamp F. Laser desorption ionization of proteins with molecular masses exceeding 10,000 daltons. *Anal Chem* 1988;60(20):2299-2301.
45. Tanaka K, Waki H, Ido Y, Akita S, Yoshida Y, Yoshida T. Protein and polymer analyses up to m/z 100 000 by laser ionization time-of-flight mass spectrometry. *Rapid Commun Mass Spectrom* 1988;2:151-153.
46. Fenn JB, Mann M, Meng CK, Wong SF, Whitehouse CM. Electrospray ionization for mass spectrometry of large biomolecules. *Science* 1989;246(4926):64-71.
47. Karas M, Gluckmann M, Schafer J. Ionization in matrix-assisted laser desorption/ionization: singly charged molecular ions are the lucky survivors. *J Mass Spectrom* 2000;35(1):1-12.
48. Guilhaus M, Selby D, Mlynski V. Orthogonal acceleration time-of-flight mass spectrometry. *Mass Spectrom Rev* 2000;19(2):65-107.
49. Beavis RC, Chait BT. Rapid, sensitive analysis of protein mixtures by mass spectrometry. *Proc Natl Acad Sci* 1990;87(17):6873-6877.
50. Karas M, Bahr U, Ingendoh A, Nordhoff E, Stahl B, Strupat K, Hillenkamp F. Principle and applications of matrix-assisted UV-laser desorption/ionization mass spectrometry. *Anal Chim Acta* 1990;241(2):175-185.
51. Glocker MO, Bauer SH, Kast J, Volz J, Przybylski M. Characterization of specific noncovalent protein complexes by UV matrix-assisted laser desorption ionization mass spectrometry. *J Mass Spectrom* 1996;31(11):1221-1227.

52. Kiselar JG, Downard KM. Preservation and detection of specific antibody-peptide complexes by matrix-assisted laser desorption ionization mass spectrometry. *J Am Soc Mass Spectrom* 2000;11(8):746-750.
53. Wattenberg A, Sobott F, Brutschy B. Detection of intact hemoglobin from aqueous solution with laser desorption mass spectrometry. *Rapid Commun Mass Spectrom* 2000;14(10):859-861.
54. Dole M, Mack LL, Hines RL, Mobley RC, Ferguson LD, Alice MB. Molecular beams of macrions. *J Chem Phys* 1968;49(5):2240-2249.
55. Yamashita M, Fenn JB. Another variation on the free-jet theme. *J Phys Chem* 1984;88(20):4451-4459.
56. Iribarne JV, Thomson BA. On the evaporation of small ions from charged droplets. *J Chem Phys* 1976;64(6):2287-2294.
57. Kebarle P. A brief overview of the present status of the mechanisms involved in electrospray mass spectrometry. *J Mass Spectrom* 2000;35(7):804-817.
58. Peschke M, Blades A, Kebarle P. Charged states of proteins. Reactions of doubly protonated alkyldiamines with NH(3): solvation or deprotonation. Extension of two proton cases to multiply protonated globular proteins observed in the gas phase. *J Am Chem Soc* 2002;124(38):11519-11530.
59. Fernandez de la Mora J. Electrospray ionization of large multiply charged species proceeds via Dole's charged residue mechanism. *Anal Chim Acta* 2000;406(1):93-104.
60. Catalina MI, Van den Heuvel RH, Van Duijn E, Heck AJ. Decharging of globular proteins and protein complexes in electrospray. *Chemistry* 2005;11(3):960-968.
61. Wilm M, Mann M. Electrospray and Taylor-cone theory, Dole's beam of macromolecules at last? *Int J Mass spectrom* 1994;136(2-3):167-180.
62. Wilm M, Mann M. Analytical properties of the nanoelectrospray ion source. *Anal Chem* 1996;68(1):1-8.
63. Sanglier S, Ramstrom H, Haiech J, Leize E, Van Dorsselaer A. Electrospray ionization mass spectrometry analysis revealed a ~310 kDa noncovalent hexamer of HPr kinase/phosphatase from *Bacillus subtilis*. *Int J Mass spectrom* 2002;219(3):681-696.
64. Ramstrom H, Sanglier S, Leize-Wagner E, Philippe C, Van Dorsselaer A, Haiech J. Properties and regulation of the bifunctional enzyme HPr kinase/phosphatase in *Bacillus subtilis*. *J Biol Chem* 2003;278(2):1174-1185.
65. Benesch JL, Sobott F, Robinson CV. Thermal dissociation of multimeric protein complexes by using nanoelectrospray mass spectrometry. *Anal Chem* 2003;75(10):2208-2214.
66. Van Montfort RL, Basha E, Friedrich KL, Slingsby C, Vierling E. Crystal structure and assembly of a eukaryotic small heat shock protein. *Nat Struct Biol* 2001;8(12):1025-1030.
67. Pinkse MW, Maier CS, Kim JI, Oh BH, Heck AJ. Macromolecular assembly of *Helicobacter pylori* urease investigated by mass spectrometry. *J Mass Spectrom* 2003;38(3):315-320.
68. Ha NC, Oh ST, Sung JY, Cha KA, Lee MH, Oh BH. Supramolecular assembly and acid resistance of Helicobacter pylori urease. *Nat Struct Biol* 2001;8(6):505-509.
69. Lengqvist J, Svensson R, Evergren E, Morgenstern R, Griffiths WJ. Observation of an intact noncovalent homotrimer of detergent-solubilized rat microsomal glutathione transferase-1 by electrospray mass spectrometry. *J Biol Chem* 2004;279(14):13311-13316.
70. Callaghan AJ, Grossmann JG, Redko YU, Ilag LL, Moncrieffe MC, Symmons MF, Robinson CV, McDowall KJ, Luisi BF. Quaternary structure and catalytic activity of the *Escherichia coli* ribonuclease E amino-terminal catalytic domain. *Biochemistry* 2003;42(47):13848-13855.
71. Ilag LL, Westblade LF, Deshayes C, Kolb A, Busby SJ, Robinson CV. Mass spectrometry of *Escherichia coli* RNA polymerase: interactions of the core enzyme with sigma70 and Rsd protein. *Structure* 2004;12(2):269-275.
72. Westblade LF, Ilag LL, Powell AK, Kolb A, Robinson CV, Busby SJ. Studies of the *Escherichia coli* Rsd-sigma70 complex. *J Mol Biol* 2004;335(3):685-692.
73. Benjamin DR, Robinson CV, Hendrick JP, Hartl FU, Dobson CM. Mass spectrometry of ribosomes and ribosomal subunits. *Proc Natl Acad Sci* 1998;95(13):7391-7395.
74. Smith RD, Light-Wahl KJ. The observation of non-covalent interactions in solution by electrospray ionization mass spectrometry: promises, pitfalls and prognosis. *Biol Mass Spectrom* 1993;369(6476):137-139.
75. Schwartz BL, Light-Wahl KJ, Smith RD. Observation of noncovalent complexes to the avidin tetramer by electrospray ionization mass spectrometry. *J Am Soc Mass Spectrom* 1994;5(3):201-204.
76. Fandrich M, Tito MA, Leroux MR, Rostom AA, Hartl FU, Dobson CM, Robinson CV. Observation of the noncovalent assembly and disassembly pathways of the chaperone complex MtGimC by mass spectrometry. *Proc Natl Acad Sci* 2000;97(26):14151-14155.
77. Rostom AA, Fucini P, Benjamin DR, Juenemann R, Nierhaus KH, Hartl FU, Dobson CM, Robinson CV. Detection and selective dissociation of intact ribosomes in a mass spectrometer. *Proc Natl Acad Sci* 2000;97(10):5185-5190.

78. Hanson CL, Fucini P, Ilag LL, Nierhaus KH, Robinson CV. Dissociation of intact *Escherichia coli* ribosomes in a mass spectrometer. Evidence for conformational change in a ribosome elongation factor G complex. *J Biol Chem* 2003;278(2):1259-1267.

79. McCammon MG, Hernandez H, Sobott F, Robinson CV. Tandem mass spectrometry defines the stoichiometry and quaternary structural arrangement of tryptophan molecules in the multiprotein complex TRAP. *J Am Chem Soc* 2004;126(19):5950-5951.

80. Aquilina JA, Benesch JL, Bateman OA, Slingsby C, Robinson CV. Polydispersity of a mammalian chaperone: mass spectrometry reveals the population of oligomers in alphaB-crystallin. *Proc Natl Acad Sci* 2003;100(19):10611-10616.

81. van Berkel WJ, Westphal AH, Eschrich K, Eppink MH, de Kok A. Substitution of Arg214 at the substrate-binding site of *p*-hydroxybenzoate hydroxylase from *Pseudomonas fluorescens*. *Eur J Biochem* 1992;210(2):411-419.

82. Shrake A, Ross PD. Origins and consequences of ligand-induced multiphasic thermal protein denaturation. *Biopolymers* 1992;32(8):925-940.

83. Hefti MH, Vervoort J, Van Berkel WJ. Deflavination and reconstitution of flavoproteins. *Eur J Biochem* 2003;270(21):4227-4242.

84. Massey V. The chemical and biological versatility of riboflavin. *Biochem Soc Trans* 2000;28(4):283-296.

85. Decker KF. Biosynthesis and function of enzymes with covalently bound flavin. *Annu Rev Nutr* 1993;13:17-41.

86. Decker KF. Vitamins. In: *Nutritional Biochemisrty*. Brody T, ed. San Diego. Academic Press, Inc., 1994:443-447.

87. Kearney EB, Singer TP. On the prosthetic group of succinic dehydrogenase. *Biochim Biophys Acta* 1955;17(4):596-597.

88. Fraaije MW, Van den Heuvel RHH, Van Berkel WJH, Mattevi A. Covalent flavinylation is essential for efficient redox catalysis in vanillyl-alcohol oxidase. *J Biol Chem* 1999;274(50):35514-35520.

89. Fraaije MW, Sjollema KA, Veenhuis M, Van Berkel WJ. Subcellular localization of vanillyl-alcohol oxidase in *Penicillium simplicissimum*. *FEBS Lett* 1998;422(1):65-68.

90. Mewies M, McIntire WS, Scrutton NS. Covalent attachment of flavin adenine dinucleotide (FAD) and flavin mononucleotide (FMN) to enzymes: the current state of affairs. *Protein Sci* 1998;7(1):7-20.

91. Tahallah N, Van Den Heuvel RH, Van Den Berg WA, Maier CS, Van Berkel WJ, Heck AJ. Cofactor-dependent assembly of the flavoenzyme vanillyl-alcohol oxidase. *J Biol Chem* 2002;277(39):36425-36432.

92. Van den Heuvel RH, Westphal AH, Heck AJ, Walsh MA, Rovida S, Van Berkel WJ, Mattevi A. Structural studies on flavin reductase PheA2 reveal binding of NAD in an unusual folded conformation and support novel mechanism of action. *J Biol Chem* 2004;279(13):12860-12867.

93. Kirchner U, Westphal AH, Muller R, Van Berkel WJ. Phenol hydroxylase from *Bacillus thermoglucosidasius* A7, a two-protein component monooxygenase with a dual role for FAD. *J Biol Chem* 2003;278(48):47545-47553.

94. Magni G, Amici A, Emanuelli M, Raffaelli N, Ruggieri S. Enzymology of NAD^+ synthesis. *Adv Enzymol Relat Areas Mol Biol* 1999;73:135-182, xi.

95. Begley TP, Kinsland C, Strauss E. The biosynthesis of coenzyme A in bacteria. *Vitam Horm* 2001;61:157-171.

96. Van den Heuvel RH, Curti B, Vanoni MA, Mattevi A. Glutamate synthase: a fascinating pathway from L-glutamine to L-glutamate. *Cell Mol Life Sci* 2004;61(6):669-681.

97. Hiro I, Tsugeno Y, Hirashiki I, Ogata F, Ito A. Characterization of rat monoamine oxidase A with noncovalently-bound FAD expressed in yeast cells. *J Biochem* 1996;120(4):759-765.

98. Yamada K, Chen Z, Rozen R, Matthews RG. Effects of common polymorphisms on the properties of recombinant human methylenetetrahydrofolate reductase. *Proc Natl Acad Sci* 2001;98(26):14853-14858.

99. Guenther BD, Sheppard CA, Tran P, Rozen R, Matthews RG, Ludwig ML. The structure and properties of methylenetetrahydrofolate reductase from *Escherichia coli* suggest how folate ameliorates human hyperhomocysteinemia. *Nat Struct Biol* 1999;6(4):359-365.

100. Van Berkel WJH, Van den Heuvel RHH, Versluis C, Heck AJR. Detection of intact megaDalton protein assemblies of vanillyl-alcohol oxidase by mass spectrometry. *Protein Sci* 2000;9(3):435-439.

101. Fraaije MW, Van Den Heuvel RHH, Van Berkel WJH, Mattevi A. Structural analysis of flavinylation in vanillyl-alcohol oxidase. *J Biol Chem* 2000;275(49):38654-38658.

102. Koshland DE, Hamadani K. Proteomics and models for enzyme cooperativity. *J Biol Chem* 2002;277(49):46841-46844.

103. Rogniaux H, Sanglier S, Strupat K, Azza S, Roitel O, Ball V, Tritsch D, Branlant G, Van Dorsselaer A. Mass spectrometry as a novel approach to probe cooperativity in multimeric enzymatic systems. *Anal Biochem* 2001;291(1):48-61.

104. McCammon MG, Scott DJ, Keetch CA, Greene LH, Purkey HE, Petrassi HM, Kelly JW, Robinson CV. Screening transthyretin amyloid fibril inhibitors: characterization of novel multiprotein, multiligand complexes by mass spectrometry. *Structure* 2002;10(6):851-863.

105. Miroy GJ, Lai Z, Lashuel HA, Peterson SA, Strang C, Kelly JW. Inhibiting transthyretin amyloid fibril formation via protein stabilization. *Proc Natl Acad Sci* 1996;93(26):15051-15056.

106. Apiyo D, Guidry J, Wittung-Stafshede P. No cofactor effect on equilibrium unfolding of *Desulfovibrio desulfuricans* flavodoxin. *Biochim Biophys Acta* 2000;1479(1-2):214-224.

107. Bollen YJ, Nabuurs SM, Van Berkel WJ, Van Mierlo CP. Last in, first out: the role of cofactor binding in flavodoxin folding. *J Biol Chem* 2005;280(9):7836-7844.

108. Aquilina JA, Robinson CV. Investigating interactions of the pentraxins serum amyloid P component and C-reactive protein by mass spectrometry. *Biochem J* 2003;375(Pt 2):323-328.

109. Entsch B, Cole LJ, Ballou DP. Protein dynamics and electrostatics in the function of *p*-hydroxybenzoate hydroxylase. *Arch Biochem Biophys* 2005;433(1):297-311.

110. Entsch B, Van Berkel WJ. Structure and mechanism of *para*-hydroxybenzoate hydroxylase. *Faseb J* 1995;9(7):476-483.

111. Schreuder HA, Prick PA, Wierenga RK, Vriend G, Wilson KS, Hol WG, Drenth J. Crystal structure of the *p*-hydroxybenzoate hydroxylase-substrate complex refined at 1.9 A resolution. Analysis of the enzyme-substrate and enzyme-product complexes. *J Mol Biol* 1989;208(4):679-696.

112. Neujahr HY. Phenol hydroxylase. In: *Chemistry and Biochemistry of Flavoenzymes II*. Muller F, ed. Florida, USA. Boca Raton, CRC Press, 1991:65-85.

113. Van Berkel WJ, Muller F. Flavin-dependent monooxygenases with special reference to *p*-Hydroxybenzoate hydroxylase. In: *Chemistry and Biochemistry of Flavoenzymes II*. Muller F, ed. Florida, USA. Boca Raton, CRC Press, 1991:1-29.

114. Gibson DT. Microbial degradation of aromatic compounds. *Science* 1967;161(846):1093-1097.

115. Van der Meer JR, De Vos WM, Harayama S, Zehnder AJ. Molecular mechanisms of genetic adaptation to xenobiotic compounds. *Microbiol Rev* 1992;56(4):677-694.

116. Eppink MH, Schreuder HA, Van Berkel WJ. Identification of a novel conserved sequence motif in flavoprotein hydroxylases with a putative dual function in FAD/NAD(P)H binding. *Protein Sci* 1997;6(11):2454-2458.

117. Ornston LN, Stanier RY. Mechanism of beta-ketoadipate formation by bacteria. *Nature* 1964;204:1279-1283.

118. Van Berkel WJ, Eppink MH, Middelhoven WJ, Vervoort J, Rietjens IM. Catabolism of 4-hydroxybenzoate in *Candida parapsilosis* proceeds through initial oxidative decarboxylation by a FAD-dependent 4-hydroxybenzoate 1-hydroxylase. *FEMS Microbiol Lett* 1994;121(2):207-215.

119. Muller F, Voordouw G, Van Berkel WJ, Steennis PJ, Visser S, Van Rooijen PJ. A study of *p*-hydroxybenzoate hydroxylase from *Pseudomonas fluorescens*. Improved purification, relative molecular mass, and amino acid composition. *Eur J Biochem* 1979;101(1):235-244.

120. Wierenga RK, Drenth J, Schulz GE. Comparison of the three-dimensional protein and nucleotide structure of the FAD-binding domain of *p*-hydroxybenzoate hydroxylase with the FAD- as well as NADPH-binding domains of glutathione reductase. *J Mol Biol* 1983;167(3):725-739.

121. Wang J, Ortiz-Maldonado M, Entsch B, Massey V, Ballou D, Gatti DL. Protein and ligand dynamics in 4-hydroxybenzoate hydroxylase. *Proc Natl Acad Sci* 2002;99(2):608-613.

122. Hoard HM, Benson LM, Vockley J, Naylor S. Microelectrospray ionization analysis of noncovalent interactions within the electron transferring flavoprotein. *Biochem Biophys Res Commun* 2001;282(1):297-305.

123. Cavanagh J, Thompson R, Bobay B, Benson LM, Naylor S. Stoichiometries of protein-protein/DNA binding and conformational changes for the transition-state regulator AbrB measured by pseudo cell-size exclusion chromatography-mass spectrometry. *Biochemistry* 2002;41(25):7859-7865.

124. Vergauwen B, Pauwels F, Jacquemotte F, Meyer TE, Cusanovich MA, Bartsch RG, Van Beeumen JJ. Characterization of glutathione amide reductase from *Chromatium gracile*. Identification of a novel thiol peroxidase (Prx/Grx) fueled by glutathione amide redox cycling. *J Biol Chem* 2001;276(24):20890-20897.

125. Bossi RT, Aliverti A, Raimondi D, Fischer F, Zanetti G, Ferrari D, Tahallah N, Maier CS, Heck AJ, Rizzi M, Mattevi A. A covalent modification of $NADP^+$ revealed by the atomic resolution structure of FprA, a *Mycobacterium tuberculosis* oxidoreductase. *Biochemistry* 2002;41(28):8807-8818.

126. Hoard-Fruchey HM, Goetzman E, Benson L, Naylor S, Vockley J. Mammalian electron transferring flavoprotein.flavoprotein dehydrogenase complexes observed by microelectrospray ionization-mass spectrometry and surface plasmon resonance. *J Biol Chem* 2004;279(14):13786-13791.

127. Tahallah* N, Van Den Berg* WA, Van Den Heuvel RH, Van Berkel WJ, Heck AJ. The FMN cofactor ensures the protection of Flavodoxin – FldA –, from *Azotobacter vinelandii*, against active site cysteine residue oxidative

damage caused by hydrogen peroxide: Evidence by a coupled Liquid Chromatography – Mass Spectrometry system. ***in prep. *Equally contributing authors*** **2005.**

128. De Jong E, Van Berkel WJH, Van der Zwan RP, De Bont JA. Purification and characterization of vanillyl-alcohol oxidase from *Penicillium simplicissimum*. A novel aromatic alcohol oxidase containing covalently bound FAD. *Eur J Biochem* 1992;208(3):651-657.

129. Fraaije MW, Pikkemaat MG, Van Berkel WJH. Enigmatic gratuitous induction of the covalent flavoprotein vanillyl-alcohol oxidase in *Penicillium simplicissimum*. *Appl Environ Microbiol* 1997;63(2):435-439.

130. Fraaije MW, Van Berkel WJH, Benen JA, Visser J, Mattevi A. A novel oxidoreductase family sharing a conserved FAD-binding domain. *Trends Biochem Sci* 1998;23(6):206-207.

131. Mattevi A, Fraaije MW, Mozzarelli A, Olivi L, Coda A, Van Berkel WJH. Crystal structures and inhibitor binding in the octameric flavoenzyme vanillyl-alcohol oxidase: the shape of the active-site cavity controls substrate specificity. *Structure* 1997;5(7):907-920.

132. Fraaije MW, Veeger C, Van Berkel WJ. Substrate specificity of flavin-dependent vanillyl-alcohol oxidase from *Penicillium simplicissimum*. Evidence for the production of 4-hydroxycinnamyl alcohols from 4-allylphenols. *Eur J Biochem* 1995;234(1):271-277.

133. Van den Heuvel RH, Fraaije MW, Laane C, Van Berkel WJ. Regio- and stereospecific conversion of 4-alkylphenols by the covalent flavoprotein vanillyl-alcohol oxidase. *J Bacteriol* 1998;180(21):5646-5651.

134. Drijfhout FP, Fraaije MW, Jongejan H, Van Berkel WJ, Franssen MC. Enantioselective hydroxylation of 4-alkylphenols by vanillyl alcohol oxidase. *Biotechnol Bioeng* 1998;59(2):171-177.

135. Fraaije MW, Mattevi A, Van Berkel WJH. Mercuration of vanillyl-alcohol oxidase from *Penicillium simplicissimum* generates inactive dimers. *FEBS Lett* 1997;402(1):33-35.

136. Van Berkel WJH, Fraaije MW, De Jong E, De Bont JAM. Vanillyl-alcohol oxidase from *Penicillium simplicissimum*: a novel flavoprotein containing 8alfa-(N3-histidyl)-FAD. In: *Flavins and Flavoproteins XI XI*. Yagi K, ed. Berlin. Walter de Gruyter & Co, 1994:709-802.

137. Kamerbeek NM, Moonen MJ, Van Der Ven JG, Van Berkel WJ, Fraaije MW, Janssen DB. 4-Hydroxyacetophenone monooxygenase from *Pseudomonas fluorescens ACB*. A novel flavoprotein catalyzing Baeyer-Villiger oxidation of aromatic compounds. *Eur J Biochem* 2001;268(9):2547-2557.

138. Willetts A. Structural studies and synthetic applications of Baeyer-Villiger monooxygenases. *Trends Biotechnol* 1997;15(2):55-62.

139. Wierenga RK, Terpstra P, Hol WG. Prediction of the occurrence of the ADP-binding beta alpha beta-fold in proteins, using an amino acid sequence fingerprint. *J Mol Biol* 1986;187(1):101-107.

140. Malito E, Alfieri A, Fraaije MW, Mattevi A. Crystal structure of a Baeyer-Villiger monooxygenase. *Proc Natl Acad Sci* 2004;101(36):13157-13162. Epub 12004 Aug 13124.

141. Pai EF. Variations on a theme: the family of FAD-dependent NAD(P)H-(disulphide)-oxidoreductases. *Curr Opin Struct Biol* 1991;1(5):796-803.

142. Cole ST, Brosch R, Parkhill J, Garnier T, Churcher C, Harris D, Gordon SV, Eiglmeier K, Gas S, Barry CEr, Tekaia F, Badcock K, Basham D, Brown D, Chillingworth T, Connor R, Davies R, Devlin K, Feltwell T, Gentles S, Hamlin N, Holroyd S, Hornsby T, Jagels K, Krogh A, McLean J, Moule S, Murphy L, Oliver K, Osborne J, Quail MA, Rajandream MA, Rogers J, Rutter S, Seeger K, Skelton J, Squares R, Squares S, Sulston JE, Taylor K, Whitehead S, Barrell BG. Deciphering the biology of *Mycobacterium tuberculosis* from the complete genome sequence. *Nature* 1998;393(6685):537-544.

143. Karplus PA, Bruns CM. Structure-function relations for ferredoxin reductase. *J Bioenerg Biomembr* 1994;26(1):89-99.

144. Fischer F, Raimondi D, Aliverti A, Zanetti G. *Mycobacterium tuberculosis* FprA, a novel bacterial NADPH-ferredoxin reductase. *Eur J Biochem* 2002;269(12):3005-3013.

145. Dym O, Eisenberg D. Sequence-structure analysis of FAD-containing proteins. *Protein Sci* 2001;10(9):1712-1728.

146. McLafferty FW. High-resolution tandem FT mass-spectrometry above 10-kDa. *Acc Chem Res* 1994;27((11)):379-386.

147. Smith RD, Cheng X, Bruce JE, Hofstadier SA, Anderson GA. Trapping, detection and reaction of very large single molecular ions by mass spectrometry. *Nature* 1994;369(6476):137-139.

148. Ganem B, Li YT, Henion JD. Observation of noncovalent enzyme-substrate and enzyme-product complexes by ion-spray mass spectrometry. *J Am Chem Soc* 1991;113(20):7818-7819.

149. Przybylski M, Glocker MO. Electrospray mass spectrometry of biomacromolecules complexes with non-covalent interactions – new analytical perspectives for supramolecular chemistry and molecular recognition processes. *Angew Chem Int Ed Engl* 1996;35:806-826.

150. Loo JA. Studying noncovalent protein complexes by electrospray ionization mass spectrometry. *Mass Spectrom Rev* 1997;16:1-23.

151. Smith RD, Bruce JE, Wu QY, Lei QP. New mass spectrometric methods for the study of noncovalent associations of biopolymers. *CHEM SOC REV* 1997;26:191-202.

152. Green BN, Bordoli RS, Hanin LG, Lallier FH, Toulmond A, Vinogradov SN. Electrospray ionization mass spectrometric determination of the molecular mass of the approximately 200-kDa globin dodecamer subassemblies in hexagonal bilayer hemoglobins. *J Biol Chem* 1999;274(40):28206-28212.

153. Yao Y, Huang L, Krutchinsky A, Wong ML, Standing KG, Burlingame AL, Wang CC. Structural and functional characterizations of the proteasome-activating protein PA26 from *Trypanosoma brucei*. *J Biol Chem* 1999;274(48):33921-33930.

154. Krutchinsky AN, Ayed A, Donald LJ, Ens W, Duckworth HW, Standing KG. Studies of noncovalent complexes in an electrospray ionization/time-of-flight mass spectrometer. *Methods Mol Biol* 2000;146:239-249.

155. Rostom AA, Robinson CV. Detection of the intact GroEL chaperonin assembly by mass spectrometry. *J Am Chem Soc* 1999;121(19):4718-4719.

156. Zhang Z, Krutchinsky A, Endicott S, Realini C, Rechsteiner M, Standing KG. Proteasome activator 11S REG or PA28: recombinant REG alpha/REG beta hetero-oligomers are heptamers. *Biochemistry* 1999;38(17):5651-5658.

157. Tito MA, Tars K, Valegard K, Hadju J, Robinson CV. Electrospray time-of-flight mass spectrometry of the intact MS2 virus capsid. *J Am Chem Soc* 2000;122(14):3550-3551.

158. van der Bolt FJ, van den Heuvel RH, Vervoort J, van Berkel WJ. 19F NMR study on the regiospecificity of hydroxylation of tetrafluoro-4-hydroxybenzoate by wild-type and Y385F p-hydroxybenzoate hydroxylase: evidence for a consecutive oxygenolytic dehalogenation mechanism. *Biochemistry* 1997;36(46):14192-14201.

159. Van Berkel WJ, Muller F. The elucidation of the microheterogeneity of highly purified *p*-hydroxybenzoate hydroxylase from *Pseudomonas fluorescens* by various biochemical techniques. *Eur J Biochem* 1987;167(1):35-46.

160. Fraaije MW, Van Berkel WJ. Catalytic mechanism of the oxidative demethylation of 4-(methoxymethyl)phenol by vanillyl-alcohol oxidase. Evidence for formation of a *p*-quinone methide intermediate. *J Biol Chem* 1997;272(29):18111-18116.

161. Benen JA, Sanchez-Torres P, Wagemaker MJ, Fraaije MW, Van Berkel WJ, Visser J. Molecular cloning, sequencing, and heterologous expression of the *vaoA* gene from *Penicillium simplicissimum CBS* 170.90 encoding vanillyl-alcohol oxidase. *J Biol Chem* 1998;273(14):7865-7872.

162. Verentchikov AN, Ens W, Standing KG. Reflecting time-of-flight mass spectrometer with an electrospray ion source and orthogonal extraction. *Anal Chem* 1994;66:126-133.

163. Morris HR, Paxton T, Dell A, Langhorne J, Berg M, Bordoli RS, Hoyes J, Bateman RH. High sensitivity collisionally-activated decomposition tandem mass spectrometry on a novel quadrupole/orthogonal-acceleration time-of-flight mass spectrometer. *Rapid Commun Mass Spectrom* 1996;10(8):889-896.

164. Muller F, Van Berkel WJ. In: *Chemistry and Biochemistry of Flavoenzymes I*. Muller F, ed. Florida, USA. Boca Raton, CRC Press, 1991:201-214.

165. Raibekas AA, Massey V. Glycerol-induced development of catalytically active conformation of *Crotalus adamanteus* L-amino acid oxidase *in vitro*. *Proc Natl Acad Sci* 1996;93(15):7546-7551.

166. Fleischmann G, Lederer F, Muller F, Bacher A, Ruterjans H. Flavin-protein interactions in flavocytochrome b2 as studied by NMR after reconstitution of the enzyme with 13C- and 15N-labelled flavin. *Eur J Biochem* 2000;267(16):5156-5167.

167. Ghisla S, Massey V. New flavins for old: artificial flavins as active site probes of flavoproteins. *Biochem J* 1986;239(1):1-12.

168. Yorita K, Misaki H, Palfey BA, Massey V. On the interpretation of quantitative structure-function activity relationship data for lactate oxidase. *Proc Natl Acad Sci* 2000;97(6):2480-2485.

169. Van Berkel WJ, Eppink MH, Schreuder HA. Crystal structure of *p*-hydroxybenzoate hydroxylase reconstituted with the modified FAD present in alcohol oxidase from methylotrophic yeasts: evidence for an arabinoflavin. *Protein Sci* 1994;3(12):2245-2253.

170. Salomon M, Eisenreich W, Durr H, Schleicher E, Knieb E, Massey V, Rudiger W, Muller F, Bacher A, Richter G. An optomechanical transducer in the blue light receptor phototropin from *Avena sativa*. *Proc Natl Acad Sci* 2001;98(22):12357-12361.

171. Swoboda BE. The relationship between molecular conformation and the binding of flavin-adenine dinucleotide in glucose oxidase. *Biochim Biophys Acta* 1969;175(2):365-379.

172. Massey V, Curti B. A new method of preparation of D-amino acid oxidase apoprotein and a conformational change after its combination with flavin adenine dinucleotide. *J Biol Chem* 1966;241(14):3417-3423.

173. Visser J, Veeger C. Relation between conformations and activities of lipoamide dehydrogenase. IV. Apoenzyme structure and flavin binding aspects. *Biochim Biophys Acta* 1970;206(2):224-241.

174. Van Berkel WJ, Benen JA, Snoek MC. On the FAD-induced dimerization of apo-lipoamide dehydrogenase from *Azotobacter vinelandii* and *Pseudomonas fluorescens*. Kinetics of reconstitution. *Eur J Biochem* 1991;197(3):769-779.

175. Lindsay H, Beaumont E, Richards SD, Kelly SM, Sanderson SJ, Price NC, Lindsay JG. FAD insertion is essential for attaining the assembly competence of the dihydrolipoamide dehydrogenase (E3) monomer from *Escherichia coli*. *J Biol Chem* 2000;275(47):36665-36670.

176. Van Berkel WJ, Van den Berg WA, Muller F. Large-scale preparation and reconstitution of apo-flavoproteins with special reference to butyryl-CoA dehydrogenase from *Megasphaera elsdenii*. Hydrophobic-interaction chromatography. *Eur J Biochem* 1988;178(1):197-207.

177. Kim J, Fuller JH, Kuusk V, Cunane L, Chen ZW, Mathews FS, McIntire WS. The cytochrome subunit is necessary for covalent FAD attachment to the flavoprotein subunit of *p*-cresol methylhydroxylase. *J Biol Chem* 1995;270(52):31202-31209.

178. Robinson CV, Chung EW, Kragelund BB, Knudsen J, Aplin RT, Poulsen FM, Dobson CM. Probing the nature of noncovalent interactions by mass spectrometry. A study of protein CoA ligand binding and assembly. *J Am Chem Soc* 1996;118(36):8646-8653.

179. Rostom AA, Robinson CV. Disassembly of intact multiprotein complexes in the gas phase. *Curr Opin Struct Biol* 1999;9(1):135-141.

180. Vis H, Dobson CM, Robinson CV. Selective association of protein molecules followed by mass spectrometry. *Protein Sci* 1999;8(6):1368-1370.

181. Van den Heuvel RH, Fraaije MW, Mattevi A, Van Berkel WJ. Asp-170 is crucial for the redox properties of vanillyl-alcohol oxidase. *J Biol Chem* 2000;275(20):14799-14808.

182. Ferridge AG, Seddon MJ, Green BN, Jarvis SA, Skilling J. Disentangling electrospray spectra with Maximum Entropy. *Rapid Commun Mass Spectrom* 1992;6:707-711.

183. Vis H, Heinemann U, Dobson CM, Robinson CV. Detection of a monomeric intermediate associated with dimerization of protein HU by mass spectrometry. *J Am Chem Soc* 1998;120(25):6427-6428.

184. Dobbek H, Gremer L, Meyer O, Huber R. Crystal structure and mechanism of CO dehydrogenase, a molybdo iron-sulfur flavoprotein containing S-selanylcysteine. *Proc Natl Acad Sci* 1999;96(16):8884-8889.

185. Enroth C, Eger BT, Okamoto K, Nishino T, Pai EF. Crystal structures of bovine milk xanthine dehydrogenase and xanthine oxidase: structure-based mechanism of conversion. *Proc Natl Acad Sci* 2000;97(20):10723-10728.

186. Gremer L, Kellner S, Dobbek H, Huber R, Meyer O. Binding of flavin adenine dinucleotide to molybdenum-containing carbon monoxide dehydrogenase from *Oligotropha carboxidovorans*. Structural and functional analysis of a carbon monoxide dehydrogenase species in which the native flavoprotein has been replaced by its recombinant counterpart produced in *Escherichia coli*. *J Biol Chem* 2000;275(3):1864-1872.

187. Shrake A, Ross PD. Ligand-induced biphasic protein denaturation. *J Biol Chem* 1990;265(9):5055-5059.

188. Van den Bremer ET, Jiskoot W, James R, Moore GR, Kleanthous C, Heck AJ, Maier CS. Probing metal ion binding and conformational properties of the colicin E9 endonuclease by electrospray ionization time-of-flight mass spectrometry. *Protein Sci* 2002;11(7):1738-1752.

189. Park IK, Kim JY. Effects of NAD or NADP on the stability of liver and pectoral muscle enzymes in 3-acetylpyridine treated quail by heat and trypsin. *Int J Biochem Cell Biol* 1998;30(11):1223-1234.

190. Woodyer R, Van der Donk WA, Zhao H. Relaxing the nicotinamide cofactor specificity of phosphite dehydrogenase by rational design. *Biochemistry* 2003;42(40):11604-11614.

191. Georlette D, Blaise V, Dohmen C, Bouillenne F, Damien B, Depiereux E, Gerday C, Uversky VN, Feller G. Cofactor binding modulates the conformational stabilities and unfolding patterns of NAD($^+$)-dependent DNA ligases from *Escherichia coli* and *Thermus scotoductus*. *J Biol Chem* 2003;278(50):49945-49953.

192. Kamerbeek NM, Olsthoorn AJ, Fraaije MW, Janssen DB. Substrate specificity and enantioselectivity of 4-hydroxyacetophenone monooxygenase. *Appl Environ Microbiol* 2003;69(1):419-426.

193. Mihovilovic MD, Rudroff F, Muller B, Stanetty P. First enantiodivergent Baeyer-Villiger oxidation by recombinant whole-cells expressing two monooxygenases from *Brevibacterium*. *Bioorg Med Chem Lett* 2003;13(8):1479-1482.

194. Alphand V, Carrea G, Wohlgemuth R, Furstoss R, Woodley JM. Towards large-scale synthetic applications of Baeyer-Villiger monooxygenases. *Trends Biotechnol* 2003;21(7):318-323.

195. Fraaije MW, Kamerbeek NM, Van Berkel WJ, Janssen DB. Identification of a Baeyer-Villiger monooxygenase sequence motif. *FEBS Lett* 2002;518(1-3):43-47.

196. Kamerbeek NM, Fraaije MW, Janssen DB. Identifying determinants of NADPH specificity in Baeyer-Villiger monooxygenases. *Eur J Biochem* 2004;271(11):2107-2116.

197. Sheng D, Ballou DP, Massey V. Mechanistic studies of cyclohexanone monooxygenase: chemical properties of intermediates involved in catalysis. *Biochemistry* 2001;40(37):11156-11167.
198. Poulsen LL, Ziegler DM. The liver microsomal FAD-containing monooxygenase. Spectral characterization and kinetic studies. *J Biol Chem* 1979;254(14):6449-6455.
199. Schmidt A, Bahr U, Karas M. Influence of pressure in the first pumping stage on analyte desolvation and fragmentation in nano-ESI MS. *Anal Chem* 2001;73(24):6040-6046.
200. Cattani L, Ferri A. The function of NADPH bound to Catalase. *Boll Soc Ital Biol Sper* 1994;70(4):75-82.
201. Pelletier JN, MacKenzie RE. Binding of the 2',5'-ADP subsite stimulates cyclohydrolase activity of human NADP($^+$)-dependent methylenetetrahydrofolate dehydrogenase/cyclohydrolase. *Biochemistry* 1994;33(7):1900-1906.
202. Mulrooney SB, Williams CH, Jr. Evidence for two conformational states of thioredoxin reductase from *Escherichia coli*: use of intrinsic and extrinsic quenchers of flavin fluorescence as probes to observe domain rotation. *Protein Sci* 1997;6(10):2188-2195.
203. Sulzenbacher G, Alvarez K, Van Den Heuvel RH, Versluis C, Spinelli S, Campanacci V, Valencia C, Cambillau C, Eklund H, Tegoni M. Crystal structure of *E.coli* alcohol dehydrogenase YqhD: evidence of a covalently modified NADP coenzyme. *J Mol Biol* 2004;342(2):489-502.
204. Grandori R, Matecko I, Muller N. Uncoupled analysis of secondary and tertiary protein structure by circular dichroism and electrospray ionization mass spectrometry. *J Mass Spectrom* 2002;37(2):191-196.
205. Poulsen LL, Ziegler DM. Multisubstrate flavin-containing monooxygenases: applications of mechanism to specificity. *Chem Biol Interact* 1995;96(1):57-73.
206. Zambianchi F, Pasta P, Carrea G, Colonna S, Gaggero N, Woodley JM. Use of isolated cyclohexanone monooxygenase from recombinant *Escherichia coli* as a biocatalyst for Baeyer-Villiger and sulfide oxidations. *Biotechnol Bioeng* 2002;78(5):489-496.
207. Snider DE, La Montagne JR. The neglected global tuberculosis problem: a report of the 1992 World Congress on Tuberculosis. *J Infect Dis* 1994;169(6):1189-1196.
208. Mycobacterium tuberculosis Structual Genomics Consortium. *http://www.doe-mbi.ucla.edu/TB*. 2002.
209. Schaffer AA, Aravind L, Madden TL, Shavirin S, Spouge JL, Wolf YI, Koonin EV, Altschul SF. Improving the accuracy of PSI-BLAST protein database searches with composition-based statistics and other refinements. *Nucleic Acids Res* 2001;29(14):2994-3005.
210. Li J, Saxena S, Pain D, Dancis A. Adrenodoxin reductase homolog (Arh1p) of yeast mitochondria required for iron homeostasis. *J Biol Chem* 2001;276(2):1503-1509.
211. Manzella L, Barros MH, Nobrega FG. *Arh1* of *Saccharomyces cerevisiae*: a new essential gene that codes for a protein homologous to the human adrenodoxin reductase. *Yeast* 1998;14(9):839-846.
212. Lambeth JD, Seybert DW, Lancaster JR, Salerno JC, Kamin H. Steroidogenic electron transport in adrenal cortex mitochondria. *Mol Cell Biochem* 1982;45(1):13-31.
213. Grinberg AV, Hannemann F, Schiffler B, Muller J, Heinemann U, Bernhardt R. Adrenodoxin: structure, stability, and electron transfer properties. *Proteins* 2000;40(4):590-612.
214. Bernhardt R. Cytochrome P450: structure, function, and generation of reactive oxygen species. *Rev Physiol Biochem Pharmacol* 1996;127:137-221.
215. De Voss JJ, Rutter K, Schroeder BG, Barry CE. Iron acquisition and metabolism by mycobacteria. *J Bacteriol* 1999;181(15):4443-4451.
216. Ziegler GA, Vonrhein C, Hanukoglu I, Schulz GE. The structure of adrenodoxin reductase of mitochondrial P450 systems: electron transfer for steroid biosynthesis. *J Mol Biol* 1999;289(4):981-990.
217. Ziegler GA, Schulz GE. Crystal structures of adrenodoxin reductase in complex with NADP$^+$ and NADPH suggesting a mechanism for the electron transfer of an enzyme family. *Biochemistry* 2000;39(36):10986-10995.
218. Muller JJ, Lapko A, Bourenkov G, Ruckpaul K, Heinemann U. Adrenodoxin reductase-adrenodoxin complex structure suggests electron transfer path in steroid biosynthesis. *J Biol Chem* 2001;276(4):2786-2789.
219. Thompson JD, Higgins DG, Gibson TJ. CLUSTAL W: improving the sensitivity of progressive multiple sequence alignment through sequence weighting, position-specific gap penalties and weight matrix choice. *Nucleic Acids Res* 1994;22(22):4673-4680.
220. Mozzarelli A, Rossi GL. Protein function in the crystal. *Annu Rev Biophys Biomol Struct* 1996;25:343-365.
221. Leslie AG. Integration of macromolecular diffraction data. *Acta Crystallogr D Biol Crystallogr* 1999;55(Pt 10):1696-1702.
222. Collaborative Computational Project Number. The CCP4 suite: programs for protein crystallography. *Acta Crystallogr D Biol Crystallogr* 1994;50(Pt 5):760-767.
223. Read RJ. Pushing the boundaries of molecular replacement with maximum likelihood. *Acta Crystallogr D Biol Crystallogr* 2001;57(Pt 10):1373-1382.

224. Cowtan K, Main P. Miscellaneous algorithms for density modification. *Acta Crystallogr D Biol Crystallogr* 1998;54(Pt 4):487-493.
225. Perrakis A, Morris R, Lamzin VS. Automated protein model building combined with iterative structure refinement. *Nat Struct Biol* 1999;6(5):458-463.
226. Perrakis A, Harkiolaki M, Wilson KS, Lamzin VS. ARP/wARP and molecular replacement. *Acta Crystallogr D Biol Crystallogr* 2001;57(Pt 10):1445-1450.
227. Murshudov GN, Vagin AA, Dodson EJ. Refinement of macromolecular structures by the Maximum-Likelihood Method. *Acta Crystallogr D Biol Crystallogr* 1997;53(Pt 3):240-255.
228. Jones TA, Zou JY, Cowan SW, Kjeldgaard E. Improved methods for building protein models in electron density maps and the location of errors in these models. *Acta Crystallogr A* 1991;47(Pt 2):110-119.
229. Laskowski RA, MacArthur MW, Moss DS, Thornton JM. *PROCHECK*: a program to check the stereochemical quality of protein structures. *J Appl Crystallogr* 1993;26:283-291.
230. Kleywegt GJ, Zou JY, Kjeldgaard M, Jones TA. Around O. In: *International tables for crystallography: crystallography of biological macromolecules F*. Rossmann MGaA, E., ed. Dordrecht. Kluwer Academic Publishers, 2001:Chapter 17.11, pp. 353-356, 366-367.
231. Kraulis PJ. *MOLSCRIPT*: a program to produce both detailed and schematic plots of protein structures. *J Appl Crystallogr* 1991;24:946-950.
232. Esnouf RM. Further additions to MolScript version 1.4, including reading and contouring of electron-density maps. *Acta Crystallogr D Biol Crystallogr* 1999;55(Pt 4):938-940.
233. Wallace AC, Laskowski RA, Thornton JM. LIGPLOT: a program to generate schematic diagrams of protein-ligand interactions. *Protein Eng* 1995;8(2):127-134.
234. Vallon O. New sequence motifs in flavoproteins: evidence for common ancestry and tools to predict structure. *Proteins* 2000;38(1):95-114.
235. Schulz GE. Binding of nucleotides by proteins. *Curr Opin Struct Biol* 1992;2(1):61-67.
236. Fraaije MW, Mattevi A. Flavoenzymes: diverse catalysts with recurrent features. *Trends Biochem Sci* 2000;25(3):126-132.
237. Almarsson O, Bruice TC. Evaluation of the factors influencing reactivity and stereospecificity in NAD(P)H dependent dehydrogenase enzymes. *J Am Chem Soc* 1993;115(6):2125-2138.
238. Dodson G, Wlodawer A. Catalytic triads and their relatives. *Trends Biochem Sci* 1998;23(9):347-352.
239. Carugo O, Argos P. NADP-dependent enzymes. I: Conserved stereochemistry of cofactor binding. *Proteins* 1997;28(1):10-28.
240. Berman HM, Westbrook J, Feng Z, Gilliland G, Bhat TN, Weissig H, Shindyalov IN, Bourne PE. The Protein Data Bank. *Nucleic Acids Res* 2000;28(1):235-242.
241. Ilag LL, Videler H, McKay AR, Sobott F, Fucini P, Nierhaus KH, Robinson CV. Heptameric (L12)6/L10 rather than canonical pentameric complexes are found by tandem MS of intact ribosomes from thermophilic bacteria. *Proc Natl Acad Sci* 2005;102(23):8192-8197.

Samenvatting in het Nederlands

Met de ontwikkeling van de “milde” electrospray ionisatie techniek aan het eind van de jaren ’80, zijn de massaspectrometrische analyse mogelijkheden enorm toegenomen. Tegenwoordig zijn niet covalente complexen van meer dan één miljoen Dalton van de oplossing naar de gasfase over te brengen. Dit maakt massaspectrometrie geschikt voor het bestuderen van eiwit oligomeren en functionele biosystemen. Deze ontwikkelingen hebben geleid tot het ontstaan van een nieuwe richting in de biomoleculaire massaspectrometrie, “natieve massaspectrometrie”, welke zich concentreert op de analyse van intacte eiwitten en eiwit complexen onder pseudo fysiologische condities. Natieve massaspectrometrie is een nieuwe techniek in het veld van structuurbiologie, en kan informatie verschaffen over de ternaire en quaternaire structuur van eiwitten, de stoichiometrie, de ligand of cofactor binding, de coöperatieve effecten en de stabiliteit en dynamica van functionele eiwitsystemen. De verkregen gegevens zijn meestal complementair aan die van de gevestigde technieken in structuurbiologie, zoals NMR, kristallografie, SAXS en electronenmicroscopie. Het doel van dit onderzoek was om informatie te verkrijgen over de structuur-functie relaties van vier flavine-bevattende eiwitten, PHBH, VAO, HAPMO en FprA, met behulp van natieve massaspectrometrie technieken. We hebben onze aandacht vooral gericht op oligomerisatie gedrag, cooperativiteits effecten, eiwit stabiliteit en cofactor binding en modificatie. Zoals blijkt uit tabel 1 van de introductie is er maar betrekkelijk weinig gepubliceerd over onderzoek naar de functionele eigenschappen van flavine-bevattende eiwitten met behulp van natieve massaspectrometrie (nano-ESI-MS).

Natieve massaspectrometrie aan niet covalente eiwitcomplexen

Hoofdstuk 2 beschrijft het belang van de nano-ESI-MS instrument parameters voor het succesvol meten van niet covalente complexen met een hoog molecuul gewicht. Hogere drukken in de eerste vacuumkamers en andere spanningsinstellingen op de inlaat openingen van de MS zijn een vereiste voor een efficiente transmissie en detectie van grote eiwit ionen. Om dit fenomeen te illustreren analyseerden we de twee flavine-bevattende eiwitten PHBH en VAO. Onze bevindingen dat zwaardere m/z ionen beter worden getransporteerd en gedetecteerd bij hogere drukken kan worden verklaard met het eerder beschreven koelende effect van botsingen[39]. Nieuw is dat op ons instrument (een enigszins aangepaste Micromass LC-T) het effect van de verhoogde druk varieert afhankelijk van de aard (grootte en gewicht) van de geanalyseerde ionen. Verandering van de druk gaat gepaard met een discriminatie in transmissie en detectie van ionen met een groot verschil in m/z, wat veroorzaakt wordt door hun verschil in kinetische energie en

effectieve botsingsdoorsnede. Voor ionen met een m/z waarde kleiner dan 1500 werd geen positief druk effect waargenomen. Bij het verhogen van het voltage op de kegelvormige inlaat opening van de massaspectrometer wordt de desolvatatie verbeterd maar kan er bij lagere m/z ionen ook dissociatie/fragmentatie optreden. Dus het zorgvuldig instellen van druk en voltage, mogelijk verschillend voor ieder eiwitcomplex of massaspectrometer zal de beste resultaten geven.

Het coöperatieve effect van cofactor binding en VAO oligomerisatie

De opgedane kennis omtrent de parameters voor nano-ESI-MS werd gebruikt om de structuur-functie relatie van het flavine-bevattende eiwit VAO te onderzoeken. Hoofdstuk 3 beschrijft de resultaten van het coöperatieve effect van FAD cofactor binding en VAO oligomerisatie. Onder natieve condities wordt wild type VAO voornamelijk gedetecteerd als octameer. Dit in tegenstelling tot apo-VAO H61T wat onder dezelfde condities voornamelijk gedetecteerd wordt als dimeer. Echter met een 10-voudige molaire overmaat FAD laat het massaspectrum van VAO H61T duidelijk de aanwezigheid van zowel dimer als octamer ionen zien. Ook laat het massaspectrum zien dat het dimeer maximaal twee FAD moleculen en het octameer maximaal acht FAD moleculen kan binden. Deze resultaten duiden op het coöperatieve effect van FAD binding en VAO octamerisatie. Toevoeging van 5'-ADP aan apo H61T gaf vergelijkbare resultaten, een sterk toegenomen octamerisatie en binding van 5'-ADP aan zowel dimeer als octameer deeltjes. De toevoeging van FMN had echter geen coöperatief effect. De verkregen ESI-MS resultaten werden gevalideerd met gel filtratie experimenten. Deze data geven aan dat natieve ESI-MS een krachtige analyse methode is voor het bestuderen van coöperatieve effecten in eiwitten. De mogelijkheid om onderscheid te maken tussen oligomere deeltjes met een verschillend aantal FAD moleculen is een bijna unieke eigenschap van deze massaspectrometrische methode.

Het eerste directe bewijs dat de permanente binding van NADP(H) aan HAPMO invloed heeft op de enzym stabiliteit.

In hoofdstuk 4 rapporteren we over het onderzoek naar de bindings karakteristieken van het nicotineamide coenzym tijdens de katalytische cyclus van HAPMO met als doel om meer inzicht te verkrijgen in het enzym mechanisme. Ook bestudeerde we hier de structurele rol van het coenzym. Voor de HAPMO homoloog cyclohexanon monooxygenase zijn er kinetische aanwijzingen dat het aanvankelijk gevormde $NADP^+$ gebonden blijft aan het enzym gedurende het substraat oxygenatie proces[197]. Dit suggereert dat het enzym eigenlijk permanent gebonden is aan het gereduceerde of het geoxideerde coenzym. Onze "real-time" ESI massa spectra laten duidelijk zien dat HAPMO, wanneer het functioneert als een NADPH oxidase, continu in complex is met het coenzym. Dit is het eerste directe bewijs van de permanente binding van een coenzym aan een

Baeyer-Villeger monoxygenase. Onze resultaten bewijzen ook dat $NADP^+$ sterk bind aan het gereduceerde enzym, maar niet aan het geoxideerde enzym. De binding met het coenzym blijkt zeer belangrijk te zijn voor de stabiliteit van het enzym. We stellen voor dat deze coenzym gestuurde stabiliteit ook belangrijk kan zijn voor vergelijkbare enzymen. Dit verklaart mogelijk ook de betrekkelijk lage stabiliteit van geïsoleerde coenzym afhankelijke enzymen. Deze "real-time" nano-ESI-MS methode is ook toepasbaar voor het verkrijgen van mechanistische informatie over de werking van andere enzymen.

FprA kan NADPO maken

In hoofdstuk 5 wordt de hoge resolutie structuur van FprA in de geoxideerde en NADPH-gereduceerde vorm beschreven. Onze bijdrage was de identificatie van een enzymatisch gemodificeerd coenzym met behulp van ESI-MS-MS. Het meest interessante kenmerk van de kristalstructuur van FprA is de covalente modificatie van $NADP^+$. De kristallografische gegevens duiden op een zuurstof atoom aan het reactieve C4 atoom van de nicotinamide ring. Het massaspectrum van natief FprA met $NADP^+$ toont een ternair complex van FprA-FAD-$NADP^+$. Helaas was het oplossend vermogen onvoldoende om te zien of er zowel $NADP^+$ als de geoxigeneerde vorm aanwezig was. Onder gedenatureerde omstandigheden toonde het massaspectrum naast apo-FprA ook pieken welke overeenkomen met $NADP^+$, het voorgestelde $NADP^+$ derivaat en FAD. Vergelijking van de MS/MS spectra van het voorgestelde $NADP^+$ derivaat en $NADP^+$ gaf specifieke fragmentionen die aantoonde dat het C4 atoom van de nicotinamide ring geoxideerd was. De MS analyse toonde onomstotelijk aan dat de vorming van dit covalente adduct plaats vindt in oplossing en dat het geen artefact is van het eiwit kristallisatie proces. Dit NADPO molecuul is nog niet eerder gedetecteerd. De fysiologische betekenis van deze reactie is nu nog niet bekend, maar het zou kunnen helpen bij "medicijn ontwerp" onderzoek, daar het NADPO een model kan zijn voor de ontwikkeling van specifieke remmers. Of de vorming van dit derivaat ook kan plaatsvinden in de celomgeving en of het dan een fysiologische rol heeft zijn onderwerpen van toekomstig onderzoek. Recentelijk is, met een zelfde benadering, een overeenkomstig $NADP^+$ derivaat, $NADP(OH)_2$, geïdentificeerd in alcohol dehydrogenase[197].

Conclusies

De in dit proefschrift gerapporteerde data tonen aan dat natieve massaspectrometrie een waardevolle techniek is voor het onderzoeken van quarternaire structuren van eiwit complexen, ligand binding, coöperatieve effecten van ligand binding en modificaties van liganden. Natieve massaspectrometrie kan dus gebruikt worden voor de bestudering van structuur-functie relaties van eiwitten, waarbij de verkregen data in hoge mate complementair zijn aan de data van klassieke structuur biologische technieken en biochemische analyses.

In dit proefschrift concentreerden we ons op homogene eiwit complexen, vaak oligomeren in complex met cofactors. We moeten echter niet vergeten dat veel functionele eiwitsystemen een heel wat complexere samenstelling hebben, zoals diverse heterogene eiwitten, nucleïnezuren en kleine moleculen. Sinds een aantal jaren kan ook natieve massaspectrometrie gebruikt worden voor het bestuderen van zulke heterogene systemen. Het meest indrukwekkende voorbeeld tot op heden is de analyse van ribosoom complexen, bestaande uit eiwitten en RNA[241]. Een grote uitdaging voor de komende jaren is het verkrijgen van structuur-functie relaties van grote heterogene systemen met behulp van natieve massaspectrometrie. Deze systemen zijn vaak dynamische eenheden met tijdelijk bindende partners en met een complexe ordening en werkingsmechanisme. Klassieke structuurbiologische technieken zijn vaak minder geschikt voor deze systemen omdat deze technieken vaak gelimiteerd zijn in de massaschaal, geen verzameling van deeltjes kunnen analyseren of grotere hoeveelheid stof nodig hebben. Om deze doelen te bereiken zijn verscheidene technologische ontwikkelingen gemaakt of moeten deze in de nabije toekomst worden gemaakt. Een belangrijk aspect is de transmissie en de detectie van grotere m/z ionen. Op dit moment is de transmissie en detectie van grote ionen met hoge m/z waarden in de massaspectrometer over het algemeen minder efficiënt dan die van ionen met lage m/z waarden. Om routinematig grotere systemen te kunnen analyseren is een toename van de gevoeligheid en efficiëntie noodzakelijk. Huidige ontwikkelingen op dit gebied zijn cryo-detectoren, die zonder verlies van gevoeligheid grote ionen kunnen detecteren, en verbeterde time-of-flight instrumenten met een hoger oplossend vermogen en gevoeligheid in het hoge m/z gebied.

Fascinerende ontwikkelingen die het mogelijk maken nog meer informatie te verkrijgen uit geïoniseerde eiwit deeltjes is ion-mobiliteits massaspectrometrie en tandem massaspectrometrie van grote eiwitcomplex ionen. De ion-mobiliteits massaspectrometrie geeft inzicht in gas-fase ionen conformaties. In een ion-mobiliteits instrument worden eiwit ionen gepulseerd naar een vlucht cel met een zwak electrostatisch veld, waarbij scheiding vindt plaats op basis van de mogelijkheid de cel over te steken. De mobiliteit van een ion is een functie van de massa, de lading en de fysieke grootte en vorm. Ion-mobiliteit gekoppeld aan massaspectrometrie combineert dus de mogelijkheid van scheiding op basis van grootte en vorm en op m/z. Tandem massaspectrometrie daarentegen kan informatie leveren over de stoichiometrie, moleculaire architectuur en bindingsenergie van de deelnemende partners (zie ook Hoofdstuk 1). Andere ontwikkelingen zijn gel filtratie gekoppeld aan massaspectrometrie en combinaties van massaspectrometrie en electronen microscopie.

De kinetische experimenten in dit proefschrift zijn uitgevoerd op een tijdschaal van minuten, dus bij lange na niet snel genoeg voor het bestuderen van het omslagpunt van een enkel enzym. Sommige onderzoeksgroepen hebben snelle mengers gekoppeld aan massaspectrometrie om het werkingsmechanisme van enzymen te bestuderen, maar tot nu toe is de benodigde

hoeveelheid eiwit veel hoger dan men kan verkrijgen van de meeste niet commerciële enzymen. Een veelbelovende benadering is de miniaturisering van deze apparatuur en het toepassen micro en nano vloeistofstromen. Deze ontwikkeling zal de mogelijkheden van het bestuderen van enzym kinetiek met behulp van massaspectrometrie enorm vergroten.

Résumé en Français

Vers la fin des années 1980, l'avènement de l'électrospray, technique d'ionisation « douce », a considérablement accru le potentiel de détection par spectrométrie de masse en termes de taille d'espèces analysables. Aujourd'hui, des entités en solution, de masse bien supérieure au million de Dalton, sont transférables en phase gazeuse. La technique accède donc à l'analyse des oligomères de protéines et des machineries fonctionnelles et une nouvelle discipline en spectrométrie de masse biomoléculaire nait, la spectrométrie de masse native, qui permet l'analyse, dans des conditions pseudo-physiologiques, de protéines et complexes protéiques intacts. La spectrométrie de masse native, méthode nouvelle dans le domaine de la biologie structurale, fournit des informations sur les structures tertiaires et quaternaires, la stoichiométrie, la stabilité et la dynamique des protéines et complexes protéiques, sur leurs liaisons avec les ligands et les cofacteurs et sur les effets de coopérativité qui en découlent. Ces données sont, le plus souvent, complémetaires à celles produites par les techniques de biologie structurales établies telles que la résonance magnétique nucléaire, la crystallographie, la diffusion de rayons X aux petits angles (SAXS) ou la microscopie électronique.

Notre projet avait pour but l'utilisation de la spectrométrie de masse native pour déterminer les relations structure-fonction de quatre protéines contenant des flavines, la PHBH, la VAO, l'HAPMO et la FprA. Nous nous sommes intéressés au comportement d'oligomérisation, à la liaison avec le cofacteur, aux effets coopératifs résultant, à la stabilité des protéines ainsi qu'à la modification du cofacteur par la protéine. Comme le révèle clairement le **Tableau I** du chapitre d'introduction, il n'y a que très peu de caractérisations fonctionnelles des flavoprotéines par spectrométrie de masse-électrospray (ESI-MS) native publiées à ce jour (12 en tout, dont 8 par notre groupe).

Analyses nano-ESI-MS de complexes non covalents

Le chapitre 2 décrit en détail l'importance des paramètres d'analyse nano-ESI-MS pour effectuer la détection des assemblages protéiques non covalents de masse moléculaire élevée. L'optimisation, en région source, de la pression (impérativement élevée) et des potentiels électriques s'avère cruciale pour la transmission et l'analyse effectives des ions protéiques volumineux. Pour illustrer ce phénomène, nous avons analysé deux flavoprotéines, PHBH et VAO, dans des conditions pseudo-physiologiques. Nos recherches ont révélé que les ions à rapport masse-sur-charge (*m/z*) élevé sont détectés plus efficacement à pressions instrumentales élevées.

Ce résultat peut s'expliquer par l'effet de refroidissement des ions par collisions précédemment décrit[39].

La nouveauté est que, sur nos instruments (2 LC-T et 1 Q-ToF-1 Micromass légèrement modifiés), l'effet de la pression élevée varie selon la nature (taille, *m/z*) de l'espèce ionique analysée. La variation de pression a un effect discriminatoire sur la détection des ions de différents *m/z*, décélérés différemment en fonction de leur vitesse (énergie cinétique) et de leur section de collision. Il n'est actuellement pas encore établi si l'effet *m/z*-dépendant observé est un phénomène général ou unique à l'équipement utilisé. A l'inverse, nous n'avons observé aucun effet de pression sur les ions de $m/z < 1500$, si ce n'est un élargissement des pics, probablement dû à une défocalisation du faisceau ionique. Par contre, il faut manipuler les tensions avec prudence car si les hauts potentiels avantagent la désolvatation, ils n'en favorisent pas moins la dissociation/fragmentation. Ainsi un ajustement précautionneux des pressions et tensions, potentiellement différents pour chaque complexe protéique et spectromètre de masse, donnera par conséquent les meilleurs résultats.

Effet de coopérativité de la liaison avec le cofacteur sur l'oligomérisation de VAO

Les acquis de ces premières recherches nous ont permis d'examiner les relations structure-fonction des protéines sélectionnées. Le chapitre 3 décrit l'étude de l'effet de coopérativité de la liaison avec le cofacteur FAD sur l'oligomérisation de VAO.

Dans des conditions natives, le sauvage VAO est presque exclusivement détecté en tant qu'octamère. En revenche, le mutant apo-VAO H61T, dans les mêmes conditions expérimentales, est essentiellement dimérique. Avec un excès de FAD, le spectre de VAO H61T révèle, sans ambiguïté, la présence de dimères et d'octamères. Tandis que le dimère est saturé par deux molécules de FAD, l'octamère apparaît comme un ensemble d'espèces contenant jusqu'à 8 molécules de FAD. Ces résultats impliquent un effet coopératif de la liaison avec FAD sur l'octamérisation. L'addition de 5'-ADP à apo-H61T, comme lors des expériences avec FAD, induit fortement l'octamérisation par liaison de 5'-ADP à la protéine. En revanche, la présence de FMN, n'a aucune incidence sur la structure quaternaire du complexe qui demeure dimérique. Ces résultats ont été validés par chromatographie d'exclusion par taille : holo-H61T VAO forme principalement des octamères alors que apo-H61T préfère s'associer en dimères. Ces recherches ont montré que la spectrométrie de masse native est une méthode puissante pour étudier les effets coopératifs dans les protéines. En fait, la spectrométrie de masse est la seule méthode capable de distinguer simultanément différents états oligomériques contenant un nombre différent de molécules de FAD.

Première mise en évidence directe de la liaison continuelle de NADP à HAPMO ; influence sur la stabilité de l'enzyme

Nous avons examiné les caractéristiques de la liaison du coenzyme NADP pendant le cycle catalytique pour obtenir des informations sur le mécanisme réactionnel ainsi que sur le rôle structural du coenzyme (chapitre 4). Pour la cyclohexanone monooxygénase, homologue de HAPMO, NADP, une fois oxidé, reste lié à l'enzyme pendant le processus d'oxygénation du substrat[197]. Ceci suggère que l'enzyme est, virtuellement, continuellement liée au coenzyme réduit ou oxydé.

Nos spectres ESI-MS en temps réel ont montré que HAPMO, lorsque'elle agit en tant que NADPH oxidase, est complexée à son coenzyme tout au long du cycle catalytique. Nous rapportons donc, pour la première fois, l'association continuelle du coenzyme à une monooxygénase Baeyer-Villiger. Nos résultats ont aussi révélé que $NADP^+$ interagit étroitement avec l'enzyme réduite mais pas avec l'enzyme oxydée. L'association avec le coenzyme s'est avérée capitale pour la stabilité de l'enzyme. Nous pensons que cet effet de stabilisation par coenzyme est aussi important pour des enzymes apparentées, ce qui expliquerait la stabilité relativement médiocre de protéines coenzyme-dépendantes qui seraient purifiées en l'absence du coenzyme en question. Nos mesures nano-ESI-MS en temps réel sont bien entendu applicables à d'autres enzymes pour l'étude de leurs mécanismes d'action.

FprA peut produire du NADPO

Dans le chapitre 5, la détermination de la structure en résolution atomique par crystallographie de FprA, oxydée et réduite en complexe avec NADPH, est détaillée. Notre contribution a été l'identification/vérification par ESI-MS du coenzyme enzymatiquement modifié par la protéine. La particularité dans la structure crystalline de FprA est la modification covalente de $NADP^+$. Les données RX suggèrent un atome d'oxygène lié à l'atome réactif C4 du nicotinamide.

La déconvolution du spectre de masse du complexe FprA-$NADP^+$ natif a révélé un complexe ternaire FprA-FAD-$NADP^+$. Malheureusement, la résolution n'a pas été suffisante pour identifier $NADP^+$ ou son dérivé. Dans des conditions dénaturantes, le spectre de masse comportait, outre les pics de l'apo-protéine FprA, des pics correspondant à FAD, à $NADP^+$ et au dérivé NADP proposé. La comparaison des spectres de dissociation induite par collision (MS/MS) sur $NADP^+$ et sur son dérivé ont révélé plusieurs fragments communs et des fragments spécifiques au dérivé, confirmant une modification correspondant à un oxygène carbonylique sur la position C4 du nicotinamide. L'analyse MS a montré sans ambiuïté que l'adduit covalent est présent en solution et

n'est donc pas un artéfact dû au processus de crystallisation. A notre connaissance, ce dérivé $NADP^+$, produit par FprA, n'avait pas encore été détecté dans d'autres enzymes. La signification physiologique de cette réaction reste à ce jour inconnue. Ceci étant, le $NADP^+$ modifié est potentiellement un composé leader pour le développement d'inhibiteurs spécifiques et pourrait aider aux recherches pharmaceutiques. La formation du dérivé en milieu cellulaire et son rôle physiologique restent à étudier. Très récemment, un dérivé $NADP^+$ similaire, $NADP(OH)_2$, a été identifié dans une alcool déshydrogénase[197] par une approche analogue à la notre.

Conclusions

Nos résultats montrent que la spectrométrie de masse native est aujourd'hui un précieux outil en biologie structurale pour l'examen des structures quaternaires de complexes protéiques homogènes, des liaisons de ligands, des effets coopératifs qui en résultent et des modifications de ligands. La spectrométrie de masse native est donc applicable à l'étude des relations structure-fonction des protéines, fournissant des données complémentaires/supplémentaires aux techniques classiques de biologie et biochimie structurales.

Dans nos recherches, nous nous sommes intéressés pour la plupart à des complexes oligomères homogènes contenant des cofacteurs. Les protéines peuvent cependant former des structures hautement plus complexes et hétérogènes avec diverses protéines, acides nucléiques et autres petites molécules. Depuis peu, la spectrométrie de masse contribue également à l'élucidation de tels assemblages. L'exemple le plus spectaculaire est la caractérisation des complexes ribosomiques formés de protéines et d'ARN[241]. Le défi de la spectrométrie de masse native est à présent de produire des informations sur les relations structure-fonction d'édifices protéiques hétérogènes imposants. Ces édifices forment souvent des structures dynamiques avec des partenaires transitoires et des mécanismes d'action/régulation très complexes. La spectrométrie de masse se prête tout à fait à l'analyse de ces structures, d'autant plus que les techniques de biologie structurale classiques sont souvent limitées par la masse des analytes ou ne peuvent analyser un ensemble d'entités ou encore requièrent une importante quantité d'échantillon.

Dans ce but, plusieurs avancées technologiques ont eu lieu mais restent encore insuffisantes. Un aspect critique est la détection des ions à *m/z* élevé. Aujourd'hui, le vol à travers l'appareil et la détection des ions macromoléculaires à haut *m/z* sont encore, en spectrométrie de masse, généralement moins efficaces que ceux des petits ions. Pour pouvoir analyser d'importantes structures de manière plus routinière, un accroissement de la sensitivité et/ou de l'efficacité de désolvatation/transmission/détection est nécessaire. Parmi les développements actuels dans ce domaine, on peut citer les cryo-détecteurs qui permettent la détection de macromolécules sans perte de sensitivité dans les région des hautes masses. D'autres progrès

fascinants, fournissant encore plus d'informations sur les ions, sont en cours de développement, notemment les instruments hybrides alliant la mobilité ionique à la spectrométrie de masse, certains permettant même la dissociation des espèces ionisées. La mobilité-ionique couplée à la spectrométrie de masse éclaire sur la conformation des ions en phase gazeuse. Dans un tel montage, les ions sont propulsés dans un dispositif de mobilité ionique puis séparés par leur capacité à traverser le courant de la cellule sous faible champ électrostatique. La mobilité est fonction de la masse, la charge, la taille et la forme globale. Cette technique allie donc séparation par la taille, la forme et le *m/z*. La spectrométrie de masse en tandem, quant à elle, renseigne sur la stoichiométrie, l'architecture moléculaire et les énergies de liaison des partenaires (voir Chapitre 1). D'autres avancées technologiques actuelles incluent le développement de couplages de la spectrométrie de masse à la chromatographie d'exclusion par taille ou à la microscopie électronique. Les deux dispositifs contribueront sans aucun doute à l'élargissement des domaines d'application de la spectrométrie de masse dans l'analyse des protéines.

Les expériences cinétiques rapportées dans cette thèse ont été effectuées à l'échelle de la minute, bien inférieure à celle des cycles catalytiques. Quelques groupes ont déjà couplé des dispositifs de mélange rapide à la spectrométrie de masse pour l'étude de mécanismes enzymatiques. Malheureusement, à ce jour, la quantité d'échantillon nécessaire pour ce type d'expériences reste importante et au-delà des quantités disponibles pour des enzymes non commerciales. Une approche prometteuse pour miniaturiser ces appareillages seraient les microfluides, un developpement qui élargirait considérablement le champ d'application de la spectrométrie de masse en permettant l'étude des cinétiques enzymatiques.

Alphabetical list of abbreviations

$AADP^+$	3-Aminopyridine adenine dinucleotide phosphate;
ADP; ATP	Adenosine diphosphate; Adenosine triphosphate;
Amu; u	atomic mass unit; mass unit;
AR	Adrenodoxin reductase;
BVMO	Baeyer-Villiger monooxygenase;
CAD; CID	Collisionally activated dissociation; Collisionally induced dissociation;
CD	Circular dichroism;
CRP	C-reactive protein;
Da; kDa; MDa	Dalton; kiloDalton; MegaDalton;
DNA	Desoxyribonucleic acid;
ESI	Electrospray ionization;
E. coli	*Escherichia coli*;
FAD	Flavin adenine dinucleotide;
FMN	Flavin mononucleotide;
FprA	Putative microbial flavoprotein oxidoreductase;
FWMH	Full width medium height;
G1	Pirani gauge located in the line between the source an the rotary pump;
G2	Pirani gauge located in the first RF-hexapole;
G3	Active inverted magnetron gauge located in the ToF-analyser;
GTP	Guanosine triphosphate;
HAPMO	4-Hydroxyacetophenone monooxygenase;
HPLC	High-pressure liquid chromatography;
HSP	Heat shock proteins;
ITC	Isothermal titration calorimetry;
LILBID	laser-induced liquid beam ionization/desorption;
LC-T	Orthogonal electrospray ionization ToF mass spectrometer;
MALDI	Matrix assisted laser desorption ionization;
MS	Mass spectrometry;
MS/MS	Tandem mass spectrometry;
NAD^+	Nicotinamide adenine dinucleotide;
NADH	Nicotinamide adenine dinucleotide reduced form;
$NADP^+$	Nicotinamide adenine dinucleotide phosphate;
NADPH	Nicotinamide adenine dinucleotide phosphate reduced form;
NADPO	$NADP^+$ oxidized derivative;
NMR	Nuclear magnetic resonance;
PheA1	Oxygenase;
PheA2	Flavin reductase;
PHBH	*para*-Hydroxybenzoate hydroxylase;
Rmsd	Root mean square deviation;
RNA	Ribonucleic acid;
SAP	Serum amyloid A protein;
SAXS	small-angle X-ray scattering;
SEC	Size-exclusion chromatography;
TEAB	Triethylammonium bicarbonate;
Th	Thomson
ToF	Time-of-flight;
UV	Ultraviolet;
VAO	Vanillyl alcohol oxidase;
3-D	Three-dimensional

List of Figures, Tables and Scheme

List of publications

Journal publications

Tahallah N, Pinkse M, Maier CS, Heck AJ. The effect of the source pressure on the abundance of ions of noncovalent protein assemblies in an electrospray ionization orthogonal time-of-flight instrument. *Rapid Commun Mass Spectrom.* **2001**;**15**(8):596-601.

Bossi RT, Aliverti A, Raimondi D, Fischer F, Zanetti G, Ferrari D, **Tahallah N**, Maier CS, Heck AJ, Rizzi M, Mattevi A. A covalent modification of $NADP^+$ revealed by the atomic resolution structure of FprA, a *Mycobacterium tuberculosis* oxidoreductase. *Biochemistry.* **2002**;**41**(28):8807-18.

Tahallah N, Van Den Heuvel RH, Van Den Berg WA, Maier CS, Van Berkel WJ, Heck AJ. Cofactor-dependent assembly of the flavoenzyme vanillyl alcohol oxidase. *J Biol Chem.* **2002**;**277**(39):36425-32.

Nanne M Kamerbeek, René Van der Ploeg, Arjen J Olsthoorn, **Nora Tahallah**, Albert JR Heck, Enrico Malito, Marco W Fraaije, Dick B Janssen. Exploring the role of the N-terminal domain of 4-hydroxyacetophenone monooxygenase. In *Biochemical properties and catalytic scope of a Baeyer-Villiger monooxygenase*. Thesis Nanne M Kamerbeek, Wageningen, The Netherlands. PrintPartners Ipskamp Enschede, **2004**, Chapter 4. Pp 55-73.

Robert HH van den Heuvel*, **Nora Tahallah***, Nanne M Kamerbeek, Marco W Fraaije, Willem JH van Berkel, Dick B Janssen, Albert JR Heck. Continuous binding of coenzyme is beneficial for the stability of 4-hydroxyacetophenone monooxygenase *J Biol Chem.* **2005;280**(37):32115 – 32121. * *Equally contributing.*

Nora Tahallah*, Willy AM van den Berg*, Kees Versluis, Robert HH van den Heuvel, Willem JH van Berkel, Albert JR Heck. The FMN cofactor ensures the protection of Flavodoxin – FldA –, from *Azotobacter vinelandii*, against active site cysteine residue oxidative damage caused by hydrogen peroxide. Evidence by LC-MS **2005** (*in prep*). * *Equally contributing.*

Conference publications

Nora Tahallah, Willy AM van den Berg, Claudia S Maier, Robert HH van den Heuvel, Willem JH van Berkel, Albert JR Heck. Cofactor-dependent assembly of the flavoenzyme vanillyl alcohol oxidase. In *Flavins and Flavoproteins*. Stephen Chapman, Richard Perham and Nigel Scrutton Eds. Rudolf Weber, Agency for scientific publications, Berlin, **2002**:387-392.

Acknowledgements

To my promoters:

To Prof. Dr. **Albert** JH Heck, I would like to address all my acknowledgments for the professional guidance, the stimulation, the trust and faith you provided at all steps of my PhD work and also for giving me the opportunity to discover Netherlands, it's landscape, culture and scientific spheres. It has been an honor to be a member of your constantly growing and promising team.

To Dr. **Claudia** S Maier. Thank you for the motivating hand you gave me in my first steps in the Biochemistry world and in the lab.

To Dr. **Robert** HH van den Heuvel. Thank you for your precious directions, help and input in the different circumstances we worked together.

Your presence has been invaluable and showed me what "Research" means.

A particular acknowledgment to "Cees" Versluis. **Kees** you have been there whenever, wherever, whatever needed. You helped me as no one to make a better living in Utrecht. Without you, I couldn't have made it the way it is. There are no words to express my gratitude to you. All those moments of sadness that you blew away with a Dutch joke, always ready to give a friendly, supportive, helpful, professional and even "spijbelende" hand. All those stories and laughs… I will never forget you. Thank you for honoring me with being my paranimf.

To all my **colleagues** and all Biomolecular mass spectrometry department **staff members**, I would like to express my thanks for the encouragements, the presence whenever needed and the "gezelligheid" that you made me come across.

To all the **members of** Dr. **Willem** JH van Berkel**'s team** that crossed my way, thank you for such a professional contribution to this project and the lovely conferences evenings that we shared.

To Dr. **Marco** W Fraaije and Dr. **Nanne** M Kamerbeek. It was a great pleasure and of great benefit to have you part of this research.

I thank M. **Carl Looijen** and the "medewerkers van Ponsen en Looijen" for their high efficiency and rapidity to get the production of my thesis ready on time.

To all **those whose way my steps crossed** during these "Dutch" years, I am thankful for all the special, interesting and instructive encounterings.

To my **room-mates.** Thank you for giving me the opportunity to discover another side of Utrecht's life and for helping my life style to become a bit more "Nederlandse".

To all my wonderful **friends in Utrecht** who shared with me laughing, crying, housing, drinking, rowing, dancing, singing, acting… I especially thank you for having endured my moods and cheered me up in all my downs. Thank you for the unforgettable moments in all my ups.

Aslı, I owe you so much that I hope life will be long enough to let me "send you back the lift".

A tous mes **amis et connaissances à Paris**, merci de n'avoir pas sauter sur l'occasion de mon départ pour m'oublier.

A **Esma** : un gros bisou à ma « grande sœur », grâce à qui j'ai cru à ma place dans la recherche.

Merci à **Cheikh Amer**, à **Nafissa**, ma troisième maman, à **Heba**, **Mona** et **Nadia**, pour leur amitié sincère, leurs merveilleux sourires et soutien et pour tous les précieux moments que nous avons partagés.

Chère **Odile**, merci d'avoir été mon premier guide dans un labo de spectrométrie de masse. **René**, merci de m'avoir initié au monde de la contrepétrie et du bon vin. Merci à tous les deux aussi pour vos visites et votre soutien réconfortant depuis que nous nous connaissons ainsi que pour les délicieux repas que nous avons partagés.

Je remercie le Dr. Francis **Maquin** de m'avoir aidé à saisir l'excellente opportunité de faire une thèse dans un domaine passionnant.

Au Pr. Dr. Jean-Claude **Tabet**, un grand merci pour m'avoir fait découvrir la spectrométrie de masse et la passion qu'elle pouvait engendrer, ainsi que pour son soutien.

Une profonde reconnaissance à Madame **Geneviève Bourg-Heckly**, ainsi qu'au Professeur **Alain Sézeur** et à Madame **Dominique Flanquart**. Sans vous je n'aurais jamais pu asseoir ma situation, atteindre mon but et découvrir de nouveaux horizons.

Valérie… Ma chère petite Bab's… Merci mille fois d'avoir toujours été si près, même bien loin. Merci d'avoir eu la force de ne jamais casser notre précieuse « cloche à fromage », ni perdre notre complice « Everest » ;-).

A tous **mes proches et amis en Algérie**. Je pense bien à vous et j'admire le courage dont vous faites preuve chaque jour. C'est pour une inspiration de tous les jours. Je regrette de ne pas vous voir aussi souvent que je le voudrais. Merci de ne pas m'avoir oubliée.

На **всички мои Български роднини, близки и приятели**. Благодаря за това че все още не сте ме забравили. Никога не ще забравя, нито вас, нито разкошните моменти и спомени, които прекарах и споделих със вас. Та нали сърцето ми е поне на половина българско…

Merci à vous, **Mathilde** et **Serge**, pour les aventures dans la neige et les succulents repas au coin du feu.

Merci à **Morwena** et **Baptiste** de m'avoir permis de me sentir moins seule dans la jungle des thésards.

To **my treasure of little family**, which being there is so out of words, price and worthiness. Мамо, от душа съм ти благодарна че ми каза: "Ако ти е много трудно и искаш да спреш, да се върнеш в къщи, вратата ще е винаги отворена." Мерси за това че вложи всичките си сили и надежди в нас. Едно се моля на живота, никога да не те разочаровам. Обичам те… « Merci » n'exprimera jamais, ni même d'une once, toute ma gratitude, mon respect, mon devouement, mon attachement et mon amour pour vous. Vous êtes ma motivation, ma raison de vivre et celle de tous mes pas dans cette merveilleuse vie.

Et enfin, *the last but not the least*, à toi Gwendal. Mon Gwen chéri, **mon tiron**, mon p'tit luce… J'espère t'apporter ne serait-ce qu'un brin des rayons de soleil que tes sourires m'envoient quand j'ai de la peine, une goutte de tous ces espoirs et confience que versent sur moi tes yeux chaque fois que je suis perdue. Ta patience, tes conseils professionnels, personnels, quotidiens, tes réconforts, tes taquineries, tes épaules et ta voix m'ont, chaque fois, rendu mon souffle et tenu la tête hors de l'eau. Merci de m'avoir fait l'honneur d'être mon paranimf. Sans toi je ne serais pas arrivée jusqu'au bout. Et aujourd'hui, avec toi, je suis heureuse. Je t'aime.

I would need more than the present pages and words to thank all the people that contributed directly or indirectly, from close or from far, personally or "via…", to make all this adventure be possible, become exciting, fruitful and eventually come to a successful end. I apologize beforehand to those who I haven't mentioned and would like them to accept my "indirect" gratefulness.

J'aurais besoin de bien plus que ces quelques pages et mots pour remercier toutes les personnes qui ont contribué directement ou indirectement, de près ou de loin, personnellement ou « via… », à faire de cette aventure une possibilité, une source de motivation, une réalité fructueuse et, somme toute, une « affaire rondement menée ». Par avance, toutes mes excuses pour ne pas vous avoir mentionnés et acceptez, s'il vous plait, mes remerciements « indirects ».

Utrecht,
October 2005,

Nora

Curriculum Vitae

Nora Tahallah was born on April the 07th 1972 in the white Algiers - Algeria. She went to the French High School Lycée Descartes and graduated in June 1990 (**Baccalauréat Série D - Sciences de la Nature** - mention AB), spending all her summer holidays with her sister in Bulgaria, her mother's country.

At the age of eighteen, she moved to the city of light, Paris - France, for her university studies at the French University Pierre et Marie Curie - PARIS VI. During her whole university studies she has had different jobs and acquired several experiences such as saleswoman, cashier in a Parisian department store but also as executive secretary and administrative assistant or also, health care for elder persons. At PARIS VI University she obtained the following diplomas: **DEUG A Sciences et Structures de la Matière** in June 1993, **Licence de Chimie** (*equivalent to a Bachelor degree in General Chemistry*) in September 1995, **Maîtrise de Chimie** - mention AB *(eqv. Bachelor degree in Chemistry, Fundamentals and Initiation to Synthesis and Organic Chemical Analyses)* in June 1998 and **DEA Spectrochimie, Analyse et Physicochimie Organiques** - mention B *(eqv. Master degree in Organic Spectrochemistry Analyses and Physical Chemistry)* in October 1999. In the frame of this latter education and to be cited among her work experiences, she performed a 6 months **laboratorial training** at the pharmaceutical company Hoechst Marion Roussel (*Actual Aventis*), Paris - France, resulting in a graduation thesis entitled "Coupling, setting and optimization of a Liquid Chromatography - Mass Spectrometry (LC/MS) system for the analyses of pharmaceutical mixtures synthesized by the Research-Production Department" under the supervision of Dr. Francis Maquin.

For the completion of her high education and the extension of her multinational culture and connections, in December 1999 she decided to join the rising international research team of Prof. Dr. Albert JR Heck at the university of Utrecht - The Netherlands to acquire a **Ph.D. degree in Biomolecular Mass Spectrometry** granted by the Dutch Organization for Scientific Research (NWO) that is described in this thesis.

« Have no fear of perfection - You will never reach it... »
SALVADOR DALI.